



<https://theses.gla.ac.uk/>

Theses Digitisation:

<https://www.gla.ac.uk/myglasgow/research/enlighten/theses/digitisation/>

This is a digitised version of the original print thesis.

Copyright and moral rights for this work are retained by the author

A copy can be downloaded for personal non-commercial research or study,
without prior permission or charge

This work cannot be reproduced or quoted extensively from without first
obtaining permission in writing from the author

The content must not be changed in any way or sold commercially in any
format or medium without the formal permission of the author

When referring to this work, full bibliographic details including the author,
title, awarding institution and date of the thesis must be given

Enlighten: Theses

<https://theses.gla.ac.uk/>
research-enlighten@glasgow.ac.uk

THE UNIVERSITY OF GLASGOW

THE GAP JUNCTION:
A SITE OF CELL TO CELL COMMUNICATION

BY

SCOTT ADDIS JOHN

A THESIS SUBMITTED TO THE FACULTY OF SCIENCE
IN CANDIDACY FOR THE DEGREE OF
DOCTOR OF PHILOSOPHY

BEATSON INSTITUTE FOR CANCER RESEARCH

JANUARY 1987

ProQuest Number: 10991918

All rights reserved

INFORMATION TO ALL USERS

The quality of this reproduction is dependent upon the quality of the copy submitted.

In the unlikely event that the author did not send a complete manuscript and there are missing pages, these will be noted. Also, if material had to be removed, a note will indicate the deletion.



ProQuest 10991918

Published by ProQuest LLC (2018). Copyright of the Dissertation is held by the Author.

All rights reserved.

This work is protected against unauthorized copying under Title 17, United States Code
Microform Edition © ProQuest LLC.

ProQuest LLC.
789 East Eisenhower Parkway
P.O. Box 1346
Ann Arbor, MI 48106 – 1346

TO MY MOTHER AND FATHER, AND FIONA

ACKNOWLEDGEMENTS

I would like to thank my supervisor, Dr. John Pitts for his insight and encouragement throughout this project. I would also like to thank Dr. Malcolm Finbow for his constructive criticism of my work.

The experiments reported in section 3.5 were carried out with the collaboration of Dr. Ephraim Kam.

This work was done while I was receiving a Scholarship from the Cancer Research Campaign, whom I thank for this support.

TABLE OF CONTENTS

Chapter	Page
I. <u>INTRODUCTION</u>	1
1.1 <u>The Structure of Gap Junctions</u>	2
1 Electron Microscopy of Thin Sectioned Tissue	2
2 Electron Microscopy of Freeze Fractured Tissue	3
3 High Resolution Electron Microscopy	4
4 Connexon Models	5
5 Conclusions	8
1.2 <u>The Permeability of Gap Junctions</u>	9
1 Electrophysiology	9
2 Dye Transfer	11
3 Metabolite Transfer	13
4 Functional and Structural Correlation	14
1.3 <u>The Modulation of Gap Junctions</u>	15
1 Voltage	15
2 Changes in Calcium Ion Concentration	16
3 Changes in Hydrogen Ion Concentration	18
4 Neurotransmitters	19
5 Alkanols	20
6 Gating of the Gap Junctional Channel	20
7 Functional and Structural Correlation	22

1.4 <u>The Function of Gap Junctions</u>	23
1 The Ubiquity of Gap Junctions	23
2 Tissue Homeostasis	25
3 Chemical Carcinogenesis	26
4 Tumourgenesis	29
5 Gap Junctions in Parturition	30
6 Gap Junctions in the Ovary	31
7 Conclusions	33
1.5 <u>The Protein Composition of Gap Junctions</u>	34
1 The Lens Fibre Protein	34
2 The Liver Protein	35
3 Antibodies	37
4 Models of Putative Gap Junctional Proteins	43
5 Conclusions	44
II. <u>MATERIALS AND METHODS</u>	46
2.1 <u>Materials</u>	46
1 Fine Chemicals	46
2 Radiochemicals	46
3 Solutions	47
2.2 <u>Methods</u>	49
1 Preparation of Gap Junctions	49
2 SDS PAGE	50
3 Protein Electroelution	51
4 Gel Scanning	51
5 Electron Microscopy of Isolated Gap Junctions	51
6 Peptide Synthesis	52
7 Coupling of Synthetic Peptide to Carrier Protein	53
8 Preparation of Site Specific Antisera	53

9 Dansyl Chloride Derivitization of 16K Protein	54
10 DABITC Derivitization of 16K Protein	54
11 Immunoblotting	55
12 Modified Immunoblotting	56
13 Agglutination of Gap Junctions	56
14 Two Dimensional Peptide Mapping	57
III. <u>RESULTS</u>	58
3.1 <u>Preparation of Site Specific Antisera</u>	58
1 Introduction	58
2 Protein Sequencing	59
3 Preparation of Polyclonal Site Specific Antisera	62
3.2 <u>Characterization of Site Specific Antisera</u>	64
1 Affinity Purification	64
2 Immunoblot Analysis	65
3 Alternative Immunoprecipitation	67
4 Agglutination	69
3.3 <u>Tissue and Species Conservation</u> <u>of Gap Junction Proteins</u>	72
1 Introduction	72
2 Microimmunodiffusion Analysis	72
3 Agglutination Analysis	74
3.4 <u>The Structural Organization of Protein</u> <u>within the Gap Junction</u>	76
1 Introduction	76
2 N-terminal Localization	76
3 Two Dimensional Peptide Mapping	79
3.5 <u>Functional Studies</u>	83

IV. <u>DISCUSSION</u>	85
4.1 <u>Introduction</u>	85
4.2 <u>Characterization of Site Specific Antisera</u>	87
1 Microimmunodiffusion Analysis	87
4.3 <u>Other Site Specific Antisera</u>	89
1 Immunoblotting Analysis	90
2 Immunoprecipitation Analysis	91
4.4 <u>Tissue and Species Conservation</u>	92
1 Tissue Conservation	92
2 Species Conservation	93
4.5 <u>Monoclonal Antibodies</u>	95
4.6 <u>Functional Studies</u>	96
V. <u>REFERENCES</u>	101

SUMMARY

1. The literature relating to the structure and function of gap junctions has been reviewed. Particular attention has been paid to papers providing evidence for the identity of the junctional proteins and to the limited information on the molecular structure of the junctional channels as this structure determines junctional permeability, which will in turn determine the possible functions of gap junctions.
2. SDS PAGE analysis of gap junction enriched fractions isolated from mouse liver shows only one major protein component, apparent Mr 16000 (16K). Application of Hopp and Woods (1981) algorithm to the known sequence of the 16K protein (amino acids 2-28) showed that the N-terminal region was the most hydrophilic.
3. The N-terminal amino acid of the 16K protein was shown by chemical analysis to be asparagine.
4. A nonapeptide was synthesized with the sequence corresponding to the N-terminal octapeptide of the 16K protein (Asn-Pro-Glu-Tyr-Ser-Ser-Phe-Phe) and a cysteine in position 9.
5. The nonapeptide was coupled through the cysteine to keyhole limpet haemocyanin and the conjugate used to raise polyclonal, site specific antisera in four rabbits.
6. An immunoglobulin (IgG) fraction was separated from the site specific antiserum. The antibodies which bound to the peptide were affinity purified.

7. The site specific antisera produced were characterized using four different techniques. All four sera had the same reactivities.

(i) immunoblotting of SDS PAGE separated protein from mouse liver gap junctional preparations and of electroeluted 16K protein, which showed the antibodies to the peptide recognize an antigenic site on the 16K protein.

(ii) microimmunodiffusion, based on the Ouchterlony technique, of SDS solubilized protein from mouse liver gap junction preparations and electroeluted 16K protein.

(iii) agglutination of isolated gap junctions (the agglutination reaction was completely inhibited by the free peptide at a concentration of 5 mM), which showed that the antigenic site is accessible in intact junctions.

(iv) ultrastructural localization using Protein-A gold and isolated mouse liver gap junctions, which showed the antigenic site is present on morphologically identifiable gap junctions.

8. Gap junctions were isolated from three different mouse tissues (brain, heart, and kidney). Analysis of these preparations by SDS PAGE showed the presence in each of one major Coomassie staining band, Mr 16000. The junctional proteins isolated from these different tissues were shown by the microimmunodiffusion assay to react with the site specific antiserum.

9. Gap junctions were isolated from tissues of different species (chicken liver, Xenopus liver, and Nephrops norvegicus hepatopancreas). The chicken and Xenopus preparations showed that one major Coomassie staining band, Mr 16000 when analysed by SDS PAGE. The preparations from Nephrops showed one major band, Mr 18000. Microimmunodiffusion analyses showed that the site specific antiserum recognized the gap junctional proteins isolated from all three species. The isolated gap junctions from Nephrops hepatopancreas also showed agglutination when incubated with the site specific antiserum.

10. The structural organization of the 16K protein within the

membrane was examined. It was shown that the N-terminus of the 16K protein (and the cross-reactive site of the 18K protein) was located on the cytoplasmic face of gap junctions. Treatment of intact junctions with pronase showed the presence of a further loop (or loops) of the 16K and 18K proteins on the cytoplasmic face of both the mouse liver and Nephrops hepatopancreas junctions. The protein fragments remaining after pronase treatment of intact junctions were sufficient to maintain the characteristic morphology of the gap junction.

11. Peptide mapping studies have been used in an attempt to determine which peptides are cytoplasmically located and more specifically to determine the orientation of the N-terminal peptide.

12. In collaboration with Dr. E. Kam, the site specific antiserum has been iontophoretically injected into Buffalo rat liver cells and shown to block cell to cell transfer of the fluorescent dye Lucifer Yellow.

13. The significance of the observations made in the course of this work are discussed and related to other published work on the protein constituents of gap junctions.

ABBREVIATIONS

Abbreviations used in this thesis are those recommended in the Biochemical Journal, Policy of the Journal and Instructions to Authors, London, 1981. All other abbreviations are specified where appropriate in the text.

CHAPTER I

INTRODUCTION

Membranes are barriers to free molecular movement: they are the sites where specific and non-specific molecular trafficking occur. The structural organization of membranes and the non-uniform distribution of its various components help to maintain the cells' individuality yet allow it to integrate with its neighbours, both near and far, to produce a fully functional organism.

Cellular integration mediated by cell to cell communication depends on both extracellular and intracellular pathways. The extracellular pathway is used by hormones and neurotransmitters.

The intracellular pathway, which is described in this thesis, is mediated by a plasma membrane specialization called the gap junction. The structure of the gap junction determines its trafficking or permeability characteristics. These characteristics in turn determine its potential functions.

There exists in the literature a dichotomy as to the identity of the structural protein of gap junctions. The work described in this thesis was started in an attempt to resolve the present uncertainty, and in the hope of adding to our knowledge of the structure and function of this membrane specialization which is found in most tissues of all metazoan animals.

1.1 THE STRUCTURE OF GAP JUNCTIONS

Gap junctions can be visualized using a variety of electron microscopic techniques: thin sectioning, negative staining, and freeze fracture. Each technique has revealed a facet of the gap junctional morphology.

1.1.1 Electron Microscopy of Thin Sectioned Tissue

Gap junctions can be seen by thin sectioning liver stained en bloc with colloidal lanthanum, an electron opaque tracer which fills the interstitial space but does not enter the cells. This reveals that the closest approach of the two apposed plasma membranes, forming the gap junction, is 2 nm (Revel and Karnovsky, 1967). The stain is not excluded from the region of apposition. This pattern of staining, in transverse section, produces the characteristic pentalaminar structure of gap junctions.

In occasional sections parallel to the plane of the membrane a loose array of particles is observed some of which have a central dot of stain. This central dot of stain suggests a pathway from the interstitial space through the core of the particle. These particles of the gap junction are called connexons (Goodenough and Revel, 1970).

Similar details are seen in the negative stained images of isolated junctions. However, isolated junctions have a more ordered hexagonal array of connexons, presumably because they have been extracted with detergents which will have removed lipid. Again each connexon has a central staining region of approximately 2 nm (Benedetti and Emmelot, 1967). In fortuitous "edge on" views of negatively stained junctions, the central staining region can be seen to span the entire length of the connexon and is continuous

with the densely staining region of the connexon in the apposing membrane, indicative of a channel connecting the cytoplasms of the neighbouring cells (Zampighi et al., 1980). A pair of connexons, one from each cell, thus form the structural unit of the gap junction.

1.1.2 Electron Microscopy of Freeze Fractured Tissue

More detailed information on the structure of the gap junction has come from other electron microscopic techniques.

One such technique is freeze fracture electron microscopy. The tissue is rapidly frozen for example, by immersion into an inert liquid such as propane cooled with liquid nitrogen. The tissue is then fractured. The tissue fractures preferentially between the two halves of the lipid bilayers of the cells membranes. This exposes two internal faces: one adjacent to the cytoplasmic compartment, the "P" face; the other adjacent to the extracellular compartment, the "E" face. The fractured tissue is then usually coated with platinum and carbon. The tissue is removed with chromic acid. Resolution of freeze fracture is limited mainly by the thickness (~ 2 nm) of the platinum-carbon coating.

Freeze fracture electron microscopy shows gap junctions to be of a characteristic macular or plaque like appearance made up from clusters of intramembranous particles (connexons?) 8-9 nm in diameter (McNutt and Weinstein, 1973). The number of connexons in a gap junction varies from a few to many thousands. The particles are loosely packed, similar to that seen in "en face" views of junctions from tissue sections. Intramembranous particles present on the P face and pits on the E face demonstrate an apparent complementarity to one another (Flower, 1972; Gilula, 1972). Recent use of rotary rather than unidirectional shadowing, has shown that the intramembranous particles have a central depression of ~ 1.5 nm diameter (Hanna et al., 1985). This depression is believed to be the channel seen in negatively stained micrographs.

The characteristic fracturing of junctions appears in nearly all species, apart from the arthropods where the particles fracture to the E face and the complimentary pits to the P face. Invertebrates also have larger intramembranous particles of 11-13 nm (Flower, 1972).

1.1.3 High Resolution Electron Microscopy

Hirokawa and Heuser (1982) have extended the findings of Goodenough and Gilula (1974) by using rapid freezing and deep etching to visualize the extracellular and cytoplasmic surfaces of the gap junction.

At gap junctions, the fracture plane jumps back and forth between the two apposed membranes, and it is not possible to visualize their extracellular surface. To do this the junctional membranes must be separated. Hirokawa and Heuser (1982) achieved this by perfusing the livers in situ with saline made hypertonic with sucrose according to the method of Goodenough and Gilula (1974), or by incubating cubes of liver in calcium free saline. Hirokawa and Heuser (1982) found after deep etching split junctions that the central 1.5 nm pore was present on the extracellular face of the connexon, in agreement with the freeze fracture studies (see section 1.1.2). They also demonstrated protrusions that extend from the external surface of the membranes which are presumably those regions of the connexon which abut against each other and thus cause the 2 nm gap.

This study also provided information on the cytoplasmic surface of the gap junction. They passed cells through narrow gauge needles to produce large plasma membrane fragments which were then washed, fixed, frozen and cleaved. Identification of the cytoplasmic faces, by continuity with fractured E faces, shows the cytoplasmic domains of the junctions appear smooth. Protrusions and depressions are noticeably absent and no lattice arrangement can be seen. The smooth cytoplasmic face of the junctions, even after glutaraldehyde fixation, shows that the cytoskeleton is not associated with the junction. Also using high resolution

replicating techniques Dermietzel et al. (1984a), show protrusions and pores on the extracellular side of the membrane and no ordered arrays or pores on the cytoplasmic surfaces. Dermietzel et al. (1984a) however used gap junctions isolated with detergents.

In summary, the general conclusions from freeze fracture studies are that the particles and pits show complementarity and that the channel varies in diameter as it traverses the membrane. The narrow region being on the cytoplasmic side and the wide region being on the extracellular side. The connexons appear not to protrude into the cytoplasm.

1.1.4 Connexon Models

1.1.4.1 Model one

In an effort to produce models of the gap junctional subunit, the connexon, three dimensional reconstruction methods have been used. Such methods depend on electron diffraction analysis of by single isolated junctions or X-ray diffraction analysis of pelleted isolated junctional plaques.

To reconstruct a three dimensional model from a two dimensional image requires Fourier analysis of diffraction patterns made at different angles i.e. by tilting junctional membranes. The information can then be combined to generate the variations of electron density across the thickness of the junction. The best resolution achieved by this technique to date is ~ 2 nm.

By using both negatively stained junctions (Unwin and Zampighi, 1980) and frozen hydrated junctions (Unwin and Ennis, 1983), the reconstruction is more complete. Images from the negatively stained junctions have contrast in those regions where the connexon protrudes from the cytoplasmic and extracellular surfaces. Images from the frozen hydrated junctions have greatest contrast in the region where the connexon is in the bilayer.

The model produced by this method (Fig 1a) shows that each connexon is made up from six, probably identical, subunits 7-7.5 nm

Figure 1

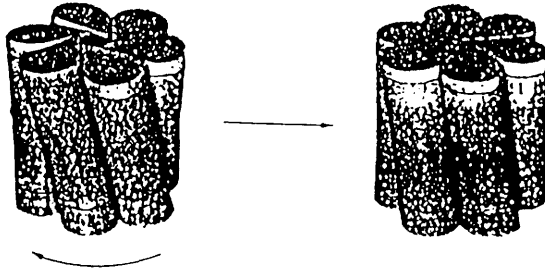
Models of Connexons

a) Model of the connexon based on the electron diffraction patterns and Fourier transforms of micrographs of isolated gap junctions (from Unwin and Zampighi, 1980). The model depicts an individual connexon with six subunits. The conformational change from the open to the closed state is produced by the addition of calcium ions. The model shows the subunit tilt changing and the entrance of the channel on the cytoplasmic face closing.

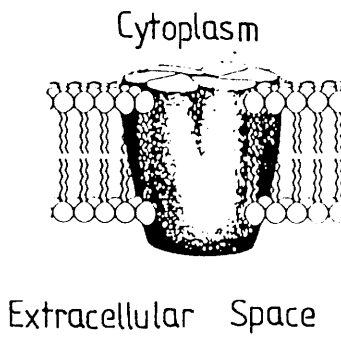
b) Schematic diagram of a connexon showing the relative position of the connexon within the bilayer of the plasma membrane (from Unwin and Henderson, 1984).

c) Drawing of the gap junction structure based on the results of X-ray diffraction studies made on isolated gap junctional plaques (from Makowski et al., 1977).

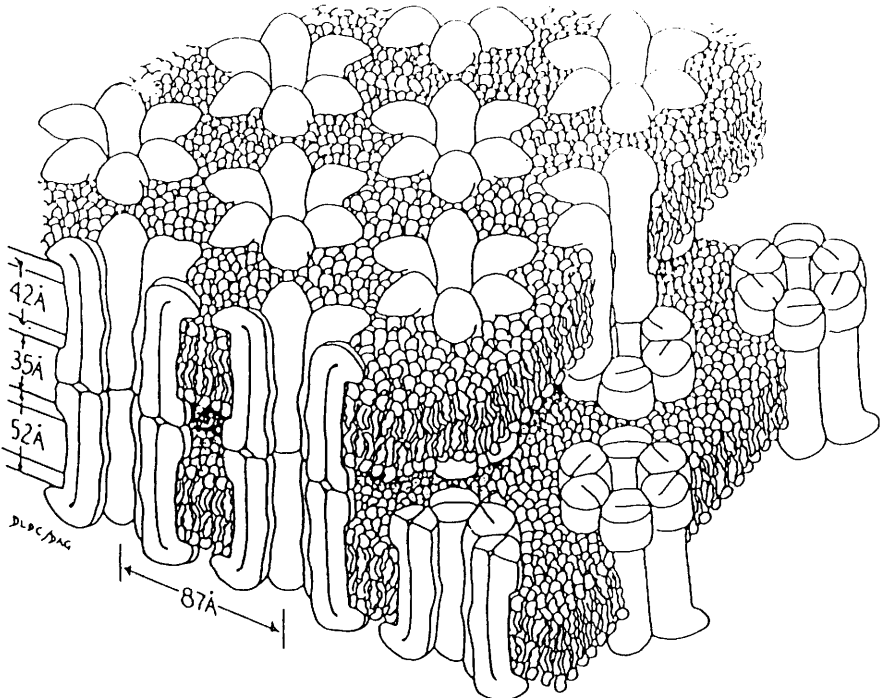
a



b



c



suggestive of a sub-structure on the cytoplasmic surface.

Zampighi et al. (1980) argue that if there were a significant protein component on the cytoplasmic face then transverse views of the junction would reveal periodic variations in stain density at the cytoplasmic surfaces, aligned with discrete densities in the gap region. Such densities were not seen despite viewing transverse sections at various angles. This would suggest that either irradiation damage removes such periodic densities or that the cytoplasmic component is small i.e. below the limits of resolution.

1.1.4.2 Model two

X-ray diffraction analysis has also been used to analyse the fine structure of gap junctions. The analysis relies on the hexagonally ordered lattice found in isolated junctions.

X-ray diffraction studies also produce electron density profiles. Meridional diffraction is produced by the electron density distribution perpendicular to the plane of the junctional membrane. Equatorial diffraction is due to the electron density distribution in the plane of the membrane. The diffraction pattern produced and a knowledge of the known electron densities of the junctional components: protein, lipid, and water enables a model to be constructed. At the present time resolution is about 1.8 nm. Not until crystals of the junctional protein are produced can this resolution be increased.

The model of the gap junction obtained by X-ray diffraction is generally similar but somewhat different in detail to that of Unwin and Zampighi (1980) (see Fig. 1c). The connexon is again shown to be made up from six subunits which form a channel that has a diameter of 2-3nm along most of its length but narrows to 1.5 nm in the extracellular region of the bilayer (Casper et al., 1977; Makowski et al., 1977). The individual subunits having a volume equivalent to 15-17000 daltons of protein with polar amino acids present in the gap and nonpolar amino acids within the bilayer (Makowski, 1985). There is a cytoplasmic component to the connexon of 5-10000 daltons, one sixth being contributed by each subunit. It

is suggested that this cytoplasmic component "intercalates" with the polar head groups of the lipid to block the channel i.e it controls the channels permeability.

The cytoplasmic domain is also susceptible to trypsin digestion, 4000 daltons being removed (Makowski et al., 1984). However, Makowski et al. (1984) to obtain this figure compared a junction preparation which had been trypsinized and then fixed with glutaraldehyde to one which had just been fixed. This comparison is suspect as glutaraldehyde may fix a non-junctional component, which is trypsin sensitive, to the junction. Makowski et al. (1984) report that the cytoplasmic domain in size and configuration is variable depending on whether, detergents and exogenous proteases, or detergents alone are used to isolate the junctions. This portion of the protein is therefore thought of as both flexible and labile (Makowski, 1985).

1.1.6 Conclusions

The two models described have many similarities with the major difference being the extent of the cytoplasmic component. Unwin and his collaborators seem to agree with the salient features of the results from negative staining, freeze fracture and deep etching. Both models appear to agree that the channel is gated at the cytoplasmic side of the junction, but the mechanism proposed is different. Unwin's model suggests that the channel is closed by a slight rotation of the subunits resulting in less tangential tilt and a narrowing of the channel at the cytoplasm. Makowski et al. (1984) argue for a movement of a cytoplasmic domain relative to the rest of the protein in the membrane.

1.2 THE PERMEABILITY OF GAP JUNCTIONS

Permeability of the gap junction channel is determined principally by its diameter. The permeants will only pass through the channel if they are small enough, though if close to the limit of permeation then shape and charge may have effects.

The structural details of the channel (section 1.1) give an indication of the theoretical limits of permeation but the functional permeability characteristics of the channel have been determined experimentally.

Three approaches have been used to characterize the functional permeability of the gap junctional channel: electrophysiology, dye transfer and metabolite transfer.

1.2.1 Electrophysiology

Using intracellular microelectrodes Furshpan and Potter (1959) demonstrated the electrical synapse: an injection of current into one nerve cell (pre-synaptic lateral giant fibre of the crayfish) produces in an adjacent nerve cell (post synaptic giant motor fibre) a voltage change. The two neurons are said to be electrically coupled. What distinguishes the electrical synapse from the chemical synapse is the lack of delay between injection of current and the recording of voltage change in the adjacent cell. However, Furshpan and Potter (1959) found that, like the chemical synapse, the transmission was uni-directional i.e. a rectifying synapse.

Numerous later studies (e.g. Watanabe and Grundfest, 1961; Hagiwara and Morita, 1962) showed that the electrical synapse is more usually considered as bi-directional i.e. injection of current into the post synaptic neuron can be transmitted into the

presynaptic neuron. Electrical synapses are not just limited to excitable tissues, they have been found in many non excitable tissues e.g. liver (Meyer et al., 1981).

1.2.1.1 Channel conductance.

Measurement of conductance for the electrical synapse has proved more intractable than many other ionic channels. The conductance value for a single channel is useful as it can be used to estimate the channel diameter. Using a double whole-cell patch clamp system, Neyton and Trautmann (1985) claim to have made the first quantitative recordings of a single channel current from a gap junction. Advantages of single channel recording are fourfold:

- (i) single channel current and thereby single channel conductance is directly measured;
- (ii) the solutions bathing both sides of the membrane can be controlled allowing relative permeabilities to be measured for different (charged) permeants (a feature of patch clamping);
- (iii) the method permits the determination of state (open or closed) of a given channel at a particular time so that conditional probability and other statistical analyses can be made;
- (iv) a channel's kinetics can be measured and rate constants of opening and closing can be determined.

Neyton and Trautmann (1985) used an unusual system. They measured the current flowing through the last remaining channels during the final stages of uncoupling in pairs of rat lacrimal cells. The measured conductance of a single channel was 120 pS. The channel discriminates poorly between cations and anions: cations are marginally more permeant. The mean open time for the channel is 2 seconds and the opening and closing of the channel is fit by an exponential function with a time constant of several tens of milliseconds.

Two other cell systems have been used to calculate the single channel conductance, the Novikoff hepatoma cell and the larval beetle epidermis. However, these determinations were not made with the

double whole-cell patch clamp technique and used additional quantitative morphological analysis to determine the area occupied by gap junctions. Such analysis assumes that the channels constitute a homogeneous population and that each connexon particle is an open channel. The values obtained for single channel conductance from Novikoff hepatoma cells (Sheridan et al., 1978) and beetle epidermis (Berdan and Caveney, 1985) of 113 pS and 94 pS respectively, agree well with the value of Neyton and Trautmann (1985).

1.2.1.2 Channel diameter calculated from channel conductance.

Theoretical conductance values for a single membrane channel can be calculated using the equation:

$$g = \pi r^2 / R_e \cdot L$$

where g is conductance, R_e is resistivity of channel (not known but set at 100 ohms/cm), cytoplasm has a resistivity of ~ 65 ohms/cm), L is the length of channel, r is radius of the channel (Berdan and Caveney, 1985).

Using this equation a channel diameter can be calculated. (Channel lengths used were those given by Berdan and Caveney, 1985). Plotting a curve of the theoretical conductance of a 20 nm long channel for invertebrates and a 15 nm long channel for vertebrates against different diameters the conductance values of 120 pS Neyton and Trautmann (1985), 113 pS Sheridan et al. (1978), and 94 pS Berdan and Caveney (1985), give channel diameters between 1.5 nm and 2.0 nm. Such diameters of channel agree with the structural determinations on gap junctions (see section 1.1.4).

1.2.2 Dye Transfer

A modification of electrophysiological methods was developed by Loewenstein and Kanno (1964). They iontophoretically injected fluorescein into electrically coupled cells. They noted that this

Mr 330 hydrophilic molecule diffused from one cell to another without entering the interstitial space. They concluded that the pathway responsible for electrical coupling is leakproof and permeable to substances other than inorganic ions. In a later series of experiments using fluorescent probes of different size, shape and charge Loewenstein and his colleagues investigated the permeability characteristics of gap junctions in situ in both vertebrate and invertebrate cells.

Using the salivary gland cells of the insect Chironomus, chosen because of their large size (~ 20 μm diameter), it was shown that all neutral molecules up to Mr 1500 pass through the junctions. Based on the limiting geometry of the largest permeant, (Simpson et al., 1977) the channels effective permeation diameter was defined as 2-3 nm. Recently Zimmermann and Rose (1985) determined the kinetics of fluorescent tracer diffusion through the same cells. Based on an inverse relationship between the tracers mean diameter and the relative rate constant for cell to cell diffusion they redefined the effective diameter as 2.9 nm. This value is somewhat larger than the structural determinations carried out on isolated gap junctions (1.5-2.0 nm). These structural determinations were on mammalian forms of gap junctions which have smaller connexon particles 8-9 nm (freeze fracture) than the 12-15 nm connexon particles of their insect counterparts (Flower, 1972).

The smaller connexon diameter of mammalian gap junctions is reflected in their permeability characteristics. Using the same series of fluorescent probes as employed in the Chironomus salivary gland cells Flagg-Newton et al. (1979) found that the effective permeability cut off is Mr 900. They also provided evidence for a negative charge in the channel. Negatively charged probes close to the exclusion limit showed decreased permeance. As described (section 1.2.1), the channel has a slightly lower permeability to anions than cations. Isolated gap junctions may retain their charge discrimination. Using anionic and cationic negative stains, Baker et al. (1985) have reported the exclusion of anionic stains from the channel of the connexon. The results are indicative of a negative charge fixed in the vertebrate junctional channel. Two other

studies have shown that a similar negative charge occurs in the invertebrate junctional channel, the arthropod (Caveney et al., 1980) and the annelid (Brink and Dewey, 1978).

1.2.3 Metabolite Transfer

Electrophysiological and dye transfer studies are invasive techniques, and in the fluorescent tracer experiments involve non-physiological molecules. A chance discovery by Subak-Sharp et al. (1966), allowed characterization of junctional permeability using non-invasive techniques and normal cellular constituents.

This discovery was based on cells which are deficient in an enzyme of a purine or pyrimidine salvage pathway. e.g. hypoxanthine: guanine phosphoribosyl transferase (EC 2.4.2.8). Mutant cells are unable to incorporate the hypoxanthine into nucleic acids unless they are grown in contact with wild-type cells. Incorporation can be followed using tritiated hypoxanthine and autoradiography. Only wild-type and mutant cells in contact with the wild-type cells are labelled. Mutant cells not in contact with the wild-type cells show no incorporation of label. The mutant cells, by contact with the wild-type cells, have undergone a phenotypic change called metabolic co-operation (Subak-Sharp et al., 1966, 1969).

Pitts (1976) has detected a phenotypic change in mutant cells at least 50 cell diameters away from the wild-type cells with an intervening gradient of incorporated labelled material.

Metabolic co-operation was shown to be due to the movement of labelled nucleotides through intercellular junctions (Pitts 1971; Pitts and Simms, 1977). As a result it was possible to extend this approach to a wider investigation into the characteristics of junctional permeability with regard both to the cell type and the metabolite being transferred. Results of these experiments showed that nucleotides, choline phosphate, amino acids and their precursors, and the vitamin derived co-factor tetrahydrofolate are all exchanged between cells which form gap junctions (Finbow and Pitts, 1981). Gap junctions from homologous and heterologous cell populations show the same permeability characteristics.

Using mixed cultures of two different mutant fibroblast cell lines, one unable to synthesize purine nucleotides and the other unable to synthesize thymine nucleotides, under the conditions of the experiment Pitts et al. (1985) have calculated, as the mixture of the cells grow at the wild type rate, that the throughput, or flux, of nucleotides between cell pairs is greater than 10^7 nucleotides per second.

1.2.4 Functional and Structural Correlation

The demonstration of electrical coupling, a passive spread of charge between cells, indicates a specialized pathway between the cells: the electrical synapse is a functional and structural term. A specialized structure must be present between the contacting surfaces of the electrically coupled cells. Metabolic co-operation demonstrates that those structures responsible for the functional electrical synapse are capable of allowing the passage of inorganic ions and nucleotides. The identification of the structural basis for electrical and metabolic coupling is however dependent upon morphological techniques (section 1.1). A correlation must be shown before one can associate one particular structure, the gap junction, with the functional structure responsible for electrical and metabolic coupling.

Many studies have shown just such a correlation e.g. for electrical coupling in excitable cells, the mammalian heart (Dahl and Isenberg, 1980), and in non excitable cells, the mammalian liver (Meyer et al., 1980), for metabolic coupling in tissue culture (Gilula et al., 1972). Correlation with morphology and metabolic coupling is well documented by Finbow (1981).

This correlation of permeability with the presence of gap junctions is supported by the good agreement between the experimentally determined permeability limits and the structural studies (sections 1.1.3 and 1.2.2). It is now generally accepted that gap junctions are the sites of intracellular communication.

1.3 MODULATION OF GAP JUNCTIONAL PERMEABILITY

Gap junctional channels are usually said to exist in one of two distinct functional states: coupled (open) or uncoupled (closed). Permeability studies (section 1.2) have been used to try and characterize the transition (gating) between the coupled and uncoupled state and to investigate the cellular mechanisms involved in modulating gap junctional permeability.

Modulation of junctional permeability is caused by several treatments: rapid and large changes in transjunctional voltage; raising the intracellular calcium ion concentration; raising the intracellular hydrogen ion concentration; and the topical application of certain alkanols (heptanol and octanol) or retinoids (retinoic acid).

1.3.1 Voltage

The voltage dependence of gap junctional conductance was first discovered between the blastomeres of Xenopus and Fundulus (Bennett et al., 1978). Increasing transjunctional voltage, V_j , of either polarity, decreases the junctional conductance, G_j . Amphibia show the steepest fall in conductance for applied voltage. On this basis Spray et al. (1984) suggest that the voltage dependence of amphibian embryos could provide a possible mechanism for gating junctions during tissue differentiation.

Obaid et al. (1983) have reported a different type of voltage dependence for junctions between cell pairs isolated from the salivary gland of the arthropod Chironomus. The junctional conductance is strongly affected by the potential between the inside and the outside of the gap junctional channel, V_{i-o} . As the cell is

depolarized the conductance of the channel decreases.

Junctions between squid embryos have high junctional conductance and in this state show no voltage dependence. If the conductance is lowered, by decreasing the intracellular pH (intracellular pH also affects junctional conductance; see section 1.3.4), then a voltage dependence develops (Spray et al., 1984) which has the same properties as those described for the amphibian and Chironomus systems (i.e. conductance is V_j and V_{i-o} sensitive).

Not all gap junctions exhibit voltage dependence. Neyton and Trautman (1985) have described a system in which they claim to be able to make single channel recordings of the rat lacrimal gap junction. They show that in this case there is no voltage dependence: transjunctional current being linearly related to the transjunctional voltage. When spontaneous uncoupling does occur a voltage dependence develops. Current does not flow until the transjunctional voltage is less than -20 mV. No voltage dependence is found for junctions between mammalian heart and liver cells (Spray et al., 1984).

1.3.2 Changes in Calcium Ion Concentration

Changes in intracellular calcium ion concentration (pCa) have been shown to have structural (in vitro) and gating (in vivo) effects on gap junctions. The structural studies of Unwin and Ennis (1984) and Wrigley et al. (1984) show that isolated mammalian junctions undergo a defined change when pCa is decreased. The channel diameter narrows on the cytoplasmic face and the tilt angle of the connexon subunits is reduced (see section 1.1.4 and Fig. 1a). Calcium ions in this case must be acting directly on the junctional membrane, but the specific site of action (lipid or protein) is unknown. It is not known if this structural change in vitro is related to the in vivo gating mechanism.

The first documented example of experimentally induced uncoupling was due to the raising of the free, intracellular calcium ion concentration (Rose and Loewenstein, 1975). Using Fundulus blastomeres Spray et al. (1982) have perfused one of a pair of cells

with buffered calcium ion solutions, while maintaining intracellular pH. They also injected the other cell (intact) with calcium ions although the amount of calcium injected was not determined. The intact cell showed only a transient decrease in coupling. The perfused cell showed decreased coupling for as long as the pCa was suprathreshold, 3.53. Complete uncoupling occurred at pCa \sim 3. The uncoupling effect of calcium ions was fully reversible.

Uncoupling has been reported at lower calcium ion concentrations in other systems. Dahl and Isenberg (1980) observed uncoupling at pCa 5.4-4.4 in the mammalian heart, but they did not measure intracellular pH. The transitory nature of uncoupling after injection of calcium ions into intact cells indicates that the cell can rapidly restore its free calcium ion concentration. Spray et al. (1982) then go on to argue that because of this, the calcium ion concentration in the intact cell, of the perfused pair, would be lower than the calcium ion concentration in the perfusion solution. Thus, they conclude that: "the calcium ions directly affect the junctional membrane rather than crossing the junctions."

Similar effects of calcium ions on junctional permeability are reported in a wide variety of cell and species types but in arthropods there appear to be specific differences, possibly related to the different voltage dependences outlined above. Increases in calcium ion concentration shift the voltage-conductance curve such that smaller depolarizations are necessary to produce a similar decrease in junctional conductance (Obaid et al., 1983).

The pCa of the cytoplasm is \sim 7 in many vertebrate and invertebrate cells. Its concentration is tightly controlled as it is a known second messenger. The levels required to cause changes in junctional conductance are much higher than those found under physiological conditions. In liver cells, Charest et al. (1983) have recently shown that α -adrenergic agonists induce increases in intracellular calcium ions from pCa 6.7 to 6.2. Levels which are still well below those reported necessary for detectable changes in junctional permeability (between hepatocytes). Therefore it seems unlikely that calcium ions regulate junctional permeability in vivo under physiological conditions. However, Iwatsuki and Peterson (1978) have reported that high calcium ion concentrations may be

reached when pancreatic acinar and lachrymal acinar cells uncouple in response to secretagogues.

Asada and Bennett (1971) suggested that calcium ions may provide a mechanism whereby dead or damaged cells i.e. permeable to extracellular levels of calcium ($pCa \sim 2.6$), may uncouple to maintain tissue integrity. Another possible action for calcium ions is to provide a means whereby precursor particles to the junction, inserted in the plasma membrane but not yet incorporated into junctions, remain closed to prevent the leakage from the cell of small cytoplasmic components.

1.3.3 Changes in Hydrogen Ion Concentration

Many studies have shown a correlation between junctional conductance and intracellular hydrogen ion concentration (pH). As intracellular pH decreases so does junctional conductance (Turin and Warner, 1977, 1980; Rose and Rick, 1978).

Spray et al. (1982), under the same conditions as those describing the modulation of junctional permeability by calcium ions (see section 1.3.3), examined the effect of intracellular pH on junctional conductance in cell pairs derived from Fundulus blastomeres. Decreasing pH by one unit causes complete uncoupling and a change of 0.6 units (smallest measured) causes greater than 50% uncoupling. Using similar arguments as those used for the effects of calcium ions Spray et al. (1982) conclude that hydrogen ions act directly on junctional membrane.

The relationship between pH and junctional conductance found in fish and amphibian embryos can be fitted to a Hill plot, giving an apparent pK for channel closure of about pH 7.3. The Hill coefficient is between 4 and 5, indicating moderate co-operativity. Similar Hill plots can be prepared from measurements made in Purkinje strands from mammalian heart (Reber and Weingart, 1982) and more recently in mammalian liver (Spray and Hertzberg, 1985). The pK values range between 6.4-6.9 with Hill coefficients varying from 1 to 8. Such pH values (6.4) are probably outwith the physiological range, but Spray et al. (1985) report that in pathological

conditions e.g. the ischaemic heart, pH values may be reached which uncouple the junctions.

Of the three potential physiological mechanisms for junctional modulation outlined above, only the lowering of intracellular pH appears to be universal. However as Turin (1985) says: "... it is difficult to even think of something less specific than the hydrogen ion in its interactions with cell constituents."

Despite the non-specificity of action of the hydrogen ion Spray et al. (1984, 1986) show that pH and voltage act independently in amphibian embryos. During acidification, to reduce junctional conductance, voltage sensitivity of the remaining conductance is unchanged, indicative of two distinct gating mechanisms. Voltage dependence of junctional conductance is thought to be due to a dipole moment change associated with a conformational change between the open and closed states, and the pH dependence due to changes in the local electric field causing conformational changes. This contrasts with the invertebrate Chironomus system where both voltage and pH act on the junctional conductance, in a manner consistent with one gating mechanism. Calcium ions are believed to act on the same site as hydrogen ions but with less affinity, thereby explaining the increased levels required for uncoupling (Spray et al., 1982).

1.3.4 Neurotransmitters

Permeability can also be modulated in vivo. For example at the electrical synapse, chemical neurotransmitters change the conductance of the nonjunctional membrane, thereby changing G_j (Spira and Bennett, 1972). This is an indirect form of modulation but recent investigations into electrical synapses between the horizontal cells of turtle retina have shown that dopamine modulates junctional permeability directly. Using electrical coupling and dye transfer to monitor coupling, Neyton et al. (1985) showed that dopamine, and pharmacological agents which produce an increase in intracellular cAMP levels, decrease the junctional permeability.

Similar effects have been observed between the horizontal cells of fish (Laseter and Dowling, 1985).

1.3.5 Alkanols

In 1980 Johnston et al. reported that octanol effectively and reversibly uncoupled crayfish axons. Since then many more cell types have been shown to uncouple in the presence of octanol e.g. amphibian embryos (Spray et al., 1984), mammalian heart muscle cells (Wojtczak, 1985) and stomach epithelial cells (Bernardini et al., 1983).

It is documented (Haydon et al., 1984) that hydrocarbons produce increased thickness of lipid bilayers, and so it may also be true of alkanols with long (7-8 carbon) hydrocarbon chains. Such thickening may cause junctional uncoupling. Seedman (1972) noted that two types of anaesthetics, neutral and positively charged, caused membrane expansion yet Wojtczak (1985) found that only the neutral anaesthetic caused junctional uncoupling. Wojtczak (1985) also showed that while octanol and octanoic acid caused uncoupling, only octanol was fully reversible. Wojtczak (1985) has speculated that this non-reversibility of octanoic acid on junctional conductance could be due to the terminal carboxyl group interacting with the hydrogen bonds in the outer bilayer of the membrane and thus disrupting the junctional membrane sufficiently to cause uncoupling.

1.3.6 Gating of the Gap Junctional Channel

Every ion channel in excitable cells that has been studied so far has one thing in common: it operates in an all or none fashion (Bennett et al., 1981; Hille, 1984).

Rose et al. (1977) suggested the possibility of transitions between open states that differ in effective pore diameter. Upon specific investigation of this point Zimmerman and Rose (1985) analysed the kinetics of fluorescent tracer diffusion through gap

junctions in Chironomus salivary gland cells. Changes in the relative flux rates of different sized tracers through the junction, at various levels of coupling, indicated that the channel had two states: open or closed. The degree of coupling appears to be dependent on the number of open channels within the whole gap junction (Zimmerman and Rose, 1985).

In response to the hormone hydroxy-ecdysone Safranyos and Caveney (1985) showed that the diffusion rates of carboxyfluorescein (Mr 371) and lissamine rhodamine B (Mr 559) when co-injected into Tenebrio melitor epidermis both increased by 33%. The ratio of their diffusion coefficients remained constant. The increase in permeability occurs in the absence of protein synthesis and a detectable change in gap junctional morphology, as judged by freeze fracture electron microscopy (Berdan and Caveney, 1985). For more definitive results, as the two tracers are of similar size, and their relative rates of flux may not change detectably in response to a graded opening of the channel, the relationship was tested between inorganic ions and organic tracers. The relationship between ionic and dye coupling remains constant over a threefold range in coupling (Caveney and Safranyos, 1985). This supports the general conclusion that the channel opens or closes in an all or none fashion. It implies that changes in permeability are due to changes in the fraction of open channels.

Neyton and Trautmann's (1985) recording of single channels show several unusual properties. The channel has a mean open time of 2 seconds, a long time when compared to other membrane channels. The transitions between open and closed states are slow, several tens of milliseconds. These slow transitions could perhaps explain the states of conductance sometimes observed, which are lower than that of the fully open channel.

Neyton and Trautmann (1985) also noted larger conductance jumps than 120 pS, some in the region of ~ 2500 pS suggestive of groups of channels acting co-operatively. Thus, it may be that the transition from coupling to uncoupling occurs in steps, which reflects on the number of channels acting co-operatively to modulate the permeability of the gap junction.

1.3.7 Functional and Structural Correlation

A number of investigators have tried to correlate gap junctional particle packing with functional coupling. For example, Kistler and Bullivant (1980), have used the change in morphological appearance of gap junctions, judged by freeze fracture, as an indicator of their functional state. Coupled junctions are suggested to have particles arranged in loose arrays, while the particles of uncoupled junctions are in ordered or crystalline arrays. Crystalline junctions have also been found in tissues treated with agents which uncouple (pH, pCa) in crayfish (Peracchia and Dalhanty, 1976) and mammalian heart (Baldwin, 1979; Dahl and Isenberg, 1980). Perrachia (1977) has proposed that crystallinity and reduced centre to centre spacing of the connexon particles is correlated with functionally uncoupled gap junctions and that this change in particle packing causes the change in permeability.

Most of the morphological studies correlating structure with the physiological state of the junction have used glutaraldehyde for fixation. Glutaraldehyde is known to uncouple gap junctions (Bennett, 1973), but this may not be as important as the time taken to fix the tissue. Those tissues which have been rapidly frozen, less than two seconds, may indicate a more accurate correlation between functional state and morphological appearance.

Using this technique Green and Severs (1984) showed that in the mammalian heart, quick frozen in situ, the junctions were always crystalline in appearance. Raviola et al. (1980) have shown a variety of particle arrangements upon uncoupling. Hanna et al. (1984) show no differences between coupled and uncoupled junctions in the tunicate heart, both showed random particle packing. They noted that when tissue was left in uncoupling medium for 1.5 hours and then rapidly frozen the junctional particle packing became crystalline. Evidence contrary to Perrachia's (1977) hypothesis that structural organization determines functional state.

From these investigations it can be concluded that the physiological state of the junction should be determined by direct functional criteria, such as those provided by the techniques outlined in section 1.2.

1.4 THE FUNCTION OF GAP JUNCTIONS

Just as the structure of the gap junction forms the framework or constraints for permeability, the permeability characteristics of the gap junction provide constraints on their possible function. Only those molecules which traverse the channel can be "effectors" in junction mediated interactions. The evidence for the functional roles of gap junctions is correlative, as at present no "effector" molecules have been unambiguously identified and there are no treatments which exclusively modulate the permeability of the gap junction.

The distribution, temporally and spatially, of gap junctions and the consequences of their permeability, form a basis for an analysis of their function.

Gap junctions could merely be passive conduits for small cytoplasmic molecules. However, other putative roles for the gap junction have been suggested e.g. tissue homeostasis and the regulation of cell growth and differentiation (Sheridan, 1976; Furshpan and Potter, 1968; Loewenstein, 1979).

In excitable tissues their function is the transmission of action potentials as well as, perhaps, some or all of those functions carried out by gap junctions in non-excitable tissues i.e. they may serve a dual function.

1.4.1 The Ubiquity of Gap Junctions

Gap junctions are found throughout the animal kingdom, from hydra (Hand and Gloebel, 1972) to hamster (Yancey et al., 1982) to human (Garfield and Hayashi, 1982). (There are functional equivalents in the plant kingdom called plasmodesmata, Gunning and

Robards, 1976.) As well as being ubiquitous within the animal kingdom they are present in most tissues. Indeed, the large number of morphological studies carried out to date suggest that virtually all normally dividing cells of complex differentiated animals are able to form gap junctions. It appears that only a limited number of terminally differentiated cell types lose coupling ability. For example some circulatory cells (e.g. red blood cells and lymphocytes), many nerve cells, and skeletal muscle cells. This widespread distribution suggests that gap junctions have important roles to play.

The ability to form gap junctions is retained by many cells in tissue culture (Revel *et al.*, 1971; Gilula *et al.*, 1972). In tissue culture gap junctions show little species specificity. Cultures of mammalian cells form junctions with other mammalian cells and cells from different classes; avian, amphibian and fish (Pitts, 1977). However mammalian cells only rarely, if ever, appear to form gap junctions with arthropod cells (Epstein and Gilula, 1977). This particular lack of communication may correlate with the differences shown by morphological studies (section 1.1.2) and permeability studies (section 1.2.3). Alternatively the lack of communication may be related to the difficulty in co-culturing both vertebrate and invertebrate species in the one medium, as invertebrate cells do not grow well in vertebrate tissue culture medium.

Cases of specificity of junction formation have been reported. Hamster fibroblast cells (BHK 21/13) and Buffalo rat epithelial cells (BRL) always form junctions at homologous contacts but rarely at heterologous contacts (Pitts and Burk, 1976). Similarly breast epithelial cells and breast fibroblasts show greater homologous than heterologous communication (Fentiman *et al.*, 1976). In mixed culture this specificity is associated with "sorting out". Islands of epithelial cells are separated by fibroblasts, forming communication compartments (Pitts and Kam, 1985). This specificity has not been found in primary cell cultures, where primary epithelial cells communicate with primary fibroblasts and the established cell lines BRL and BHK (Hunter and Pitts, 1981).

This general lack of species and often tissue specificity in

tissue culture reinforces the view of functional conservation of gap junctions and perhaps more importantly the conservation at a structural level, at least of the gap junctional protein. A point which will be returned to in section 1.5.

1.4.2 Tissue Homeostasis

The metabolic co-operation assay described earlier (section 1.2.3) and the results of Sheridan et al. (1979) which showed that intermediate metabolites form common pools shared by all coupled cells in a culture, showed that coupled cell populations behave as metabolic units. This indicates a homeostatic role for the gap junction integrating and co-ordinating the control of cellular metabolic activity. This is probably one of the most basic physiological roles of gap junctions.

Another way of showing tissue homeostasis in cells is by measuring the electrical space constant. An extended array of cells connected by gap junctions will resemble a single elongated cell in an applied electrical field if electrically coupled. On the assumption that the extracellular resistance is comparable to the cytoplasmic resistance an equation can be derived where:

$$\lambda = \sqrt{(r_m / 2r_i)}$$

λ is the space constant, r_m is the membrane resistance, and r_c is the resistance of the cytoplasm.

If the cells were not equilibrated, with regards to the electrically permeant ions, then the space constant would be similar in size to that of the cell.

The salivary gland of Chironomus is composed of a linear string of about 20 cells each having a length of about 70 μm (Lowenstein, 1966). In Chironomus salivary gland the space constant is approximately 1 mm (Cooper, 1984); i.e. the population of cells is equilibrated as regards inorganic ions. From values of r_m , r_c , given in Berdan and Caveney (1985) on the epidermal cells of the beetle Tenebrio molitor the space constant is 1.4 mm. The cell

diameter is ~ 40 μm .

1.4.3 Chemical Carcinogenesis

It has been proposed that chemical carcinogenesis occurs via a two step initiation-promotion scheme. In this scheme initiators are believed to act on DNA as mutagens. Mutagenesis is rapid and irreversible, however it does not manifest itself in the form of a tumour (malignant cell growth) until the cells are promoted. Promotion of initiated cells can be brought about by several means but only one particular promotor, 4 beta phorbol-12 tetradecanoate-13-acetate, (TPA) shall be discussed here. The process of promotion is not as rapid as initiation and treatment with TPA has to be repeated many times.

Studies in tissue culture systems have indicated that the primary site of action of tumour promoters is the plasma membrane. TPA can cause increased membrane fluidity, altered cell adhesion and increased turnover of membrane lipids (Weinstein et al., 1979; Blumberg, 1980). There are also several reports that tumour promoters can inhibit junctional communication between Chinese hamster V-79 cells (Yotti et al., 1979), and epidermal and 3T3 cells (Murray and Fitzgerald, 1979) growing in tissue culture.

The inhibition of cell to cell communication could provide a mechanism for the promotion phase of the two step scheme outlined above (Newbold, 1981). A pre-malignant cell may be suppressed after initiation by gap junctional interactions with the surrounding uninitiated cells. The initiated cell may only become malignant if the maintenance of the "normal" phenotype by surrounding cells is interrupted.

Hartman and Rosen (1985) have shown that a one minute exposure to TPA is sufficient to inhibit metabolic co-operation between V-79 cells. This is considerably shorter than the original 79 h exposure described by Yotti et al. (1979). The dose response curve of inhibition against TPA concentration obtained by Hartman and Rosen (1985) is biphasic. The rise in the curve is linear from 0.1 ng/ml to 1 ng/ml and then levels off at maximal inhibition, until the

concentration of TPA reaches 1000 ng/ml. At this point it begins to decrease slightly. Similar dose response effects have been described by Dorman and Boreiko (1983), although they used much longer exposure times. It is important to note that at no concentration was TPA able to completely inhibit metabolic co-operation. The shape of the curve seems to indicate that some cell activity is either fully inhibited or fully excited at TPA concentrations of about 100 ng/ml and this change in activity then acts to inhibit gap junctional communication.

Enomoto et al. (1981) examined the effects of TPA on electrical coupling in FL epithelial cells derived from human amniotic membrane. When 100 ng/ml of TPA was added to the culture the percentage of coupled cells decreased to 6% compared to 89% in controls. Enomoto et al.'s (1981) dose response curve is similar to that described by Hartman and Rosen (1985) but at 1 ng/ml TPA, little uncoupling was observed. This concentration has a marked effect when assayed by metabolic co-operation, a reflection perhaps on the sensitivity of this assay of junctional communication.

Cells incubated with TPA for 24 h during which time cell coupling remained suppressed, showed that coupling returned to control levels within 4 h of removal of TPA (Enomoto et al., 1981). Similar effects have been reported for 3T3 cells (Yamasaki and Enomoto, 1985) and V-79 cells (Pitts and Burk, 1986).

The effect of TPA on junctional communication could be twofold, either it acts on the formation/removal of gap junctions and/or it modulates the permeability of the gap junctions already within the membrane. It seems that Hartman and Rosen (1985) and Enomoto et al. (1981) are showing different mechanistic effects on gap junctional communication. A one minute exposure followed by culture for a further 140 h (assay time) could be investigating the long term effects (Hartman and Rosen, 1985 i.e. junctional turnover). Whereas Enomoto et al. (1981) are analysing short term effects, i.e modulation of permeability. The two may therefore not be comparable.

Yancey et al. (1982) have shown that V-79 cells incubated with 10 ng/ml of TPA for 16 h caused a 95% decrease in morphologically detectable gap junctions, as examined by freeze fracture electron

microscopy. It is not possible to say from these results, whether the TPA effect is a result of reduced capability to form and/or maintain gap junctions. A recent study by Pitts (1986) ^{by Pitts} suggests that TPA does act by reducing the ability of cells to form and maintain gap junctions. It is interesting that as in the metabolic co-operation and electrical coupling experiments described above, the number of junctions seen by freeze fracture morphometry did not fall to zero.

Another effect of tumour promoters, including TPA, not mentioned previously is that they are potent activators of protein kinase C and are believed to act like the physiological activator diacylglycerol (DG). DG increases protein kinase C's affinity for calcium ions bringing the calcium ion requirement down to physiological levels pCa 6 (Nisizuka, 1986). Could a similar mechanism apply for increasing the gap junctional proteins affinity for calcium ions? and thereby allow modulation of junctional permeability at physiological calcium ion concentrations.

Studies by Davidson et al. (1985) have shown that protein kinase C may have an effect upon junctional communication. Inhibitors of protein kinase C, chlorpromazine and trifluoperazine, showed antagonistic effects to TPA, in their presence TPA did not inhibit junctional communication to the same extent as when they were absent. Further evidence for protein kinase C having an effect on junctional permeability is that the addition of a synthetic analogue of DG, 1-oleoyl-2 acetyl glycerol (OAG), causes inhibition of junctional communication. Gainer and Murray (1985) have shown that OAG inhibits gap junctional communication in cultured epidermal cells.

A further possibility which appears in Davidson et al.'s (1985) report is that TPA increases membrane permeability to calcium ions, which is a known modulator of junctional permeability (see section 1.3.2). In the absence of extracellular calcium, TPA inhibition was less pronounced. At odds with this was the finding that in the presence of 1 mM extracellular calcium and the calcium ionophore A23187, synergism with TPA could not be demonstrated.

It is clear that TPA is having an effect upon junctional communication. Indeed all known tumour promoters to date have an

inhibitory effect upon metabolic communication. Metabolic co-operation is now an assay to test chemicals for their tumour promoting ability (Trosko et al., 1984).

1.4.4 Tumourgenesis

The scheme outlined above involves gap junctions in a way which means that they are not involved as a primary event of transformation. However, Loewenstein (1968) hypothesized that gap junctions control cell proliferation directly. He suggested, on the basis of lack of cell coupling between certain tumour cells (Loewenstein and Kanno, 1967), that their absence causes abnormal, unregulated cellular growth i.e. tumours. Further studies however, showed that cell coupling was present in some tumour cells (Sheridan, 1970). These studies were merely addressing the question of whether gap junctions are present or absent in particular tumours. Quantitative studies and the development of model systems in tissue culture have enabled the questions to become more refined. Are changes in gap junctional permeability a causitive factor in tumourgenesis?

One model system which has been used to try and answer this question is that of Atkinson et al. (1981). Cells were transformed with a temperature sensitive mutant of the src gene of Rous sarcoma virus (RSV). The advantage of using a temperature sensitive mutant is that transformation can rapidly be induced by temperature shifts.

Normal rat kidney cells (NRK) infected with the RSV mutant (LA 25) show reduced junctional permeability, as judged by Lucifer Yellow dye transfer, when changed from 40°C to the transformation permissive temperature of 35°C. The changes in junctional permeability respond quickly, over a time course of 15 min, to the temperature shift. The temperature effect is reversed with a similar time course by switching the cells back to the original growth temperature. Atkinson et al. (1986) have analysed gap junctions from NRK and LA 25-NRK cells at permissive and non permissive temperatures by freeze fracture electron microscopy. They found that the number and size of the junctions do not change

in conjunction with the changes in junctional permeability. They conclude that junctional permeability is being changed by direct modulation of existing channels.

As an aside, they also report that the particle packing order increases in the non transformed state i.e. higher junctional permeability. Further evidence for the difficulty in predicting the state of coupling from junctional morphology (see section 1.3.4).

Azarnia and Loewenstein (1984) have extended these findings by showing that quail embryo, chick embryo, and mouse 3T3 cells, infected with a similar temperature sensitive mutant of RSV, all showed decreased junctional permeability when grown at the permissive temperature. Azarnia and Loewenstein (1984) also showed that the change in junctional permeability was not due to protein synthesis as cycloheximide did not prevent the increase in permeability when the cells were shifted to the non permissive temperature.

These results and the studies on the effects of tumour promoters are supportive of the general view that reduced junctional communication and cell transformation are correlated. There is at present though no unequivocal evidence that communication through gap junctions is involved directly with the control of cell proliferation.

1.4.5 Gap Junctions in Parturition

A good example of temporal distribution of gap junctions is found in uterine smooth muscle. Smooth muscle is divided into two physiologically distinct types: multi-unit and single unit. As the names imply multi-unit smooth muscle acts as though made up from many units. Single unit smooth muscle functions synchronously.

One theory for parturition, as defined by Garfield *et al.* (1978), which relates to gap junctions is described below. However, the cause for parturition has not been determined unequivocally. Some workers believe that the foetus signals the uterus to contract.

At parturition the uterine smooth muscle undergoes a change

from multi-unit to single unit, which enables strong, regular, and synchronous contractions to expel the foetus. The switch from multi-unit to single unit is closely associated with the development of large numbers of gap junctions between the myometrial cells. In rats gap junctions are present in low frequency and small size in non pregnant, preterm and postpartum animals. In pregnant animals, the junctions begin to form prior (0-24 h) to the start of labour (Garfield et al., 1977). In vitro electrical coupling studies (Sims et al., 1982) have shown improved electrical coupling with the concomitant rise in the number of gap junctions.

In contrast, Zelcer and Daniel (1979) have shown that there is no increase in electrical coupling between preterm and term tissue but have noted a significant degree of coupling in the non pregnant uterus despite the low occurrence of gap junctions, as judged by electron microscopy.

Parturition is believed to be due to the progesterone concentration falling below the threshold level required to suppress contraction. Garfield et al. (1977) have therefore administered progesterone to rats and shown that parturition does not occur, but neither does the rapid development of gap junctions. Garfield et al. (1977,1978) suggested that the onset of labour was due to the development of gap junctions and that progesterone inhibited their formation.

1.4.6 Gap Junctions in the Ovary

In the ovary of mammals the germ cell, the oocyte, is surrounded by an acellular layer of protein and mucopolysaccharide, the zona pellucida. The zona pellucida is in turn surrounded by granulosa cells. Neither the oocyte nor the granulosa cells are in direct contact with any capillaries. Gap junctions are believed to be required for the transfer of nutrients to the oocyte and the control of maturation (Dekel et al., 1981).

In vivo mammalian oocytes, which are non atretic, are arrested in the first meiotic division. A preovulatory gonadotrophin surge releases the oocyte, usually one but sometimes

two, from meiotic arrest.

In vitro, when oocytes are isolated from the granulosa cells they undergo spontaneous meiotic maturation, this occurs in the absence of hormones, and they then progress through meiosis until the second metaphase (Pincus and Enzmann, 1935). These observations have led to the hypothesis that the follicular environment inhibits oocyte maturation until the preovulatory surge of gonadotrophins (Pincus and Enzmann, 1935).

Gap junctions were first shown between the oolemma and the granulosa cells by Anderson and Albertini (1976). Gilula et al. (1978) showed that these gap junctions, formed from heterologous cells, were functional by electrical coupling and dye transfer studies. Moor et al. (1980) showed the transfer of tritiated metabolites derived from choline, uridine and inositol.

Both Gilula et al. (1978) and Moor et al. (1980) noted that communication was constant just prior to ovulation. Gilula et al. (1978) showed that the granulosa cell processes retracted from the oolemma prior to ovulation and thus uncoupled. But Moor et al. (1980) found that whilst a marked decrease in functional coupling occurs it is not complete.

These observations suggested the possibility that the maintenance of meiotic arrest and the level of coupling between oocyte and granulosa cells might be correlated. Based on Gilula et al.'s (1978) observation, Dekel and Beers (1981) suggested that it is the termination of coupling and therefore a loss of transmission of an inhibitory substance which allows maturation.

Moor et al. (1980) on the other hand proposed that it is a quantitative or qualitative change in the signal communicated to the oocyte through gap junctions, which allows maturation, as coupling markedly but not completely decreased before ovulation.

A further possibility is that gap junctions merely breakdown after the "signal" for maturation to resume has reached some suprathreshold value as part of the maturation process.

Other studies though suggest that junctional communication is not involved in oocyte maturation. Eppig (1982) has followed junctional communication at various stages before and after oocyte maturation in mice, induced by injection of human gonadotrophin.

Oocyte maturation occurred in advance of any change in granulosa-oocyte coupling.

Recently Canipari et al. (1984) have cultured mouse oocytes, which cannot mature, in the presence of fibroblast monolayers and fibroblast conditioned media. They found that the number of days in culture and the age of the donor cell amounted to 15 days before isolated oocytes resumed meiosis. In vivo 15 days of age represents the time at which growing mouse oocytes, belonging to the first wave of growing follicles, first acquire the competence to mature. Thus the oocytes follow the same developmental time program in vitro as they do in vivo. Canipari et al. (1984) conclude that the ability to mature is based on a definitive time program which is independent of: (i) the presence of surrounding granulosa cells (ii) the existence of heterologous gap junctions [follows from (i)] (iii) the maintenance of normal growth as oocytes in culture do not grow in size as they do in vivo.

It appears most likely therefore that gap junctions are present to enable the passage of nutrients from the granulosa cells to the developing oocyte providing metabolic support rather than being involved in signal transduction.

1.4.7 Conclusions

The above discussion has focused upon a variety of putative functions for gap junctional communication and how they might be involved in controlling and coordinating growth and differentiation in complex organisms. To further delineate the functions of gap junctions a means of either specifically interrupting or controlling gap junctional communication is required. One possibility to do this is by using antibodies directed against the junctional protein. Such antibodies to the putative junctional proteins will be discussed in section 1.5. The injection of antibodies, directed against the junctional protein, into cells may be one way of perturbing cell to cell communication specifically. Experiments along these lines will be described in the Discussion.

1.5 PROTEIN COMPOSITION OF GAP JUNCTIONS

Identification of the gap junctional structural protein is a prerequisite for any complete analysis of the functional role of gap junctional communication.

Plasma membrane preparations made by modifications of Neville's (1960) procedure have been used as a starting point for gap junction fractionation from three major sources: lens, liver and heart.

1.5.1 The Lens Fibre Protein

In the vertebrate lens there are two major cell types: epithelial and fibre. Bendetti et al. (1976) observed that the lens fibres are joined by extensive gap-junction like structures. These structures are similar but not identical to those found in the liver (see section 1.1). By freeze fracture electron microscopy loosely packed intramembranous particles are observed ~ 8-9 nm in diameter (Benedetti et al., 1976; Peracchia, 1978), which are similar in size to the connexons found in the liver. However, in thin sectioned material fibre-fibre junctions do not reveal a gap (Fitzgerald et al., 1983) and appear as pentalaminar structures of 16-17 nm overall thickness (Zampighi et al., 1982). Other junction structures are also found which consist of "orthogonal arrays" of particles (Kistler and Bullivant, 1980; Zampighi et al., 1982). In thin section they also have no gap but are thinner with an overall thickness of 12-13 nm (Zampighi et al., 1982).

The epithelial cells are joined to one another by small gap junctions similar in appearance to those found in other tissues (Goodenough, 1979). Fibre cells are functionally coupled to each

other and to coupled epithelial cells (Miller and Goodenough, 1985).

Miller and Goodenough (1985) have produced evidence that there are two physiologically distinct gap junctions in the embryonic chick lens. Bathing the lens in 90% CO₂-equilibrated media causes a decrease in junctional permeability as judged by fluorescent dye transfer. High CO₂ media blocks intra-epithelial dye transfer but not fibre to epithelial, nor fibre to fibre dye transfer.

On the basis of the quantitative relationship between the lens fibre junctions and a 26K protein, which is the main protein component of isolated lens fibre membranes (and therefore referred to as major intrinsic protein, MIP 26) it was suggested that MIP 26 is the major protein component of lens fibre gap junctions (Benedetti et al., 1976) i.e. those structures which are similar to those found in the liver consist of MIP 26.

This view has recently been challenged by Zamphigi et al. (1982), and Paul and Goodenough (1983) as immunolocalization studies with antibodies directed against MIP 26 (Paul and Goodenough, 1983) show non-junctional staining. However, Bok et al. (1982) and Fitzgerald et al. (1983) have used similar techniques to Paul and Goodenough (1983) and have found evidence for MIP 26 throughout the plasma membrane, including localization to both thick and thin structures. Moreover, Sas et al. (1985) showed, with gold immunolocalization, the labelling of both types of junctions on their cytoplasmic faces, with a monoclonal antibody directed against bovine MIP 26.

At the present time therefore, there is no clear cut answer as to which protein constitutes the lens gap junction. A similar situation has recently developed in the identification of the liver and heart gap junctional protein(s).

1.5.2 The Liver Protein

High resolution imaging studies (see section 1.1.4) on liver gap junctions have indicated that the connexon is made up of six, probably identical, protein subunits. Each subunit with an estimated

mass, determined from the estimated volume, of ~ 20-30000 daltons. The resolution of the techniques is not sufficient to determine the exact molecular size, conformation of the protein within the membrane, or the number of polypeptides in each subunit.

The structural and functional studies (sections 1.1 and 1.4.1, respectively) indicate that the gap junction structure is highly conserved. The structural studies further show that the gap junctional structure is maintained even after treatment with detergents such as Sarkosyl (Goodenough and Stoeckenius, 1972), deoxycholate (Benedetti and Emmelot, 1968), Triton X-100 (Henderson et al., 1979), proteolytic enzymes such as collagenase and trypsin (Goodenough and Stoeckenius, 1972; Makowski et al., 1984; Casper et al., 1984), six molar urea (Finbow et al., 1983); and alkali solutions at pH 11 (Hertzberg, 1984).

Studies over the past fifteen years have produced a variety of putative gap junctional proteins varying in size from 10000 daltons (Goodenough, 1974) to 38000 daltons (Culvenor and Evans, 1977), as judged by SDS PAGE. However, today the majority of investigators accept that a protein of molecular weight 27000 daltons (27K) is the major structural constituent of liver gap junctions.

The 27K protein has been isolated by two different procedures. Both start with plasma membranes, one enriches for gap junctional areas (Hertzberg and Gilula, 1979; Henderson et al., 1979; Finbow et al., 1980) by the use of urea and detergents followed by purification on sucrose density gradients. The other, recently developed by Hertzberg (1984), enriches for gap junctions by extraction of plasma membranes with alkaline solutions (pH 11), again followed by purification on sucrose density gradients. This latter procedure has greatly increased the yield of the 27K protein: 30 rat livers give 3-4 mg of protein as compared to 200-300 µg. As Hertzberg (1984) starts with a plasma membrane preparation (10% recovery as judged by 5'-nucleotidase activity, Hertzberg and Gilula, 1979) his yield is equivalent to ~ 100 µg/g wet weight liver which is rather high.

Based on a maximum mass for each connexon of ~ 170,000 daltons (Unwin and Ennis, 1984); 180,000 connexons per hepatocyte (Revel et al., 1980; Meyer et al., 1981); and 2.4×10^8 cells/g wet weight

liver (Leslie, 1955) of which 80% are hepatocytes the theoretical yield is 10 µg/g wet weight liver.

1.5.3 Antibodies

Further characterization of the constituent protein in gap junctions has, in part, relied on raising antibodies against either gap junctional plaques or SDS PAGE purified protein. An immunological approach should provide direct evidence for a protein being of junctional origin whereas other approaches are only correlative (see section 1.2.5).

After initial failures antibodies have now been raised in several laboratories.

Traub et al. (1982) have raised an antiserum in rabbits against SDS PAGE band purified 26K mouse liver protein (the slightly different molecular weight ascribed to this protein is due to the use of different molecular weight standards). The antiserum has been used in immunoprecipitation studies to follow the quantitative changes of 26K protein after partial hepatectomy (Traub et al., 1983). The precipitable protein decreases to 15% of control values 28-35 hours after partial hepatectomy. This is in reasonable agreement with the earlier morphometric data of Yee and Revel (1979), and Yancey et al. (1979) which shows that the gap junctional plaques decrease to 1.7% of control values 28-36 hours after partial hepatectomy.

The anti-26K antiserum has been used in gold immunolocalization studies (Janseen-Timmen et al., 1983). The antiserum has been used to localize the 26K protein to isolated gap junctions both in thin sections and negative stained preparations by Protein-A gold. However, antibody binding to gap junctional plaques in plasma membrane preparations was less than that to gap junctions. Purified plaques bound 1176 +/- 276 gold particles / µm² using anti-26K antiserum and 39 +/- 24 gold particles / µm² using preimmune serum. In plasma membranes native gap junction plaques the binding was much reduced, the number of gold particles / µm² for anti-26K antiserum was 401 +/- 104. This compares to the preimmune of 193 +/- 64

particles/ μm^2 .

The 26K protein polyclonal antiserum has been affinity purified against total SDS soluble proteins from a mouse liver gap junction preparation (Dermietzel et al., 1984b). The affinity purified antibodies bind to 26K proteins in immunoblots from liver, pancreas, and kidney. However, the immunoblotting data is dubious as there is binding to a variety of other bands as well as a band at 26K. The antibodies have also been shown to bind to mouse liver and pancreas gap junctional plaques seen in ultrathin frozen sections using Protein-A gold immunolocalization studies (Dermietzel et al., 1984b).

Dermietzel et al. (1984b), have also used the affinity purified antibodies to examine the distribution of the 26K protein by immunofluorescent cytochemistry. They showed discrete spots in mouse pancreas, kidney, and small intestine from both mouse and rat. It does not however stain the rat myocardium, a tissue known to be rich in gap junctions.

This last result contrasts with data of Hertzberg and Skibbens (1984). Their antiserum was raised in sheep against whole rat liver gap junctions and was affinity purified against total SDS soluble proteins in this preparation.

Using immunoblot analyses Hertzberg and Skibbens (1984) showed that their affinity purified antibodies bind to a 27K protein in liver extracts from mouse, human, monkey, rabbit, sheep, goldfish, and chicken. The antibodies also bind to a 27K protein in extracts of rat pancreas, stomach, heart, kidney, brain and adrenal gland. In addition the antibodies also bind to a 30K protein from rat, mouse, rabbit and sheep liver when the tissue extract is boiled for 2 mins in SDS prior to electrophoresis. Similarly treated extracts of chicken, human, goldfish and monkey show no labelling. The antibodies react with the 47K dimer of the 27K protein, which is increased in abundance by boiling in 1% SDS, in all rat tissues except heart and stomach.

Paul (1985) has reported on an antiserum raised in rabbits against whole calf liver gap junctions and affinity purified against SDS PAGE band purified 27K protein from calf liver. In immunoblot studies the affinity purified antibodies do not bind to any proteins

from whole tissue homogenates of calf liver, kidney, heart or pancreas. However, they do bind to a 27K protein from isolated liver junctions. If extreme precautions are taken to prevent endogenous proteolysis, such as keeping the tissue frozen with liquid nitrogen, then the affinity purified antibodies bind to 27K, 47K and 54K proteins in whole tissue homogenates of pancreas but not heart.

In common with Paul (1985), Warner et al. (1984) describe two antisera raised in rabbits against the SDS PAGE band purified 27K protein from rat liver which cross react with a 54K protein as well as the 27K (and 47K dimer) putative junctional protein. Cross reactivity, by immunoblotting, is shown against all these proteins in tissue homogenates from rat liver and also unfertilized Xenopus eggs. In homogenates of Xenopus embryos at the eight cell stage, reactivity is only detected against the 54K protein. This is unexpected because gap junctions are not present in unfertilized eggs and only develop at the 8 cell stage of embryogenesis. The disappearance of the reactivity against the 27K and 47K proteins between the egg and the eight cell stage does not fit the explanation provided by Warner et al. (1984) that " all material necessary for progression through development to the blastula stage must, therefore, be available in the unfertilized egg. This would include the production of gap junctions...".

Both Paul (1985) and Warner et al. (1984) argue that the 54K protein maybe a precursor to the 27K gap junctional protein because the 54K protein shares common antigenic sites with the 27K, although neither the antisera of Hertzberg and Skibbens (1984) nor Traub et al. (1982) detected a 54K protein. This could be due to failure to take necessary precautions against endogenous proteolysis.

Using his antiserum affinity purified against the rat liver 27K protein, Paul (1986) has isolated a rat liver cDNA clone, from a cDNA expression library in lambda gt11. This 1494 bp cDNA codes for a protein with a molecular weight of 32007 daltons which has the same N-terminal sequence as the 27K protein (determined by Nicholson et al., 1983). From this it is clear that there cannot be a "precursor/product" relationship between the 54K protein and the protein encoded by the cDNA clone. Northern blot analyses indicate

that brain, kidney and stomach also express an mRNA of similar size and sequence to the rat liver mRNA but heart appears to only express a smaller mRNA (1.3 kbp) which can only just be detected at low stringency of hybridization.

A puzzling feature of the antisera described above (excluding that of Warner et al. (1984) which has not been tested), is that they all, when used for immunofluorescent histochemistry, show punctate spots on liver tissue sections which appear to exceed both the size of individual junctions and the junctional area per cell of that particular tissue. The area of plasma membrane in a liver cell occupied by gap junctions measured by morphometry of freeze fractured samples is ~ 2-3 % (Meyer et al., 1981). A 10 μ m section through a cell could only reveal a percentage of this 2-3% yet quite clearly the immunofluorescence is covering a large area (e.g. ~ 20 % Dermietzel et al., 1984b) of the cytoplasmic surface of the cell membrane.

As described earlier, most attempts to isolate the junctional protein have started by preparing enriched fractions of the plasma membrane because gap junctions are plasma membrane organelles.

More recently Finbow et al. (1983) have isolated gap junctions on a different basis, namely that they are one of the few organelles not associated with the cytoskeleton. Tissue culture cells and tissue homogenates are solubilized in 1% Triton X-100, 0.15 M NaCl and centrifuged at low speeds (3000 rpm) which separates gap junctions and soluble cytoplasmic components from the remainder of the cell which stays intact. As with the other isolation procedures the junctions are further purified by their resistance to Sarkosyl and 6 M urea with a final sucrose density centrifugation step.

This method gives preparations containing a single Coomassie staining band, after analysis on SDS PAGE, running at 16000 daltons (16K). When a trypsin treatment step is included in the method (at the urea extraction step) the junctional purity is increased as judged by electron microscopy after negative staining but it does not change the gel profile (Finbow et al., 1983).

Further biophysical characterization showed that those fractions which contained identifiable gap junctions after centrifugation of the final preparations to equilibrium on potassium iodide isopycnic gradients (bouyant density 1.195 g/cm³) also contained the 16K protein (Finbow et al., 1983).

Hertzberg and Gilula (1979) reported a bouyant density value for gap junctions, determined in the more viscous medium of sucrose, as 1.165 g/cm³. Fractions from these gap junctions contain a major Coomassie staining band at 27K. Intuitively one would expect the values to be the other way around, the larger protein having the greater density. The actual result could be due to either non-equilibrium in the more viscous sucrose, or the lipid content of the Hertzberg and Gilula (1979) junctions is greater.

Finbow et al. (1983) have also carried out a similar study to Traub et al. (1983) and obtained similar results. After partial hepatectomy the area of gap junction decreases by 98.3% between 28 and 36 hours after the operation. Finbow et al. (1983) showed that the recoverable protein decreases by 90%, 30 hours after the operation. (Traub et al. 1983, showed an 85% decrease).

In a quite different system the gap junctional area has been shown to decrease (reversibly) by 93% after the application of TPA to V-79 chinese hamster lung cells in culture and Finbow et al. (1983) reported a 90% (reversible) decrease of recoverable 16K protein.

Correlative studies on the morphology and corresponding protein profiles, as gap junctions are progressively solubilized in SDS solutions of increasing concentration, show that the gap junction structure disintegrates over the 0.1-0.3% SDS range with the directly concomitant appearance of the 16K protein in the soluble fraction (Finbow et al., 1983).

Finbow et al. (1984) described an antiserum raised in rabbits against intact chicken liver gap junctions. The crude polyclonal antiserum recognizes the 16K proteins from chicken and mouse liver gap junctions and an 18K protein from Nephrops norvegicus (lobster) hepatopancreas gap junction. The antiserum has been affinity purified against SDS PAGE purified mouse liver 16K protein and

Nephrops 18K protein. The affinity purified antibodies recognize the chicken and mouse 16K proteins and the Nephrops 18K protein.

Biophysical characterization of the isolated arthropod gap junctions shows the junctions have a higher bouyant density in potassium iodide gradients, as might be predicted, of 1.260 g/cm^3 . However junctions isolated with a trypsin treatment step, unlike the mouse liver junctions, show a change in bouyant density to 1.245 g/cm^3 . This corresponds to a loss of approximately 5% of the protein. The change in bouyant density is not reflected in an altered SDS PAGE profile. The arthropod gap junctions are solubilized in SDS in the 0.1-0.2% range (compared to mouse gap junctions, 0.1-0.3% SDS).

Recently Van Eldik et al. (1985) have isolated gap junctions from crayfish hepatopancreas. They isolated two proteins, by a triton method similar to Finbow et al. (1984) of 16K and 17K. Even though the two bands have been assigned slightly lower relative molecular weights one may be the same protein as that described by Finbow et al. (1984), as calculating the molecular weights of proteins by SDS PAGE can vary depending upon which markers are used as standards. However further characterization of these proteins is needed before "relatedness" can be established.

The above discussion shows that there are still difficulties in ascribing a particular protein to the gap junction structure. The different results of the various laboratories could be explained in several ways.

One explanation is that each laboratory is isolating a particular type of gap junction. Close examination of the electron micrographs does not support this view, although minor structural variations may not be apparent at this resolution. Furthermore this contention could only hold if the different methods of junction preparation somehow resulted in different classes of gap junctions being isolated on the basis of these (unknown) subtle differences.

Another explanation could be that the two proteins are present in the same structure but that the isolation procedures remove one component at the expense of the other. There may be some support for this view as junctional preparations have been isolated which

contain both 16K and 27K proteins (Finbow et al., 1986). Hertzberg (1985) has reported that the antisera raised against gap junctions prepared in his laboratory recognize a 16K component in a gap junction preparation from Finbow et al.'s laboratory.

Similarly, samples of gap junctions prepared by Hertzberg and Traub, both of which contain the 27K (or 26K) protein as a major Coomassie staining band, show a 16K band by immunoblotting with the antiserum raised against chicken gap junctions (Finbow et al., 1986). The explanation of both proteins in the gap junctional structure might be resolved by using double label gold immunolocalization studies as one antiserum has been raised in sheep and another in rabbits. In contrast to this explanation, preparations from rat or mouse have not been found to contain any detectable 27K protein by immunoblotting (Finbow et al., 1986).

A further explanation maybe that the two proteins are in someway related i.e. 16K is a proteolytic fragment of 27K. However, extensive peptide mapping studies (Finbow et al., 1986) show no common tryptic peptides between the two proteins. The recent published sequence deduced from cDNA, coding for the 27K protein, (Paul, 1986; Kamur and Gilula, 1986) also shows that the partial 16K protein sequence available (50 amino acids) is not present in the 27K protein. These two findings rule out any arguments for a precursor/degradation product relationship.

1.5.4 Models of Putative Gap Junctional Proteins

The primary structure of the 27K liver protein as deduced from the cDNA can be used to predict the secondary and tertiary structure of the protein. Such predictions cannot define the function nor establish its identity as a gap junctional protein. They can be used to devise experiments to test any models produced by the predicted structure and compare the results to those found using isolated plaques.

A hydrophobicity plot (Paul, 1985) shows four major hydrophobic regions, which have predicted beta pleated-sheet

secondary structure. If these four regions are assumed to be transmembrane then two models for their arrangement are possible. One has the C-terminus on the cytoplasmic face (model one), which had previously been proposed by Nicholson *et al.* (1981). The other has the C-terminus on the extracellular face (model two). The N-terminus is buried within the membrane (see below) and so the path of the polypeptide can either be towards the cytoplasm or the extracellular compartment.

Protease studies on isolated junction plaques, where only the cytoplasmic domains are accessible, should show agreement with one of these models, if 27K is the gap junctional protein. If trypsin is used, then with model one two major fragments should be produced: ~ 10000 and 8400. With model two then three major fragment should be produced: 12000, 4800, 3700. On SDS PAGE where trypsin has been included in the gap junctional preparation only the 16K protein has been found. A 10K "connexin" originally described by Goodenough (1974,1976) has been proposed as a limit digest of trypsin treated junctions (Nicholson *et al.*, 1981). However this protein migrates, in the absence of reducing agents, as multimers of 10K. i.e. it contains disulphide bonds. 27K is not affected by the presence or absence of reducing agents.

A 10K fragment produced by trypsin (Nicholson *et al.*, 1981), has been sequenced and it agrees with the N-terminal region of that predicted from the cDNA clone. This result would mean that the N-terminus is buried in the membrane. However no further fragments have been isolated.

However Pitts and Finbow (1986) report that the inclusion of a trypsin treatment step in either of the methods for preparing the 27K protein results in extensive degradation and no proteins of size thought to be sufficient to maintain the gap junctional structure have been observed on SDS PAGE.

1.5.5 Conclusions

From the above discusson it is clear that the case for the widely accepted 27K protein as the gap junctional protein is not as

sound as is implied in the literature. Furthermore, recently Manjunath and Page (1984) have proposed a protein of 46K as the heart gap junctional protein. It is obtained when serine proteases are inhibited during the preparation. The junctions so produced have "fuzzy" coats, as judged by thin section electron microscopy (Manjunath et al., 1984) and on freeze fracture followed by deep etching (Shibata et al., 1985) are not smooth on the cytoplasmic face like the liver junctions (Hirokawa and Heuser, 1982). However if the preparation is not made in the continual presences of inhibitors then a 17K component is lost from the cytoplasmic face of the junctions and the junctions become less "fuzzy".

The work on the 46K protein is not as extensive as that described above on the liver gap junctional proteins. Until further immunological methods are used to characterize this putative heart junctional protein then the evidence for it being a junctional protein is mainly correlative.

Until the problem of which protein is the junctional protein has been satisfactorily solved any progress in the functional analysis of gap junctional communication will be slowed. With this particular problem of identifying the liver gap junctional protein in mind, work in this thesis has been carried out in the hope of providing evidence for the junctional origin of 16K.

CHAPTER II

MATERIALS AND METHODS

2.1 MATERIALS

2.1.1 Fine Chemicals

Acetonitrile and trifluoroacetic acid, were supplied by Rathburn Chemicals, Peebles, Scotland.

Dimethylformamide, piperidine and dichloroethane were supplied by Cruachem, Livingston, Scotland.

Fluorenylmethoxycarbonyl (Fmoc) amino acids were purchased from Cambridge Research Biochemicals, CRB Cambridge, England.

Hydroxybenzotriazole and dicyclohexylcarbodiimide were supplied by Aldrich, Poole, England.

Low molecular weight standards for SDS PAGE, and Coomassie Brilliant Blue R250 were obtained from Bio-Rad, Irvine, California.

Phosphotungstic acid was supplied by EMScope, London.

All other reagents used were supplied by Sigma Chemical Co. Dorset, England.

2.1.2 Radiochemicals

Na ^{125}I (13.4 mCi/ μg), ^{125}I labelled anti-rabbit whole antibody from donkey (750-3000 Ci/mmol), and ^{125}I labelled streptavidin (20-40 $\mu\text{Ci}/\mu\text{g}$) were supplied by Amersham International, Amersham, England.

2.1.3 Solutions

i) Isolation buffer

NaHCO ₃	0.084 g
CaCl ₂	0.056 g
H ₂ O upto	1.00 l
pH	7.4

ii) Extraction buffer

NaCl	17.54 g
Na ₂ HPO ₄	1.15 g
NaH ₂ PO ₄ ·2H ₂ O	0.30 g
H ₂ O upto	2.00 l
pH	7.4

iii) Electrophoresis buffer

Glycine	14.42 g
Tris	3.03 g
SDS	1.00 g
H ₂ O upto	1.00 l
pH	8.2

iv) Solubilization buffer

Glycerol	20.00 g
SDS	2.00 g
Tris	1.21 g
MgCl ₂ ·6H ₂ O	20.30 mg
H ₂ O upto	0.10 l
pH	6.8

v) Blotting buffer

Glycine	43.26 g
Tris	9.09 g
SDS	3.00 g
Methanol	0.60 l
H ₂ O upto	3.00 l
pH	7.4

v) Wash Buffer

NaCl	18.0 g
Tris	2.42 g
H ₂ O upto	1.00 l
pH	7.4

2.2 METHODS

2.2.1 Preparation of Gap Junctions

Gap junctions were prepared from various mouse tissues (brain, heart, kidney and liver), Chicken liver, Xenopus laevis liver and Nephrops norvegicus hepatopancreas. Tissues were removed immediately after death and homogenised in a domestic blender ("Osterizer") set at full for 30 s in 200 ml isolation buffer (IB, 1 mM NaHCO₃, 0.5 mM CaCl₂, pH 7.4). Tissue homogenates were diluted with IB to an approximate final ratio of 50 g wet weight starting tissue to 2.1 l final volume except for Nephrops hepatopancreas where the ratio was increased to 100 g wet weight starting tissue to 2.1 l final volume. After standing the homogenates for 5 min on ice they were filtered through cheese-cloth and centrifuged for 15 min at 3000g in a Sorvall RC2 or RC5 centrifuge (GS-3 rotor). The supernatants were carefully poured off and discarded and the centrifugation repeated after suspending the pellets in half of the initial volume of IB. The pellets were taken up in extraction buffer (ExB, 0.15 M NaCl, 5 mM Na₃PO₄, pH 7.4) containing 2% (v/v) Triton X-100 (300 ml of ExB per 100 g wet weight starting material). The suspensions were centrifuged for 10 min at 4000g in the Sorvall centrifuge (GS-A rotor) and the supernatants retained. N-lauroyl sarcosine was added to a final concentration of 0.5% (w/v) and the suspensions centrifuged for 30 min at 40,000g in the Sorvall SS-34 rotor. The pellets were re-suspended in 1 mM NaHCO₃ and the centrifugation repeated. The pellets were then suspended by vortexing in 6 M urea (6 ml per 50 g of starting material) containing trypsin (Type XI) (1.5 mg per 6 ml 6 M urea) and the samples incubated at 37°C for 30 min with occasional shaking. N-lauroyl sarcosine was added to a final concentration of 0.5% (w/v) in 6 M urea (final volume of all samples 35 ml) and centrifuged for

30 min at 40,000g in the Sorvall SS-34 rotor. The pellets were suspended in a small volume of 1 mM NaHCO₃ and layered on top of a discontinuous sucrose gradient containing 4 ml 32% (w/v) and 3.5 ml 50% (w/v) sucrose (vertebrate preparations) or 60% (w/v) sucrose (Nephrops preparation) and centrifuged at 209,000g for 90 min in an International B-60 ultracentrifuge (6 x 14 rotor). Gap junctions were collected at the interface of the two sucrose densities, diluted to 13.5 ml with 1 mM NaHCO₃ and centrifuged at 209,000g for 30-60min. After pelleting the gap junction preparations the pellets were suspended in a small volume of water and stored frozen at -20°C. All steps were carried out at 5°C unless otherwise stated.

2.2.2 SDS PAGE

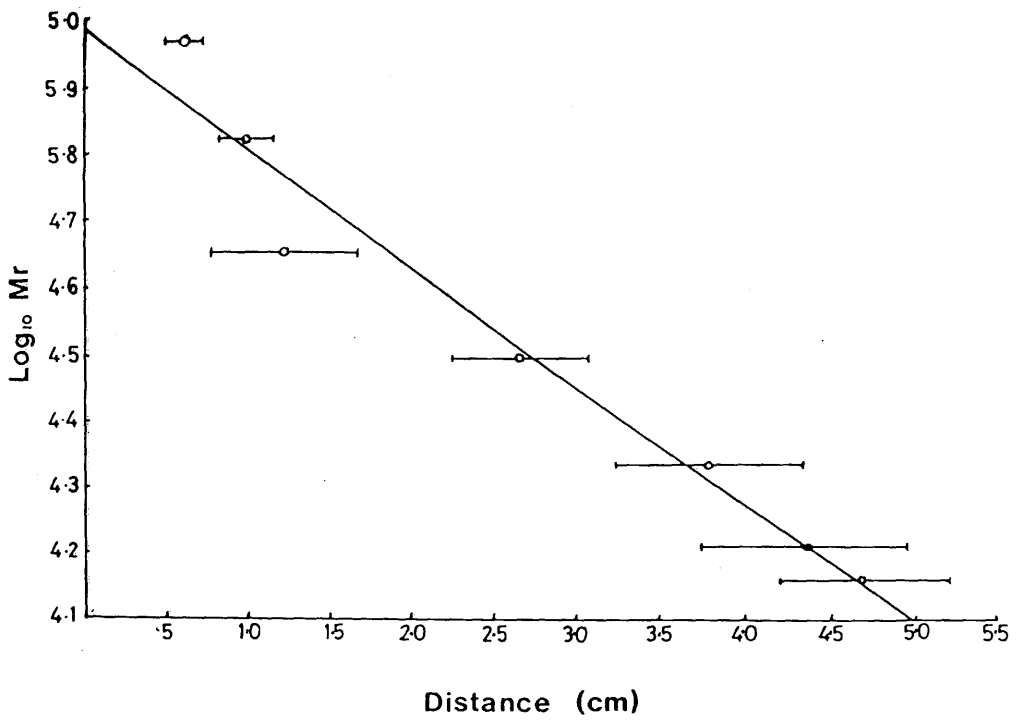
Microslab (6.5 cm x 0.75 mm running gel with a 1 cm stacking gel) polyacrylamide gel electrophoresis was carried out as described by Laemmli (1976). Running gels were 13.7% acrylamide, 0.3% N,N methylene bis acrylamide (w/v) in 0.375 M tris-HCl buffer, pH 8.8. Stacking gels were 6% acrylamide, 0.15% N,N methylene bis acrylamide (w/v) in 0.125 M tris-HCl buffer, pH 6.8. Samples were solubilized in an equal volume (upto ~ 20 µl) of solubilization buffer (SB, 0.125 M tris-HCl, pH 6.8, 2% SDS, 20% glycerol, 1 mM MgCl₂·6H₂O) Electrophoresis was carried out at 15mA for 1-2 h using the electrophoresis buffer (EB, 0.052 M tris, 0.53 M glycine and 0.01% SDS, pH 8.2). Gels were stained in 0.125% Coomassie Brilliant Blue R250 in 5% acetic acid, 12.5% isopropanol in water (v/v). Gels were destained in several changes of 5% acetic acid, 16% methanol in water (v/v). SDS PAGE gels with the Bio-rad low molecular weight standards and "16K" protein were measured and the resulting graph of distance migrated versus log₁₀ Mr plotted (Fig. 2). The data from 14 runs were plotted and the best straight line was constructed by linear regression analysis (correlation -0.993) using a Texas Instrument Ti 51-III calculator. The resulting plot (Fig. 2) shows that the SDS PAGE determined molecular weight for "16K" is 16000 +/- 3500 daltons.

Figure 2

SDS PAGE Calibration Graph for Estimation of Molecular Weight

Graph of log M_r versus electrophoretic mobility in 13.7% running gel. Bio-rad low molecular weight markers of phosphorylase B (92,500), bovine serum albumin (66,200), ovalbumin (45,000), carbonic anhydrase (31,000), soyabean trypsin inhibitor (21,500) and lysozyme (14,400) were used as standards. Standard deviations are shown for the standards (—○—) and for the "16K" protein (—●—).

SDS PAGE and the data from 14 runs was plotted as described in section 2.2.2.



2.2.3 Protein Electroelution

13.7% polyacrylamide preparative slab gels (1.5 mm thick) were stained with Coomassie Blue (5-10 min) then rinsed in destain until the protein band was visible (10-15 min). The band was excised and placed in a dialysis tube (long enough to take the gel slice plus 2 cm at either end) containing EB. Most of the buffer was squeezed out, carefully to avoid the inclusion of air bubbles. A flat-bed tank was filled with EB such that it just covered the dialysis bag. Electrophoresis was carried out for 3-20 h at constant current (20-150 mA). The current was then reversed for 30 s. The gel slice was removed from the bag and the protein solution was dialysed against 0.1% SDS for 2-3 days at 4°C. The protein solution was lyophilised to dryness.

2.2.4 Gel Scanning

Slab gels were scanned using a Helena Laboratory Densitometer. To determine the relative amounts of protein in the bands the peaks on the chart paper were cut out and weighed. To convert peak weights to amounts of protein, gels were run with different amounts of bovine serum albumin (BSA), the peaks of the densitometer scans were cut out and weighed and a standard curve was constructed. There was found to be a linear relationship between area under the peak and the amount of BSA.

2.2.5 Electron Microscopy of Isolated Gap Junctions

Gap junction pellets were suspended in a small volume of 1 mM NaHCO_3 , pH 7.4. An aliquot (2 μl) of the suspension was mixed with an equal volume of 4% phosphotungstic acid, pH 7.4. This mixture was then placed on a carbon coated copper grid (300 mesh). The liquid was carefully removed, either with filter paper or by pipette. The grid was air dried and viewed in a Phillips 301 electron microscope operated at 60 or 80 kV.

2.2.6 Peptide Synthesis

Peptide was synthesised by the solid phase method developed by Sheppard and his colleagues (Atherton et al., 1978) using polar supports for synthesis and the base labile protecting group fluorenylmethoxycarbonyl (Fmoc). Pepsyn KA resin (CRB, Cambridge) was swollen in dimethylformamide (DMF) and deprotected for 7 min in 20% piperidine in DMF (vol/vol) and washed in DMF. The reaction cycle for addition of a single Fmoc amino acid consisted of:

- 1) DMF 5 x 1 min
- 2) 20% piperidine in DMF 10 min
- 3) DMF 10 x 1 min
- 4) Acylation in DMF 60-90 min
- 5) DMF 5 x 1 min

Symmetrical anhydrides were prepared from the protected amino acid and dicyclohexylcarbodiimide for 10 min at room temperature in dichloroethane solution. The following N-protected amino acid symmetrical anhydrides, or their active esters were coupled in the presence of hydroxybenzotriazole (as a catalyst) in DMF using a Cruachem Synthesiser.

1 Fmoc-L-Cys(Trt)-OH, 2 Fmoc-L-Phe-OH, 3 Fmoc-L-Phe-OH, 4 Fmoc-L-Ser(Bu^t)-OH, 5 Fmoc-L-Ser(Bu^t)-OH, 6 Fmoc-L-Tyr(Bu^t)-OH, 7 Fmoc-L-Glu(OBu^t)-OH, 8 Fmoc-L-Pro-OH, 9 Fmoc-L-Asn-ONp.

The remaining blocking groups were removed by 20% piperidine in DMF. The peptide-resin conjugate was washed 2 x 10 min in DMF. The synthesised peptide was cleaved from the resin by treating with 10 ml of 5% ethanedithiol in trifluoroacetic acid (TFA) (vol/vol) for 3 h. Ethanedithiol was present to maintain a reduced sulphurhydryl group for coupling to keyhole limpet hemacyanin (KLH). The peptide was purified by gel permeation chromatography using a Bio-rad polyacrylamide P2 gel column (10 cm x 1 cm) eluted with 0.03 M NH₄CO₃ (pH 7.9) at a flow rate of 0.6 ml/min. The fractions containing the peptide were identified by monitoring the eluate at 260 nm. The eluted peptide was lyophilized to dryness. Analysis of a sample by high performance liquid chromatography (HPLC) on a reverse phase TSK C18 column with a linear gradient of 0-100% acetonitrile in 0.1% TFA (vol/vol) gave one major peak (Fig. 3).

Figure 3

HPLC Analysis of Laboratory Synthesized Peptide

A sample of the laboratory synthesized peptide was dissolved in 20 μ l of 0.1% trifluoroacetic acid in distilled water (vol/vol) and applied to a TSK C18 reverse phase column and developed:

Temp: Ambient

Flow: 1 ml/min

Detector: 230 nm

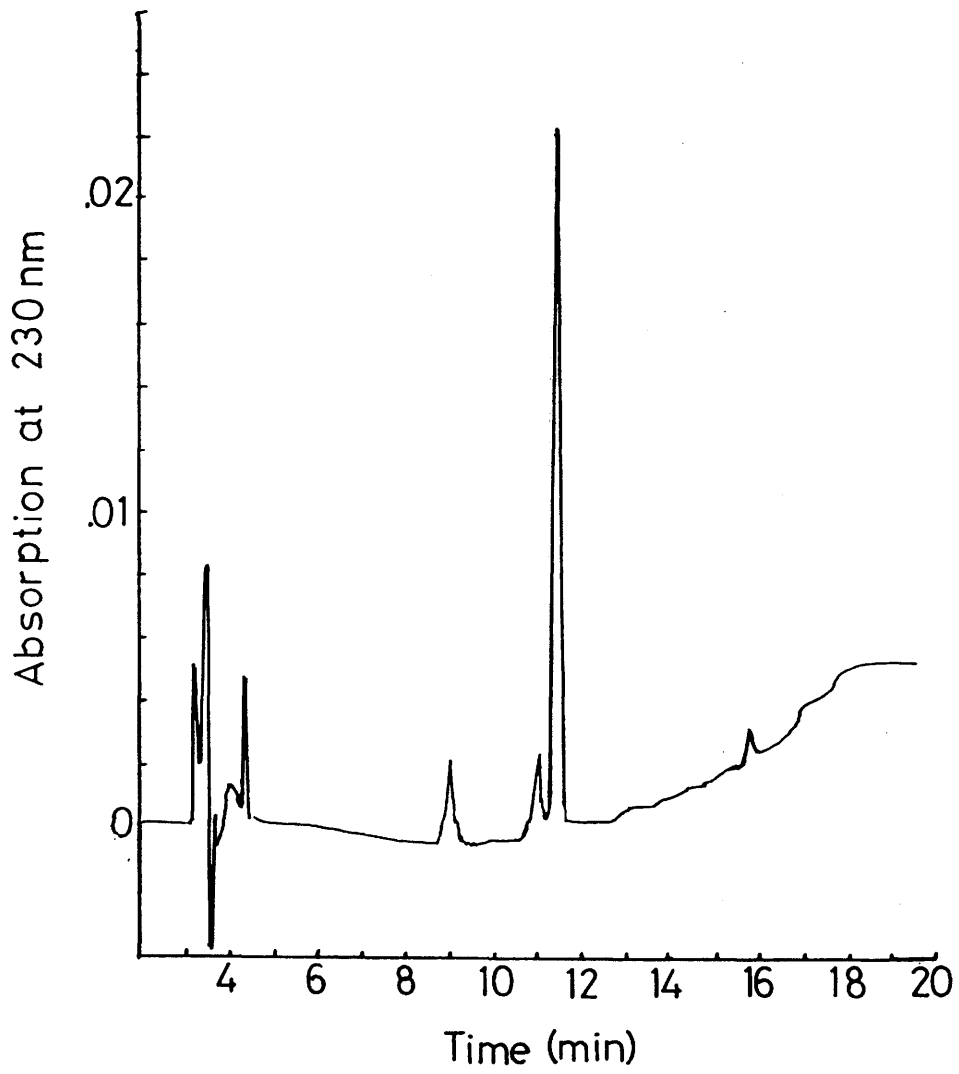
Chart Speed: 30 cm/h

Gradient:

solvent A: 0.1% trifluoroacetic acid in distilled water (vol/vol).

solvent B: 0.1% trifluoroacetic acid in acetonitrile (vol/vol).

Time(min)	%B
0	0
20	100



Amino acid analysis (attempted by CRB, Cambridge) was not successful. Subsequently a sample of the same peptide was purchased from CRB which had the following amino acid analysis after acid hydrolysis (6 M HCl, 110°C, 18 h): Asp 1.10 (1), Ser 1.61 (2), Glu 1.08 (1), Pro 1.03 (1), Cys 0.48 (1), Tyr 0.95 (1), Phe 2.00 (2).

Under these acid hydrolysis conditions serine undergoes a certain degree of degradation and cysteine is almost totally degraded.

Fast atom bombardment mass spectrometry when run in the positive ion mode, showed a molecular ion (M) 1093 and a M+Na⁺ ion at 1115 both being consistent with a compound having a molecular weight of 1092 (the theoretical molecular weight). The commercial peptide, when analysed by HPLC (linear gradient of 0-100% acetonitrile in TFA, vol/vol) gave a single peak eluting at the same time as the peptide made in the laboratory.

2.2.7 Coupling of Synthetic Peptide to Carrier Protein

The peptide was coupled to the carrier protein KLH through the cysteine residue, with maleimido-benzoyl-N-hydroxysuccinimide ester (MBS) as the coupling agent. KLH (4 mg in 0.25 ml of 10 mM sodium phosphate buffer, pH 7.2) was treated with 0.7 mg MBS (dissolved in DMF), added dropwise and stirred for 30 min at room temperature. The reaction product KLH-MB was passed through a Bio-rad P10 column (15 cm x 1 cm) equilibrated with 50 mM sodium phosphate buffer (pH 6.0) to remove free MBS. KLH-MB was then treated with 4 mg peptide dissolved in PBS (pH 7.5). The pH was adjusted to 7-7.5 and the reaction mixture was stirred for 3 h at room temperature. The conjugate was then frozen and stored at -20°C until used for injection.

2.2.8 Preparation of Site Specific Antisera

Four female New Zealand white rabbits were injected subcutaneously at multiple sites along the back with the KLH-peptide conjugate mixed with Freund's adjuvant. The following procedure was used: first injection of 200 µg conjugate (total) in complete

Freund's adjuvant (1:1) on day 0, second injection of 200 µg conjugate (total) in incomplete Freund's adjuvant (1:1) on day 14. Animals were bled on days 21, 28 and 32 after the first injection and then once every fortnight. The rabbits were boosted every 2-3 months with 200 µg conjugate in Freund's incomplete adjuvant. Serum was collected from an ear vein and allowed to clot at room temperature for 1 h and then overnight at 4°C before spinning to clarify the serum (MSE bench top microfuge). Serum was aliquoted and stored at -20°C.

2.2.9 Dimethylamino-napthalene-5-sulphonyl Chloride Derivitization of 16K Protein

The 16K protein was dansylated as described by Gray and Hartley (1969). Electroeluted 16K protein (50 µg) was dialysed against 0.1% SDS. The protein was lyophilised to dryness in a chromic acid cleaned test-tube. 0.2M NaHCO₃ (50 µl) was added followed by 50 µl of dansyl choride in acetone (2.5 mg/ml). The test tube was sealed and incubated for 1 h at 37°C. The derivitized protein was then lyophilised. 6 M HCl (200 µl) was added and the test tube was heat sealed. The protein was hydrolysed at 110°C overnight and then dried down as before. The hydrolysate was dissolved in ethanol and the dansylated amino acids analysed by thin layer chromatography on polyamide sheets.

2.2.10 Dimethylaminoazobenzene-isothiocyanate Derivitization of 16K Protein

Dimethylaminoazobenzene-isothiocyanate (DABITC) derivitization was carried out as described by Chang *et al.* (1978). Electroeluted 16K protein was dried in an Eppendorf tube (see section 2.2.3). To the dried protein 20 µl 50% pyridine/water (vol/vol) and 10 µl DABITC 2.82 mg/ml in pyridine was added. DABITC was freshly prepared for each cycle by making a stock solution in acetone (4 mg/ml), drying down an aliquot and then adding pyridine. The Eppendorf was flushed with oxygen free nitrogen, mixed by vortexing and sealed. The reaction was incubated at 55°C for 20 min.

Phenylisothiocyanate (5 µl) was added and the Eppendorf was again flushed with nitrogen, sealed and incubated for 20 min at 55°C. The amino acid was extracted (3x) with 200 µl heptane/ethyl acetate (2/1, vol/vol) saturated with 67% pyridine/water and vortexed and spun on a MSE bench top microfuge. The aqueous phase was removed taking care not to remove any of the protein which is at the interface (as it is a highly hydrophobic protein) and the aqueous layer was dried. To the dried residue TFA (20 µl) was added and the Eppendorf again flushed with nitrogen, sealed, mixed and incubated for 20 min at 55°C. 25 µl water and 100 µl butyl acetate was added followed by mixing, spun on a MSE bench top microfuge to separate and carefully drawing off the butyl acetate. The butyl acetate extract was dried down and 20 µl 50% TFA/water (vol/vol) was added. The Eppendorf was flushed with nitrogen, sealed, mixed, and incubated for 15 min at 80°C. The residue was dried down and identified by HPLC.

2.2.11 Immunoblotting

Immunoblotting was carried out as originally described by Towbin et al. (1979). The SDS PAGE separated proteins were transferred to nitrocellulose supports in blotting buffer (BB, 0.025 M tris-HCl, pH 8.3, 0.15 M glycine, 20% methanol, 0.1% SDS) for 2-3 h at 30 V in a Bio-Rad Trans-Blot Cell. Transfer to Nylon supports (Amersham) was performed in the same manner except sometimes the methanol was omitted from the BB. Nitrocellulose supports were blocked at 37°C for 1 h in wash buffer (WB, 0.9% NaCl, 10 mM tris-HCl, pH 7.4) containing 3% bovine serum albumin (BSA) (w/vol). Nylon supports were blocked for 3 h in WB with 10% BSA at 60°C. Blots were washed for 30 min in several changes WB with 0.1% Tween-20 (polyoxyethylene sorbitan monolaurate) added. Blots were incubated in WB with 1% BSA with various dilutions (range 1:1-1:1000) of primary antisera at 37°C for 1 h and then washed as before (30 min in 0.1% Tween-20 in WB). Blots were transferred to 30 ml WB + 3 detergents (3D WB, 1% Triton X-100, 1% sodium deoxycholate, 0.1% Tween-20) with 3% BSA and either of two detection reagents, biotinylated second antibody at appropriate dilutions

(range 1:100-1:100,000), or iodinated second antibody (approx 1 x 10⁶ cpm per track). Blots were incubated with the detection reagent 1 h at 37°C, washed as before and, if biotinylated second antibody used, ¹²⁵I-streptavidin was added to 2 x 10⁶ cpm/track in 3% BSA in WB and incubated for 15 min at room temperature. Blots treated with either ¹²⁵I labelled second antibody or ¹²⁵I labelled streptavidin were washed in WB as before. The blots were air dried and exposed to X-Omat film with Cronex screens at -70°C.

2.2.12 Modified Immunoblotting

The protocol as outlined in section 2.2.11 was carried out. After incubation with iodinated second antibody, blots were further washed with 3% BSA in 3D WB + 1 M KI for 10 min at room temperature before placing in WB and 0.1% Tween, rinsing drying and exposing as before.

2.2.13 Agglutination of Gap Junctions

Gap junction pellets were suspended in a small volume of PBS with 3% BSA. The suspensions were then pelleted in a MSE bench top microfuge. The supernatants were removed and the pellets resuspended in PBS with 3% BSA (final concentration approximately 2 µg of 16K protein/µl). An aliquot was removed and added to an equal volume of either immune or preimmune serum. The suspension was mixed in a pipette tip and 2 µl viewed on a microscope slide. (If junctions were too dense the reaction mix was diluted with PBS with 3% BSA). The reaction mix in an Eppendorf tube was then put on a Luckman orbital shaker at maximum rotation for 1 h. The reaction mix (2 µl) was then placed on a microscope slide covered with a cover slip and sealed with "Glyceel". The microscope slide was incubated in a humid chamber for 2-3 h and viewed under the microscope. Sometimes the agglutination reaction was allowed to proceed overnight before photographing with Ilford HP5 on a Vario-Orthomatic Leitz microscope.

2.2.14 Two-dimensional Peptide Mapping

Gap junction preparations were labelled with ^{125}I using chloramine T (Hunter and Greenwood, 1962). To 10 μl of suspended junctions (approx 10-20 μg 16K protein) 500 μCi ^{125}I were added, followed by 10 μl chloramine T (1 mg/ml in PBS). After incubation for 30 s at room temperature 10 μl sodium metabisulphite (1 mg/ml in PBS) were added. The reaction mix was layered onto 9 ml 32% sucrose (w/v) and centrifuged at 209,000g for 60-90 min in an International B-60 ultracentrifuge (6 x 14 rotor). To prepare labelled 16K protein the ^{125}I labelled gap junctions were electrophoresied on SDS PAGE. After electrophoresis the gels were briefly exposed to X-ray film to visualize the labelled protein bands which were then cut out and eluted overnight from the gel slices in 0.5 ml H_2O . The samples were lyophilised and re-dissolved in 20 μl of H_2O containing 20 μg of ovalbumin. The proteins were precipitated at 0°C by adding 20 μl of 40% (w/v) trichloroacetic acid (TCA) and pelleted using a MSE bench top microfuge. The precipitates were washed (2x) with 100 μl 20% TCA and then extracted (3x) with diethyl ether before suspending in 100 μl of 1% (w/v) NH_3HCO_3 containing 10 μg of trypsin (type XI) and incubating at 37°C. After 1 h a second 100 μl aliquot of 1% NH_4HCO_3 containing 10 μg trypsin was added and the samples digested for 16-18 h. The digests were lyophilised, suspended in a small volume of electrophoresis buffer (acetic acid/formic acid/water 8/2/19, vol/vol/vol, pH 2.1), and 10 μl aliquotes were spotted on cellulose thin layer chromatography plates (20 cm x 20 cm). Electrophoresis was carried out at 22°C for 45 min at 600 V and chromatographic separation was carried out at room temperature in acetic acid/butanol/pyridine/water (1/5/4/4, vol/vol/vol/vol). The plates were then exposed to Kodak X-Omat X-ray film with Cronex screens at -70°C.

CHAPTER III

RESULTS

3.1 PREPARATION OF SITE SPECIFIC ANTISERA

3.1.1 Introduction

The review of the literature presented in section 1.5 has shown that the identity of the gap junctional protein is not as clear as is sometimes made out. The identification of the gap junctional protein is required for a better understanding of structure and a further analysis of the functional role of gap junctional communication.

Finbow et al. (1983) have proposed that the gap junction is likely to be conserved at the protein level because it appears to be conserved at both the structural and functional levels. Such a proposal is consistent with their findings that the protein Mr 16000 (16K), isolated from mouse liver gap junction preparations, is indistinguishable in different tissues and conserved over a wide range of species. This 16K protein is unrelated to the more generally accepted Mr 27000 (27K) junctional protein.

Finbow et al. (1983) propose that the 16K protein is a major structural component of gap junctions but do not necessarily expect it to represent the protein in its native state as some endogenous proteolysis could occur during isolation. They have also shown that the 16K vertebrate proteins are immunologically related to a corresponding set of related invertebrate Mr 18000 (18K) proteins of which the best characterised is the 18K protein found as a major component of Nephrops norvegicus hepatopancreas gap junctional preparations (Finbow et al., 1984).

One important aim of this thesis therefore, is to provide more direct evidence that the 16K protein is a gap junctional protein.

Most of the antisera used to characterize gap junctions which have been described in the literature have been raised against either preparations containing gap junction plaques (Hertzberg, 1984; Finbow et al., 1984), or proteins isolated from gap junction preparations (Traub et al., 1982; Warner et al., 1984; Paul, 1985). Both approaches have their merits but the antigens prepared by either method contain contaminants, and hence may produce antisera with mixed activities. An alternative approach which overcomes this particular problem is to synthesize peptides, based on the sequence of a putative junction protein and use them to raise antisera. The antisera so produced would be polyclonal but site specific. Such a strategy has been adopted in this thesis for the 16K protein. A similar approach has been adopted by Evans and his colleagues (Hope et al., 1984; Zervos et al., 1985) with respect to the 27K putative liver gap junction protein. The results of these investigations will be compared in the Discussion (section 4).

3.1.2 Protein Sequencing

Some sequence data for the 16K protein was available at the outset of this work; namely amino acids 2-27. The N-terminal residue was not identified because it was bound, like all residues with free amino groups, to the support material used in the sequenator (John Walker LMB, Cambridge, personal communication). Using the Hopp and Woods (1981) algorithm, a hydrophilicity plot for this sequence was constructed (Fig. 4). This shows that of the known sequence the N-terminal region is the most hydrophilic and as hydrophilic regions of proteins are regarded (e.g. Hopp and Woods, 1981) to have the most potential for antigenicity, it was chosen as the candidate sequence for the synthesis of the peptide.

However, the missing residue made it impossible to select the most appropriate synthetic peptide for synthesis and so it was necessary to identify the N-terminal amino acid.

Figure 4

Predicted Hydropathic Indices of the 27 Amino Acids of the 16K
Protein N-terminal Sequence

The algorithm of Hopp and Woods (1981) is used with the MicroGenie software (Beckman, Glenrothes, Scotland). The sequence is listed vertically, with each amino acid given by its standard three letter code. The vertical line represents a hydropathic index of 0. The plot shows the running average (over 6 residues) of the amino acid hydropathic indices. Hydrophilic regions of the protein appear on the right of the vertical line and hydrophobic regions to the left.

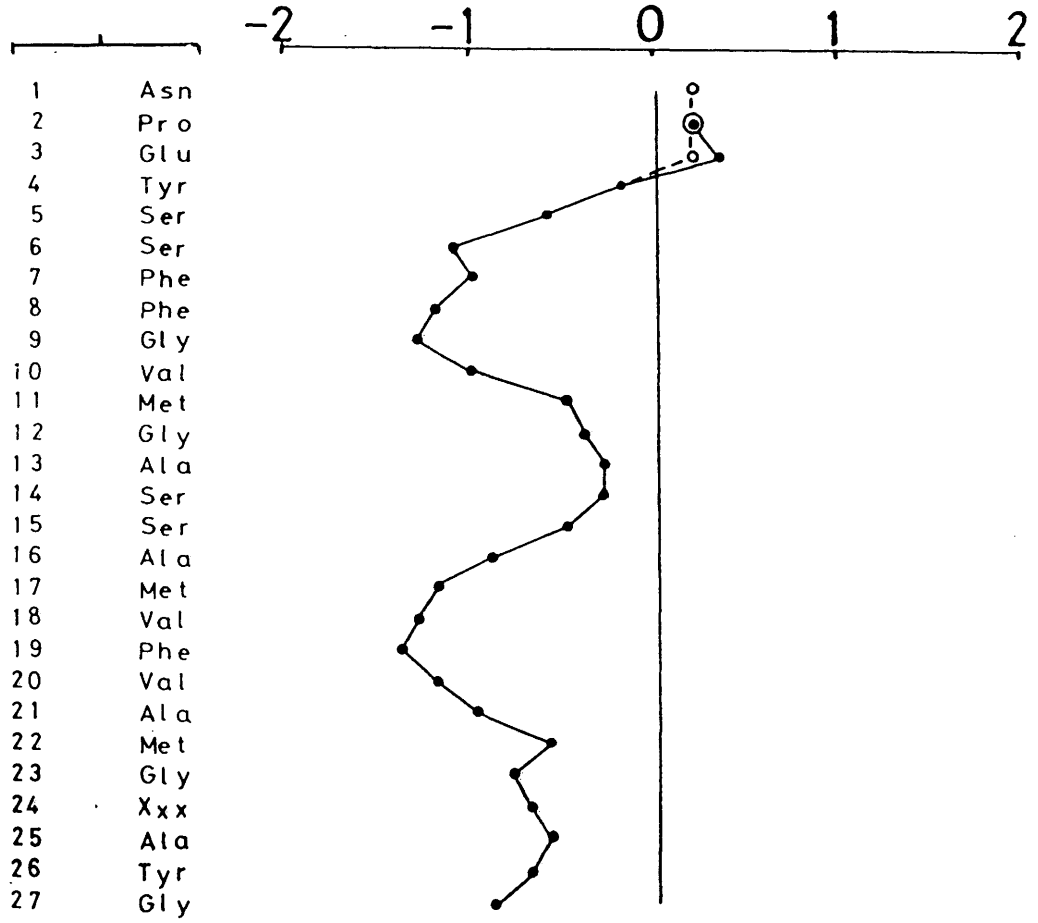
----- = hydropathic index with N-terminal asparagine.

————— = hydropathic index without N-terminal asparagine.

(from residue 4 the two plots are identical)

Amino Acid
Residue

Predicted
Hydropathic Index



The initial approach was based on the use of the fluorescent chromophore dansyl chloride (1-dimethylamino-naphthalene-5-sulphonyl chloride), which reacts with free amino groups in proteins (Gray and Hartley, 1969). Mouse liver gap junctions (Fig. 5a) were prepared (see section 2.2.1) and 16K protein was obtained by preparative SDS PAGE followed by electroelution (Fig. 5b) (see section 2.2.3). Two bands are obtained 16K bands dimer 26K, (Finbow et al., 1983). The protein was then derivitized with dansyl chloride and hydrolysed with 6 M HCl as described in section 2.2.9.

To identify the dansylated amino acid residues of the 16K protein, standard dansyl amino acids (Sigma) were chromatographed on polyamide TLC plates. Most dansyl amino acids produce a bright yellow fluorescence when exposed to UV light. However, certain breakdown products of dansyl chloride, dansyl hydroxide and dimethylamino-naphthalene-5-sulphonic acids have bright blue fluorescence. These different colours are useful for identification and orientation purposes but cannot be distinguished on the black and white photographs (Fig. 6).

Dansyl chloride treatment of proteins labels the amino group of the N-terminal amino acid, the ϵ -amino group of lysine, the amino groups of histidine and arginine and the hydroxyl group of tyrosine. Therefore, on the chromatogram of the hydrolysate of the dansylated 16K protein, there will be fluorescent signals arising from the internally located lysine, histidine, arginine and tyrosine residues, as well as a signal arising from the N-terminal amino acid. Stronger signals should come from the lysine, histidine, arginine and tyrosine residues because they are likely to occur several times within the 16K protein.

Using the chromatographed standards as a guide, the N-terminus was tentatively identified as aspartic acid or asparagine (Fig 6). Due to the conditions used for hydrolysis (6 M HCl, 24 h, 110 °C) asparagine is converted to aspartic acid. To confirm that the extra spot was aspartic acid (Fig. 6a, position 3) an aspartic acid standard was co-chromatographed on the opposite side of the double-sided TLC plate. Co-migration supported the identification.

Figure 5

Electron Microscopy of Negative Stained Mouse Liver Gap Junctional
Preparation and SDS PAGE of Electroeluted 16K Protein

a) Electron micrograph of negatively stained gap junctions from mouse liver. Gap junctions were prepared as described in section 2.2.1, and electron microscopy was carried out as described in section 2.2.5.

Magnification 105,000x

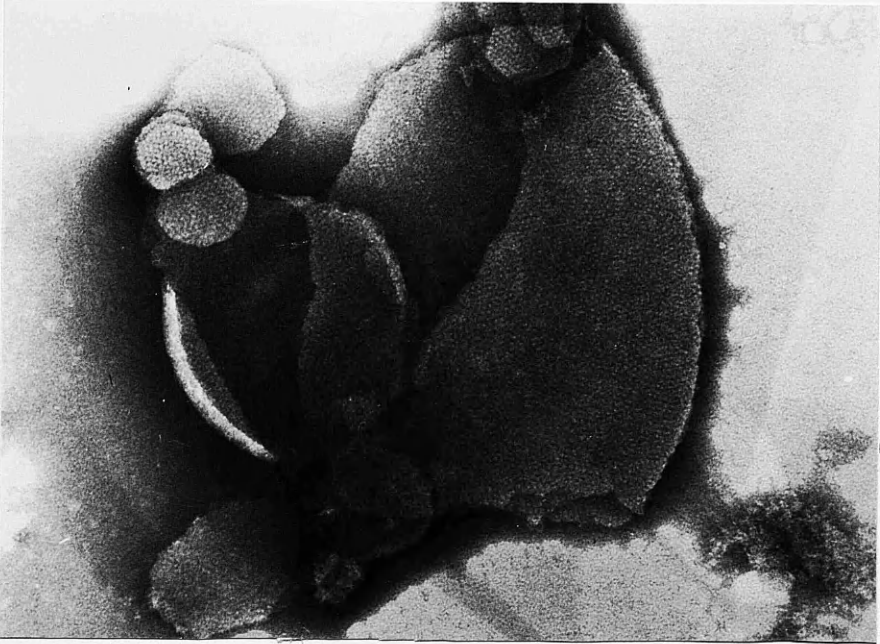
b) Coomassie stained SDS PAGE of electroeluted 16K protein.

Lane 1 Bio-rad. Mol.Wt marker proteins ($M_r \times 10^{-3}$)

2 Electroeluted 16K protein.

16K protein was electroeluted as described in section 2.2.3.

a



b

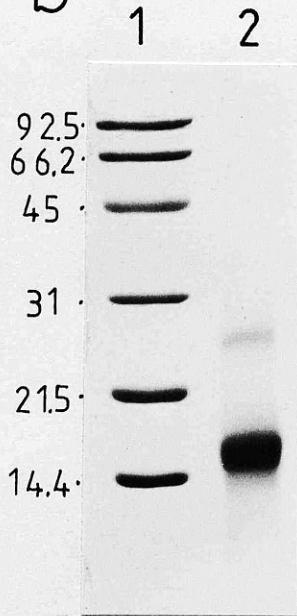


Figure 6

Chromatography of Dansylated Amino Acids

a) diagram showing distribution of standard dansyl amino acids:

1 Dans-OH, 2 dans-(arginine, and ϵ -lysine), 3 dans-aspartic acid, 4 dans-glutamic acid, 5 dans-histidine, 6 dans-serine, 7 dans-O-tyrosine, 8 dans-threonine, 9 dans-tryptophan, 10 dans-methionine, 11 dans-bis-lysine, 12 dans-glycine, 13 dans-bis-tyrosine, 14 dans-phenylalanine, 15 dans-alanine, 16 dans-leucine, 17 dans-valine, 18 dans-isoleucine, 19 dans-proline, 20 dans-NH₂.

b) Chromatography of selected dansylated amino acids used as markers (4, 6, 9, 14, 19) overlaid with a copy of (a) to show relative positions.

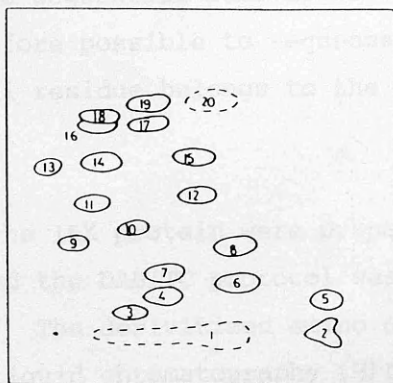
c) Chromatography of acid hydrolysate of the mouse liver 16K protein after dansylation. Four spots are visible: the brightest is dans-(arginine, and ϵ -lysine) position 2, and the other three correspond to dans-O-tyrosine (position 7), dans-NH₂ (position 20) and to dans-aspartic acid (position 3). The identification of dans aspartic acid was confirmed by co-chromatography with the standard dansylated aspartic acid on the reverse side of the polyamide TLC plate.

Chromatography solvent 1 (left to right): 1.5% formic acid.

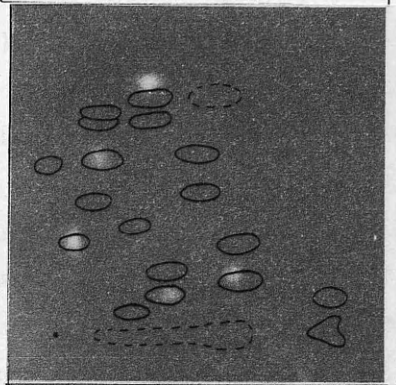
Chromatography solvent 2 (bottom to top): toluene/acetic acid 9/1 (vol/vol).

Chromatography solvent 3 (bottom to top): ethyl acetate/ methanol/ acetic acid. 20/1/1 (vol/vol/vol).

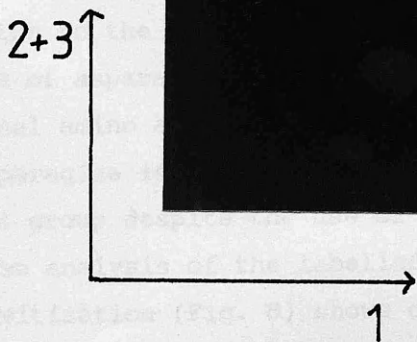
a



b



c



In order to distinguish between aspartic acid and asparagine an approach was required which used less harsh conditions for cleaving the labelled amino acid from the protein. The procedure chosen was a labelling technique using dimethylaminoazobenzene-isothiocyanate (DABITC). This procedure has the added advantage that it can be combined with Edman degradation (Chang et al., 1978), which allows sequential removal of the N-terminal amino acid. It is therefore possible to sequence the protein to confirm that the N-terminal residue belongs to the previously determined sequence.

Samples of the 16K protein were prepared by electroelution (section 2.2.3) and the DABITC protocol was followed as described in section 2.2.10. The derivitized amino acids were identified by high performance liquid chromatography (HPLC) using a C18 reverse phase column and elution with an acetonitrile gradient. The amino acids asparagine and aspartic acid were derivitized with DABITC to use as standards (see section 2.2.10). In addition proline and glutamic acid were derivitized as these correspond to residues two and three in the known sequence of the 16K protein.

Figure 7 shows the elution profile for the N-terminal amino acid. There are two major peaks on the trace. The first peak elutes at a time corresponding to aspartic acid and the second peak at a time corresponding to asparagine. When the asparagine standard and the N-terminal amino acid were applied to the column together the height of the second peak increased in direct proportion to the amount of asparagine standard loaded. The presence of asparagine even with some aspartic acid identifies the N-terminal amino acid as asparagine. The presence of aspartic acid with asparagine is due limited hydrolysis of the amide group to the carboxyl group despite the use of milder conditions.

The analysis of the labelled products from the second round of derivitization (Fig. 8) shows only one major peak. Using the same procedure as before, the co-injection of a standard derivitized amino acid, the identity of this peak was confirmed as proline. The third amino acid determined in this way corresponds to glutamic acid (Fig. 9), continuing the partial sequence produced

Figure 7

HPLC Analysis of Dimethylaminoazobenzene-thiohydantoin N-terminal
Amino Acid

HPLC analysis of (a) N-terminal amino acid-DABTH, (b) asparagine-DABTH standard, (c) N-terminal amino acid-DABTH + asparagine-DABTH standard. Samples (dissolved in solvent A) were applied to a TSK C18 reverse phase column and developed:

Temp: Ambient.

Flow: 1 ml/min.

Detector: 436 nm

Chart speed: 15 cm/h.

Gradient:

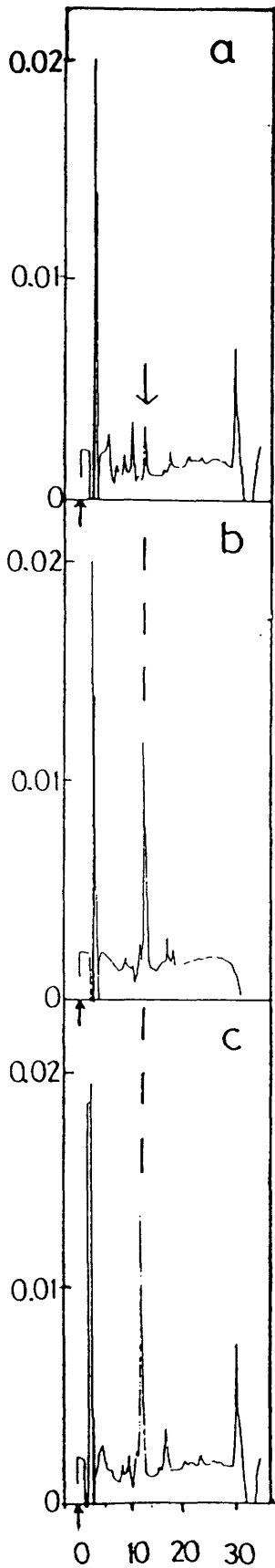
solvent A 0.029 M sodium acetate pH 5

solvent B 1% ethylene dichloride in acetonitrile (vol/vol).

Time	%B
0	35
20	50
21	85
25	85
30	35

Upward arrow indicates injection. Downward arrow and dotted lines indicate asparagine peak and the same time after injection.

Absorption at 436 nm.



Time (min)

Figure 8

HPLC Analysis of Dimethylaminoazobenzene-thiohydantoins Second
Amino Acid

HPLC analysis (a) second amino acid-DABTH, (b) proline-DABTH standard, (c) second amino acid -DABTH + proline-DABTH standard. Samples (dissolved in solvent A) were applied to the TSK reverse phase column and the column was developed as described in the legend to figure 7.

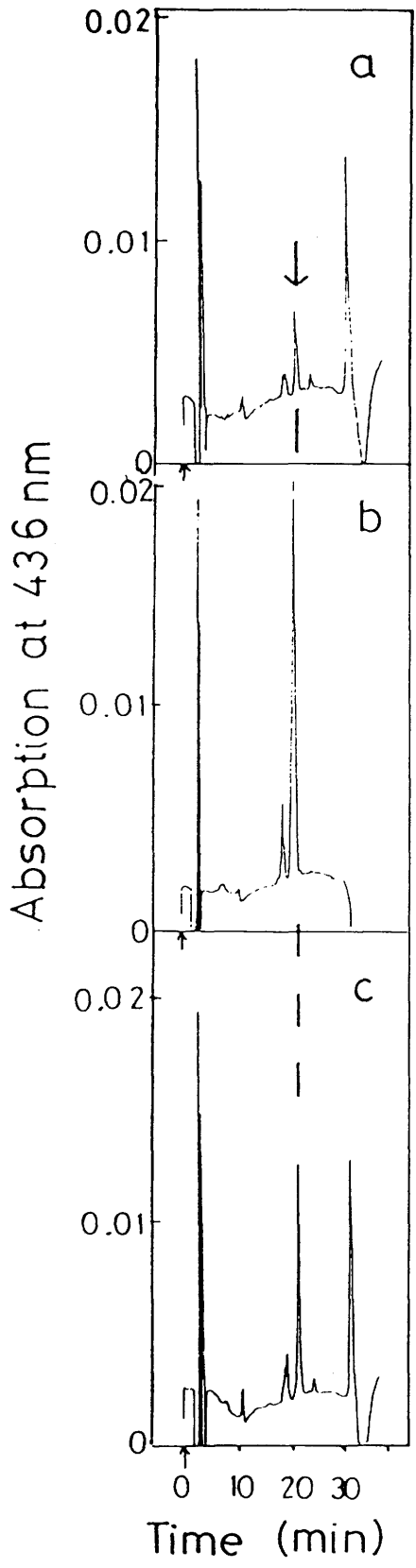
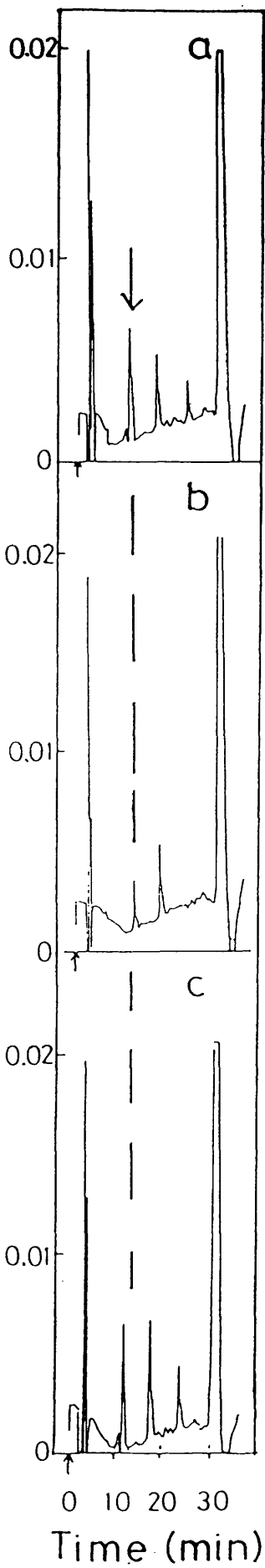


Figure 9

HPLC Analysis of Dimethylaminoazobenzene-thiohydantoins Third
Amino Acid

HPLC analysis of (a) third amino acid-DABTH, (b) glutamic acid-DABTH standard, (c) third amino acid-DABTH + glutamic acid-DABTH. The samples were dissolved in solvent A and applied to the TSK C18 reverse phase column and developed as described in in the legend to figure 7.

Absorption at 436 nm.



for the 16K protein. Subsequent sequence analysis of the 16K protein by J.-P. Revel and L. Hood (California Institute of Technology) and by J. Findlay (University of Leeds) has confirmed that the N-terminal residue is asparagine and also confirmed (to amino acid residue 19) the sequence determined by Shuttleworth and Walker (personal communications).

This analysis also shows that the N-terminus of the isolated protein is not blocked and provides further evidence that the 16K protein seen after Coomassie staining of SDS PAGE is composed of a single protein. (There could be contaminating proteins with blocked N-termini.)

3.1.3 Preparation of Polyclonal Site Specific Antisera

The hydrophilicity plot using the Hopp and Woods (1981) algorithm for the 16K protein, modified by the incorporation of the N-terminal asparagine is shown in figure 4 as a broken line. The asparagine adds to the hydrophilic nature of the N-terminal region of the protein and makes this region a better candidate for an antigenic site.

On this basis an octapeptide was synthesized which correlated to the N-terminal eight amino acids of the 16K protein. A C-terminal cysteine was added to the octapeptide so that it could be coupled to the carrier protein, keyhole limpet haemocyanin (KLH).

The peptide was initially synthesized in the laboratory (see section 2.2.6) using the solid phase methodology developed by Sheppard and his colleagues (Atherton *et al.*, 1978), but later a further supply of peptide was purchased from Cambridge Research Biochemicals (CRB, Cambridge).

Amino acid analysis and fast atom bombardment (FAB) mass spectrometry was carried out on both peptides by CRB. Only the commercially bought peptide analysis was complete. This showed that the peptide had the correct amino acid composition and gave a

major peak on FAB mass spectrometry at Mr 1092, which corresponds to the predicted molecular weight of the peptide. CRB confirmed that both peptides migrate as a single spot on TLC analyses detected by ninhydrin and potassium iodide staining. The laboratory synthesized peptide was coupled to KLH with the coupling reagent maleimido-benzoyl-N-hydroxysuccinimide ester (MBS) (section 2.2.7). The peptide-KLH conjugate was injected into two female New Zealand white rabbits (see section 2.2.8). Subsequently the commercially prepared peptide was also coupled to KLH and used to raise antisera in two further New Zealand white rabbits. The two peptide preparations produced antisera with similar activities.

3.2 CHARACTERIZATION OF SITE SPECIFIC ANTISERA

3.2.1 Affinity Purification

One advantage of raising antisera against a synthetic peptide is that the antisera can be affinity purified using the immunogen (without the carrier) coupled to an inert support. The nonapeptide was coupled to a polylysine agarose support through the cysteine of the peptide with the coupling reagent MBS. Sufficient peptide was coupled to the column such that, under the conditions used, the bound peptide would not be a limiting factor in the binding of antibodies during affinity purification. The resin chosen couples through the ϵ - amino groups of lysine providing good availability for antibody binding, and as the same coupling reagent was used to couple the peptide to the carrier protein (see section 2.2.7), the orientation of the peptide should be similar to that used as the immunogen.

The sera were first fractionated on a Sepharose Protein-A column to enrich for immunoglobins of the IgG class. The IgG fraction was then fractionated on the affinity column. After extensive washing the affinity purified antibodies were eluted with 0.2 M glycine pH 2.2 (see legend to Fig. 10).

SDS PAGE profiles (Fig. 10) of the various fractions at different stages of purification show that after the fractionation on the Protein-A and affinity columns the major protein recovered has Mr ~150K consistent with it being IgG. Upon reduction with dithiothreitol the ~150K band is reduced to its heavy chain (~50K) and light chain (~25K) components, again consistent with the isolated reactive immunoglobulins being IgG (Fig. 10b).

Table 1 shows the yields of the affinity purified IgG as a percentage of total IgG applied to the affinity column. The yield

Figure 10

SDS PAGE Analysis of Fractionated Rabbit Site Specific Antiserum

a) Coomassie stained SDS PAGE analysis of fractionated rabbit site specific antiserum.

- Lane 1 Bio-Rad M. Wt marker proteins ($M_r \times 10^{-3}$).
- 2 Sample of unfractionated rabbit serum.
 - 3 Sample of eluate from Sepharose Protein-A column.
 - 4 Sample of eluate from affinity column.
 - 5 Bio-Rad M. Wt marker proteins.

The rabbit site specific antiserum was incubated with a Sepharose Protein-A column overnight at 4°C. The column was washed with PBS containing 0.1% Tween-20. The eluate was monitored at 280 nm. When absorption fell below 0.02 the column was equilibrated with PBS to remove Tween-20, the bound antibody was eluted with 0.2 M glycine-HCl buffer, pH 2.2, which was then immediately neutralized with 1 M tris-HCl buffer, pH 8.2. The same protocol was used when the Protein-A eluted IgG was applied to the peptide/agarose affinity column.

Samples were dissolved in an equal volume of SB and run on a 13.7% acrylamide gel as described in section 2.2.2.

b) Coomassie stained SDS PAGE analysis of reduced and non reduced affinity purified antibodies

- Lane 1 Affinity purified antibodies before reduction.
- 2 Affinity purified antibodies after reduction.

Affinity purified antibodies were heated with an equal volume of SB containing DTT for 5 min at 100° C. The samples were then run on a 13.7 % acrylamide gel as described in section 2.2.2. Both (a) and (b) were stained with coomassie blue as described in section 2.2.2.

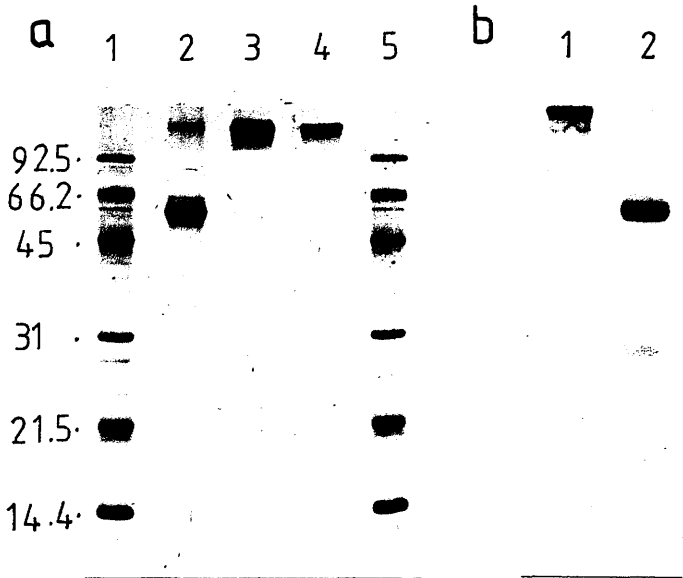


Table 1

Recovery of Affinity Purified Antibodies from IgG Applied to
Affinity Column

Amounts of IgG were calculated from the measured absorption at 280 nm (1.4 O.D. units = 1 mg). The site specific antiserum (SS) from two rabbits were fractionated as described in the legend to figure 10.

SS Serum No:	A IgG applied to affinity column (mg)	B IgG recovered (mg)	B/A × 100 % yield
1	8.76	0.69	7.9
1	11.93	0.61	5.1
1	9.14	0.52	5.7
3	12.44	0.68	5.5
3	17.21	0.77	4.5
3	9.39	0.46	4.9

of affinity purified site specific antibodies, ~5% of IgG applied to affinity column, is similar to that reported by Gullick et al. (1985) for affinity purified antibodies directed against the autophosphorylation site of epidermal growth factor.

The affinity purification suggests that the sera contain antibodies directed against the octapeptide derived from the 16K N-terminal sequence.

3.2.2 Immunoblot Analysis

A major step towards the characterization of the site specific antisera however, is to find out whether they will specifically bind to the mouse liver 16K protein. Initial attempts to characterize the sera by immunoprecipitating ¹²⁵I labelled 16K protein, with Sepharose Protein-A, as used for the IgG affinity purification (section 3.2.1), were unsuccessful. This suggests that the antibody-protein interaction is affected by the iodination of the 16K protein as the Sepharose Protein-A has been shown to bind the antibodies (Fig. 10). One possible explanation is because the tyrosine is labelled by the iodination technique, thereby modifying the antigen such that the antibodies failed to recognize it.

The technique of immunoblotting as developed by Towbin et al. (1979) was therefore tried as an alternative approach (see section 2.2.11).

A systematic analysis was undertaken to determine the conditions necessary to selectively detect the 16K protein by immunoblotting. Initial attempts involved using the successfully characterized (Finbow et al., 1984) anti-chicken gap junction antiserum (RaC 16K) as a positive control and the site specific antiserum without affinity purification. When tested against nitrocellulose blots of SDS PAGE separated KLH, KLH coupled to the peptide, marker proteins and two samples from a mouse liver gap junctional preparation (containing 0.1 µg and 1 µg of 16K protein), using the conditions described by Finbow et al. (1984), the positive

control antiserum (RaC 16K) detected the 16K protein and the dimer (26K) at both sample concentrations (Fig. 11) but the site specific antiserum only detected the KLH and KLH coupled to the peptide (Fig. 11).

At lower stringency, using blots of only the marker proteins and a mouse liver gap junction sample (~1 µg 16K protein) (Fig. 12), the 16K protein was detected but all the marker proteins (to differing degrees) gave a positive reaction (Fig.13). The same result was obtained using various dilutions of both the primary antiserum and the secondary detection reagent, iodinated anti-rabbit IgG or a biotinylated anti-rabbit IgG with ¹²⁵I streptavidin (Fig. 13). The preimmune serum however, under these low stringency conditions, only labelled the marker proteins suggesting that some specific anti-16K activity was present in the site specific antiserum (Fig. 13).

Further analyses were therefore carried out using an unmodified nylon support. Nylon has a higher affinity for proteins than nitrocellulose so the methanol normally used in electrotransfer from gel to support can be omitted. However, both with and without methanol, specific detection of the 16K protein was not achieved (Fig. 13). Even the RaC 16K failed to detect the 16K protein in immunoblots using the nylon support (Fig. 13). This result shows that the support can affect the binding of the antiserum to the 16K protein. One disadvantage of nylon, compared to nitrocellulose, is that staining of transferred protein is not possible.

To more quantitatively compare the nylon and nitrocellulose supports, blots using marker proteins, gap junctional proteins from mouse liver and Nephrops norvegicus hepatopancreas, KLH coupled to the peptide and KLH were used. The proteins were solubilized with 1% SDS buffer and applied directly to the support i.e. omitting the potentially variable transfer step. The dot blots were then probed with preimmune serum, site specific antisera and affinity purified antibodies. The results (Fig. 14 and Table 2) show that there are minor differences in the detection of antibody binding using the two supports and that the affinity purified antibodies show decreased binding to KLH but not significantly increased binding to

Figure 11

Immunoblots Using Site Specific Antiserum and Anti-chicken Liver
Gap Junction Antiserum on Nitrocellulose Supports

a) and (b) autoradiographs of duplicate immunoblots using RaC 16K antiserum (a) or site specific antiserum (b).

Lane 1 Bio-rad Mol. Wt. marker proteins.

2 KLH coupled to peptide.

3 Mouse liver gap junctional preparation (0.1 μ g 16K protein).

4 KLH.

5 Mouse liver gap junctional preparation (1 μ g 16K protein).

6 KLH coupled to peptide.

7 Bio-rad Mol. Wt. marker proteins.

All samples (1-7) were dissolved in an equal volume of SB at room temperature and run on 13.7% acrylamide gels and electrophoretically transferred to nitrocellulose supports as describrd in section 2.2.11.

a

b

1 2 3 4 5 6 7 1 2 3 4 5 6 7

26
16

26
16

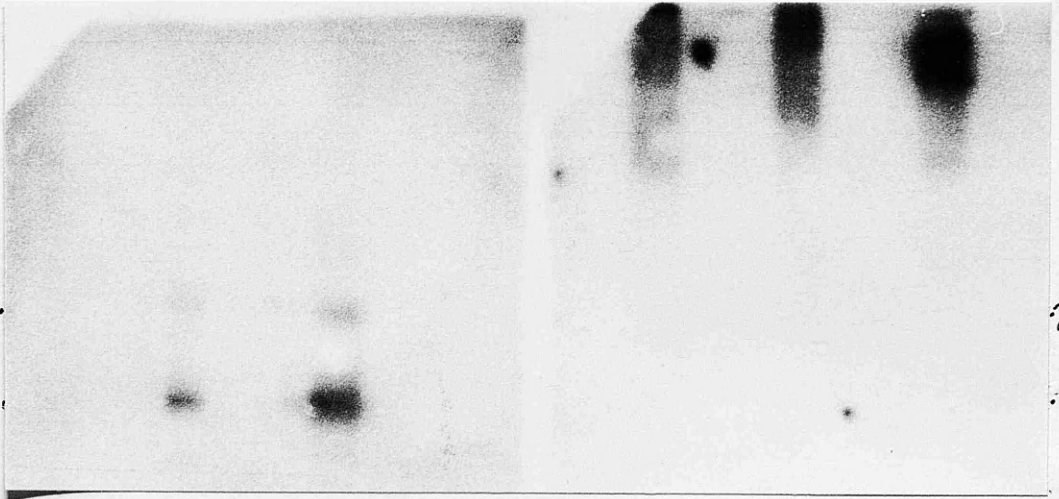


Figure 12

Amido Black Stained Nitrocellulose Replica of Electrophoretically
Transferred Proteins After SDS PAGE

Amido black stained nitrocellulose support after the electrophoretic transfer Bio-rad Mol. Wt proteins and a mouse liver gap junctional preparation.

Lane 1 Bio-rad Mol. Wt. marker proteins ($M_r \times 10^{-3}$).

2 Mouse liver gap junctional preparation showing 16K band.

A 13.7 % acrylamide gel was run with Bio-rad Mol. Wt. markers and a mouse liver gap junctional preparation. The proteins were electrophoretically transferred to the nitrocellulose support as described in section 2.2.11. The nitrocellulose support was stained with 0.1% amido black (w/v) in methanol/acetic acid/water (45/10/45, vol/vol/vol) for 5 min and destained with methanol/acetic acid/water (90/2/8, vol/vol/vol).

Similar replicas were used for probing with antisera, see figure 13.

1 2

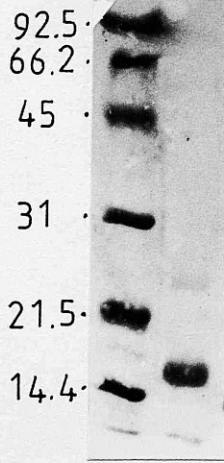


Figure 13

Immunoblots Using Two Different Detection Reagents with the Preimmune Serum and Site Specific Antiserum and Two Supports Using the Site Specific Antiserum and the Whole Rabbit Anti-chicken Liver Gap Junction Antiserum

- a) Autoradiographs of nitrocellulose immunoblots of Bio-rad Mol.Wt.marker proteins (1) and mouse liver gap junctional preparation (2) using the preimmune serum (Pre I) and site specific antiserum (SS). Iodinated sheep anti-rabbit antiserum was used as detection reagent for both immunoblots.

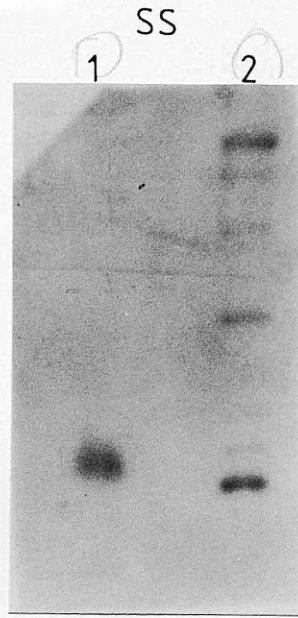
- b) Autoradiographs of immunoblots as in (a) but using donkey biotinylated anti-rabbit and iodinated streptavidin as detection reagents for both immunoblots.

- c) Autoradiograph of a nylon immunoblot of marker proteins (1) and mouse liver gap junctional preparation (2) but using whole anti-chicken liver gap junction antiserum, (RaC 16K). Iodinated sheep anti-rabbit antiserum was used as detection reagent.

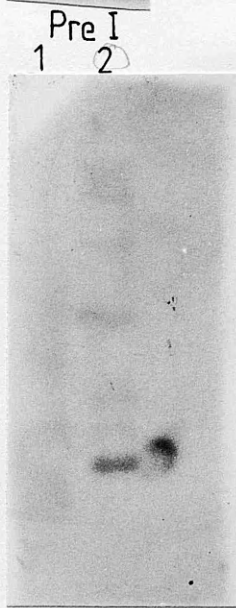
- d) Autoradiograph of an immunoblot as in (c) but using site specific antiserum. Iodinated sheep anti-rabbit was used as detection reagent.

Immunoblotting was carried out as described in section 2.2.11.

a

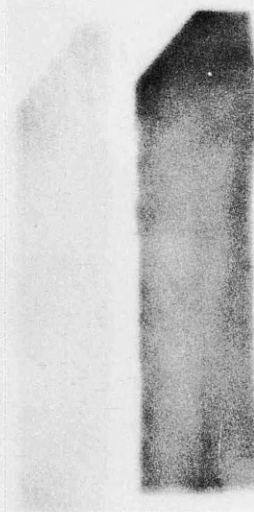


b



c

1 2



d

1 2

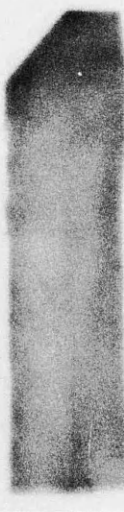


Figure 14

Comparative Dot Blots of Various Antigens on Nylon and Nitrocellulose Membrane Supports

Autoradiograph of dot immunoblots of marker proteins (MP), mouse liver gap junctions (ML GJ), keyhole limpet haemocyanin (KLH), KLH coupled to peptide 1 (KLH/P₁), KLH coupled to peptide 2 (KLH/P₂), Nephrops hepatopancreas gap junctions (NH GJ). Each immunoblot (1) Nitrocellulose support, (2) Nylon support was probed with preimmune serum (PreI), site specific affinity purified serum 1 (Aff 1), site specific affinity purified serum 3 (Aff 3), unfractionated site specific antiserum 1 (SS 1), unfractionated site specific antiserum 3 (SS 3). All antigens were solubilized in an equal volume of SB. 2 µl volumes were directly applied to the membrane supports and allowed to air dry. Detection of antibody binding was carried out as described in section 2.2.11.

Quantitation of dot immunoblots is shown in table 2.

PreI

1 2

Aff1

1 2

Aff3

1 2

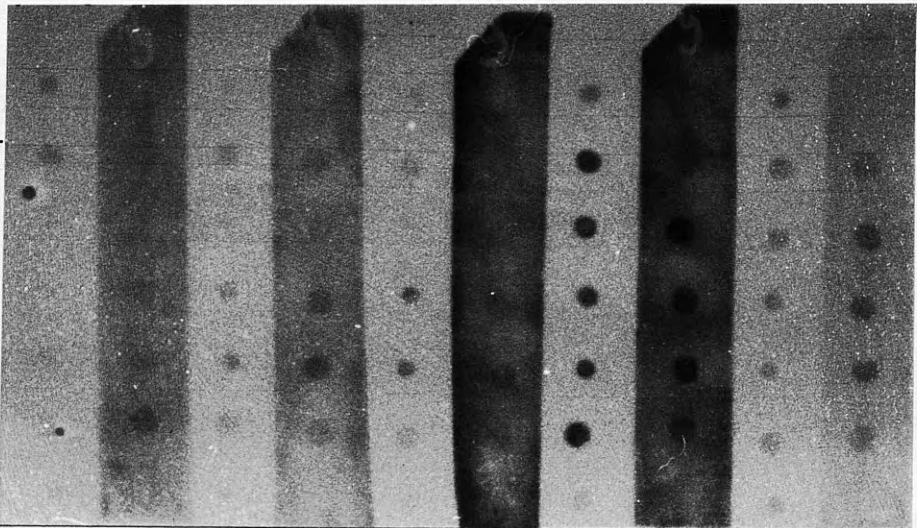
SS1

1 2

SS3

1 2

MP
MLGJ
KLH
KLH/P₁
KLH/P₂
NHGJ
MP



Quantitation of Microdensitometer Traces of Figure 14
Autoradiograph

The abbreviations are explained in the legend to figure 14. The autoradiograph of figure 14 was scanned in a Helena Laboratories Gel Scanner. Gel scans were quantitated as described in section 2.2.4. The integrated values of density were then normalized (integrated density value of dot/integrated density value of preimmune dot) to the values determined for the preimmune serum. Values greater than 1 show that the detected binding was greater than that found with the preimmune serum and values less than 1 show that the detected binding was less than that found with the preimmune serum.

SERUM										
Antigen	Pre I		SS1		Aff 1		SS3		Aff 3	
	Nitro-cell.	Nylon								
MP	1	1	0.84	0.5	0.16	0.2	0.63	0.8	0.35	0.4
MLGJ	1	1	1.69	2.8	0.29	1.4	1.2	12	0.5	1.3
KLH	1	1	17.81	45.7	0.8	0.7	4.4	16.7	16	0.33
KLH/P ₁	1	1	9.9	27.1	3.1	2.6	4.6	3.78	8.9	1.33
KLH/P ₂	1	1	8	36.7	6.8	3.5	3.4	28	7.3	3.7
NH GJ	1	1	4.2	17	1.93	0.21	1.22	0.4	1	0.3

the gap junctional preparations.

This failure to obtain a specific blotting or immunoprecipitation reaction was a serious setback, however the data from Table 2 suggested that affinity purification may better be achieved by purifying the antiserum not against the peptide but against the 16K protein itself i.e. enriching for those antibodies which bind to the 16K protein preferably when bound to a nitrocellulose support.

In addition, recent work in the laboratory has been directed towards raising monoclonal antibodies to junctional proteins. Analyses using these antibodies are also difficult and it was necessary to modify the original Towbin *et al.* (1979) immunoblotting technique. This modified technique (see section 2.2.12) was also used for the analysis of the site specific antiserum. The inclusion of 1M KI in the final wash of the immunoblotting technique improves the signal to noise ratio. The antibody binding to the marker proteins is decreased to below detection limits. The higher ionic strength of the wash buffer presumably reduces non-specific ionic interactions between the antibody and the proteins on the nitrocellulose while sufficient antibody still binds to the 16K protein (Fig.15a)

Furthermore application of the same blotting procedure to whole mouse plasma membranes (Fig. 15b) using antibodies from the site specific antiserum affinity purified against 16K protein bound to nitrocellulose (see legend to Fig. 15), shows activity against bands which migrate in the same position as the higher molecular weight aggregates of the 16K protein. The immunoblot also shows the affinity purified antibodies react with the 16K protein from a mouse gap junctional preparation and gel purified electroeluted 16K and 26K proteins. The 26K band co-migrates with the 26K band labelled in the plasma membrane fraction.

3.2.3 Alternative Immunoprecipitation

As already suggested one possible explanation for the failure to immunoprecipitate iodinated 16K protein is that the iodination of the tyrosine in position four of the sequence (near the middle of the nonapeptide) may change the antigenic to such an extent that the antibodies fail to bind to the protein. Immunoprecipitation

Figure 15

Immunoblots Using Whole Site Specific Antiserum and Nitrocellulose
Affinity Purified Fraction

a) Autoradiograph of an immunoblot similar to that shown in figure 12, Bio-rad Mol. Wt. marker proteins (1), and mouse liver gap junctional preparation (2) probed with the whole site specific antiserum.

b) Amido black stained nitrocellulose support after the electrophoretic transfer of mouse liver gap junctional preparation (1), mouse plasma membrane preparation (2), and a heated (100°C, 5 min in 1% SDS) mouse liver gap junctional preparation (3).

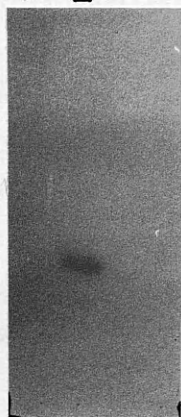
c) Autoradiograph of a corresponding immunoblot to (b) using nitrocellulose affinity purified fraction from site specific antiserum.

Proteins were electrophoretically transferred to nitrocellulose and immunoblotted as described in section 2.2.12. The nitrocellulose affinity purified fraction was different to that previously described. Nitrocellulose squares (1 cm²) were incubated overnight at 4°C with ~ 10 µg of mouse 16K protein, electroeluted from preparative SDS PAGE (see section 2.2.3). The derivitized squares were then incubated for 2 h at 37°C in PBS containing 10% foetal calf serum, rinsed briefly in PBS and treated with 200 µl of rabbit site specific antiserum at 4°C overnight. The antiserum treated squares were washed in several 100 ml changes of PBS over a 2 h period and eluted with 0.2 M glycine/HCl buffer, pH 2.2. The eluate was rapidly neutralized with 1 M Tris/HCl buffer, pH 8.

a

1 2

16

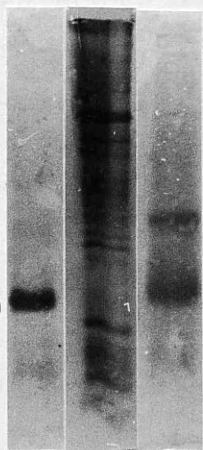


b

1 2 3

16

26

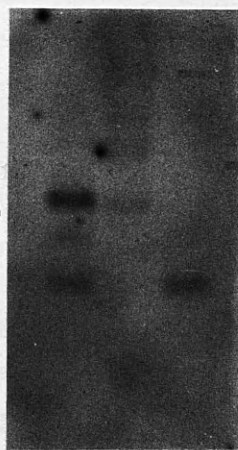


c

3 2 1

26

16



was therefore tried using a microimmunodiffusion (Ouchterlony) assay system with unlabelled protein.

Agarose (1%) microimmunodiffusion plates were cast as described in the legend to figure 16. The site specific antiserum and affinity purified antibodies were tested against SDS solubilized mouse liver gap junctions and electroeluted 16K protein. Figure 16 shows the SDS PAGE profile of the two antigens and the results of the microimmunodiffusion analysis. Both the site specific antiserum and the affinity purified antibodies recognize, as shown by precipitin lines stained with Coomassie blue, a precipitable antigen in the solubilized gap junctions and the electroeluted 16K protein. The precipitin lines are joined which suggests that the antiserum is recognising the same antigen in the electroeluted 16K protein and the mouse liver gap junctional preparation. The preimmune serum does not form detectable precipitates.

The activity of the antiserum was titrated by testing serial dilutions against a constant amount of antigen (SDS solubilized gap junctions), and by serially diluting the antigen against a constant antiserum concentration. Placing serial dilutions of the antiserum, in successive wells produces a spiral precipitate around the central antigen well. The precipitin lines decrease in intensity when the antigen is serially diluted and placed in the outer wells (Fig. 17).

The site specific antiserum is directed against an octapeptide, a relatively short sequence, and it is perhaps surprising that it forms an immunoprecipitate in the microimmunodiffusion system. One explanation is that precipitation is due to a combination of 16K protein multimerization (dimerization or aggregation to higher molecular weight forms) and crosslinking with the antibodies. To examine this possibility mouse liver gap junction preparations were heated so as to induce multimerization to the dimer and higher molecular weight aggregates. If this explanation is correct then the immunoprecipitates should form in the same position.

Figure 16

Microimmunodiffusion Analysis of Mouse Liver Gap Junction
Preparation and Electroeluted 16K Protein

a) Coomassie stained SDS PAGE analysis of antigens used in the microimmunodiffusion analysis.

Lane 1 Bio-rad Mol. Wt. marker proteins ($M_r \times 10^{-3}$).

2 Mouse liver gap junction preparation.

3 Electroeluted 16K protein.

b) Coomassie stained microimmunodiffusion plate.

GJ mouse liver gap junction preparation.

EE electroeluted 16K protein.

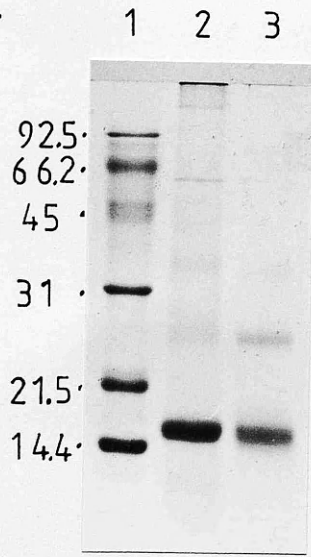
SS site specific antiserum.

Aff 1 affinity purified antibodies.

PreI preimmune serum.

The antigens were placed in the outer wells (the same for each set) and the sera in the inner wells of 1% agarose gels (buffer PBS). The microimmunodiffusion plates were incubated overnight at 4 °C. Washed over 3-4 h with several changes of PBS and stained with Coomassie Brilliant Blue, the same as SDS-polyacrylamide gels.

a



b

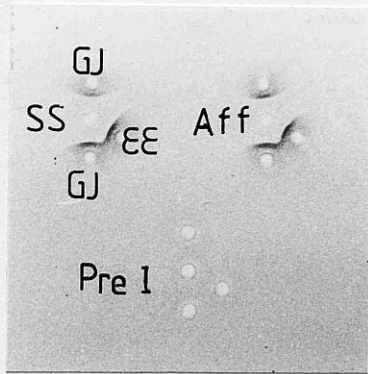


Figure 17

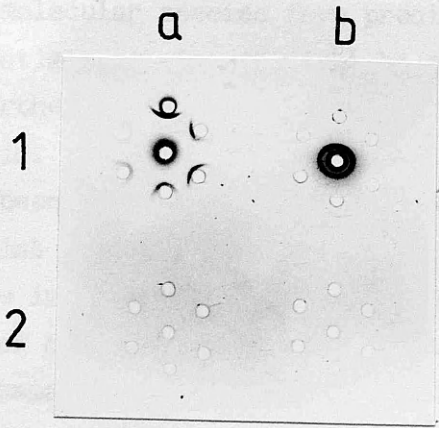
Titration of Site Specific Antiserum

(a,1) Serial dilutions (1:2, 1:4, 1:8, 1:16, 1:32) of solubilized mouse liver gap junctional preparation, as in figure 16, was placed in the outer wells of 1% agarose plate. The site specific antiserum was placed in the central well.

(b,1) Serial dilutions (1:2, 1:4, 1:8, 1:16, 1:32) of site specific antiserum were placed in the outer wells. A solubilized mouse liver sample was placed in the inner well.

(a,2) and (b,2) were the same as in (a,1) and (b,1) except that the preimmune replaced the site specific antiserum.

The agarose plate was incubated overnight at 4^o C and then washed over 3-4 h with several changes of PBS before staining with Coomassie blue.



The SDS PAGE profile of the heated antigen (Fig. 18a) shows that heating at 100 °C gradually increases the formation of multimers of 16K protein (Finbow *et al.*, 1983). Microimmunodiffusion analysis shows that precipitin lines are formed at the same distance from the antigen well with the heated and non-heated samples. If the multimers seen in SDS PAGE are stable under immunodiffusion conditions then a possible explanation for the formation of the immunoprecipitates is that multimers of the 16K protein (which would have multiple antibody binding sites) interact with the site specific antibody. However the actual aggregation state of the 16K protein cannot be ascertained at the point of precipitation and it is possible that the monomer itself, if the N-terminal octapeptide can bind two antibody molecules, could be responsible for the precipitates. Because single precipitin lines are formed at the same position with all the samples (which have marked differences in their monomer to multimer ratios), it seems unlikely that both molecular species form precipitin lines.

In unheated antigen samples it might be expected that dimerization and further aggregation will occur as the SDS diffuses away from the protein. Reduction of the SDS concentration during electroelution has been shown to induce multimer formation (e.g. Fig. 16a). This point will be discussed further (section 4) in conjunction with the immunoblotting data (Fig. 15) which appears to show the presence of higher molecular aggregates of the 16K protein in crude plasma membrane preparations (Fig. 15).

3.2.4 Agglutination

The microimmunodiffusion and the immunoblotting results show that the site specific antiserum binds to the 16K protein and its higher molecular weight aggregates. The immunoblotting results of antibody binding to the higher molecular weight aggregates in liver plasma membrane homogenates (Fig. 15) are consistent with the 16K protein being a plasma membrane component but further data is necessary to confirm localization of the antigen in the gap junction structure. An assay system was therefore devised which depends on antibody binding to intact gap junctions and can be used to show the specificity of the antiserum.

Isolated whole gap junctions, when incubated with the site specific antiserum form clumps which are visible under the light microscope (Fig. 19). Preimmune serum does not clump gap junctions (Fig. 19). To show that these clumps are aggregated gap junctions

Figure 18

Aggregation of 16K Protein and Microimmunodiffusion Analysis

a) Coomassie stained SDS PAGE of mouse liver gap junctional preparations heated at 100 °C for the following times.

Lane 1 Bio-rad Mol. Wt. marker proteins ($M_r \times 10^{-3}$).

2 20 min.

3 15 min.

4 12 min.

5 9 min.

6 6 min.

7 3 min.

8 0 min.

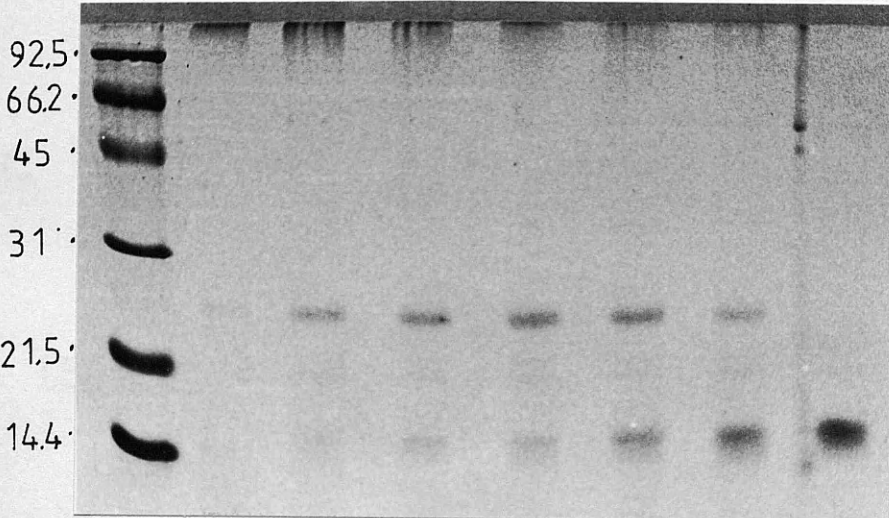
b)(i) Coomassie stained microimmunodiffusion analysis. The well numbers correspond to the lane numbers given above. The samples were put in alternate wells. The site specific antiserum was placed in the central well. Duplicate patterns are shown with smaller distances between the central and outer wells.

b)(ii) conditions as b(i) but immunodiffusion analysis was carried out in adjacent wells to examine continuity of precipitin lines.

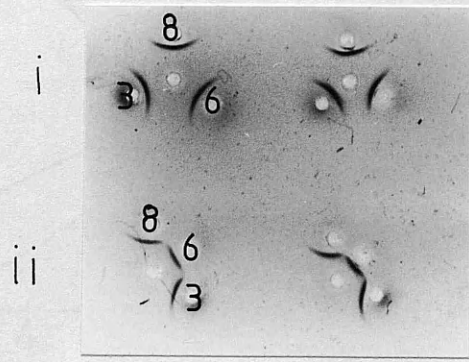
c) Graph based on densitometer scans of the SDS polyacrylamide gel shown in (a), showing the amounts of the monomer (16K, ●—●), the dimer (26K, ○—○), the highly aggregated material (-----) at the top of the running gel is unresolved.

a

1 2 3 4 5 6 7 8



b



C

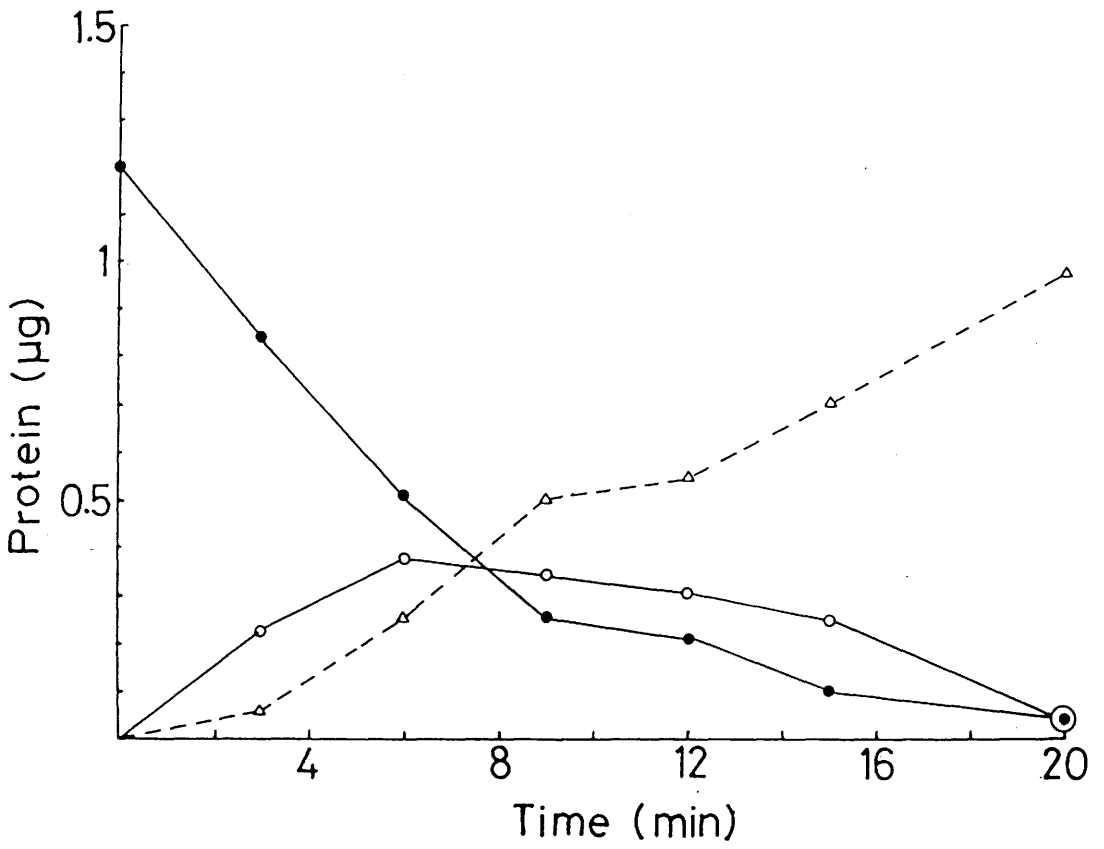


Figure 19

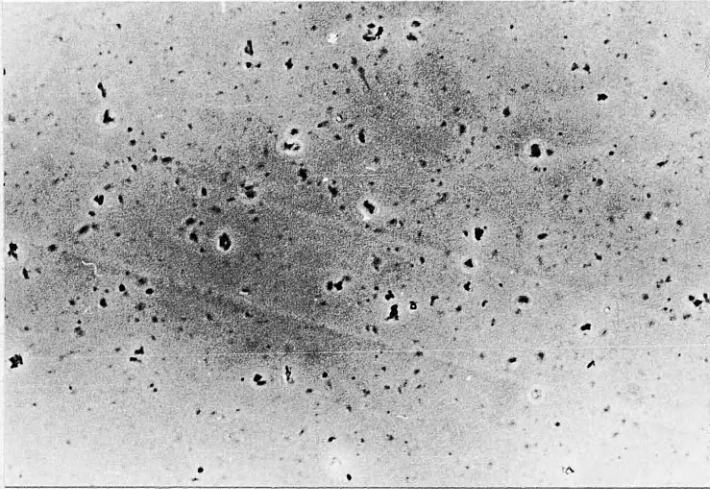
Agglutination of Mouse Liver Gap Junctional Preparation

Phase light micrographs of mouse liver gap junctional preparation incubated with preimmune serum (a), site specific antiserum (b), and affinity purified antibodies (c).

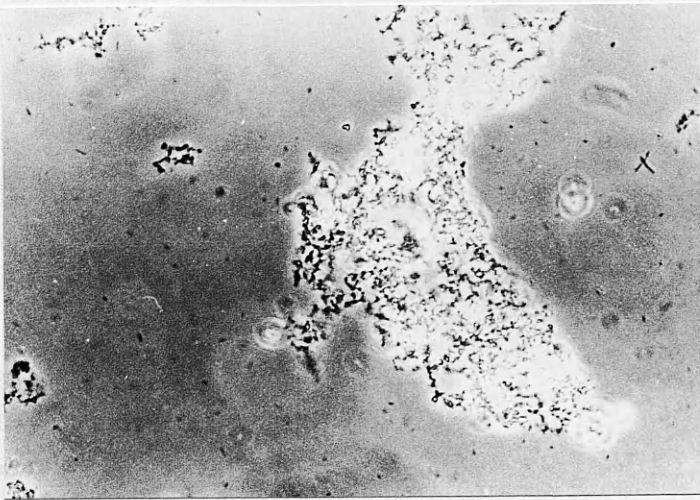
Magnification 900x

The agglutination reaction was carried out as described in section 2.2.13.

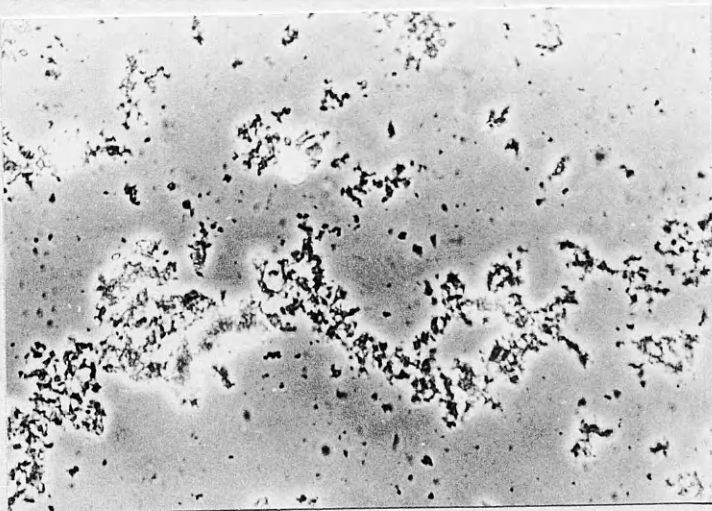
a



b



c



the "agglutination" assay was performed in droplets on electron microscope grids. Figure 20 shows the appearance of clumps of gap junctions, negatively stained with PTA, after incubation with the site specific antiserum.

Serial two-fold dilution of the site specific antiserum produces an end point to the agglutination assay (Fig. 21). There is no detectable clumping with further dilutions.

As the agglutination assay has an easily determined endpoint and it is done in solution it is amenable for the analysis of potential inhibition by the free peptide used as the initial immunogen.

Aliquots of site specific antiserum were incubated overnight with concentrations of peptide over the range of 1 μ M to 10 mM. They were then serially diluted, maintaining the peptide concentrations and mixed with junctions which had also been suspended with the peptide at the same concentrations. The state of agglutination in each sample was scored in terms of three values: agglutination = 1, partial agglutination = 0.5 and no agglutination = 0. Examples of these states of agglutination are shown in figure 22a. These values were plotted against the serial dilutions of the antiserum for the various peptide concentrations. The results are shown graphically in figure 22b. The graphs show that at concentrations above 5 mM the formation of the antibody-junction complex is completely inhibited. At concentrations below 1 μ M no inhibition is detectable. The titrations of the antiserum between these two concentrations show intermediate degrees of inhibition.

The affinity purified antibodies are predominantly IgG and the class of antibody binding to the junctions was also shown to be IgG by incubating the agglutinated junctions with biotinylated anti-rabbit IgG (Fig. 23). The anti-rabbit IgG was detected with fluorescein conjugated streptavidin. Neither the biotinylated anti-rabbit IgG nor the streptavidin causes agglutination when incubated separately with the intact gap junctions.

The agglutination of isolated gap junctions indicates that the N-terminus is available for antibody binding i.e. it is on the edge or the cytoplasmic face of the gap junction. The fluorescent

Figure 20

Electron Microscopy of Negative Stained Agglutinated Mouse Liver
Gap Junction Preparation

Electron micrographs of mouse liver gap junction preparation agglutination complexes.

The agglutination reaction was carried out as described section 2.2.13 except a carbon coated electron microscope copper (300 mesh) grid was used. The complexes were stained with PTA (pH 7.4), as described in section 2.2.5.

- a) magnification 20,000x
- b) magnification 40,500x
- c) magnification 63,000x
inset magnification 190,000x

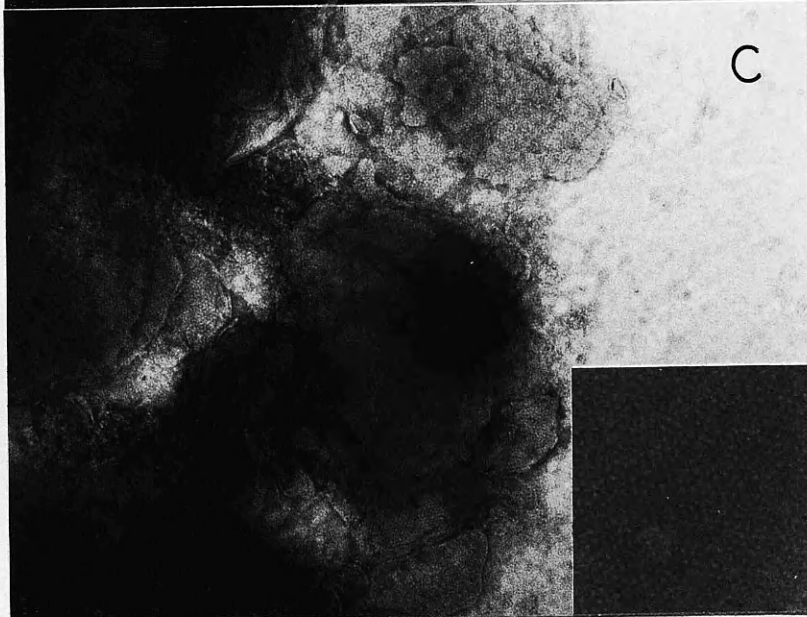
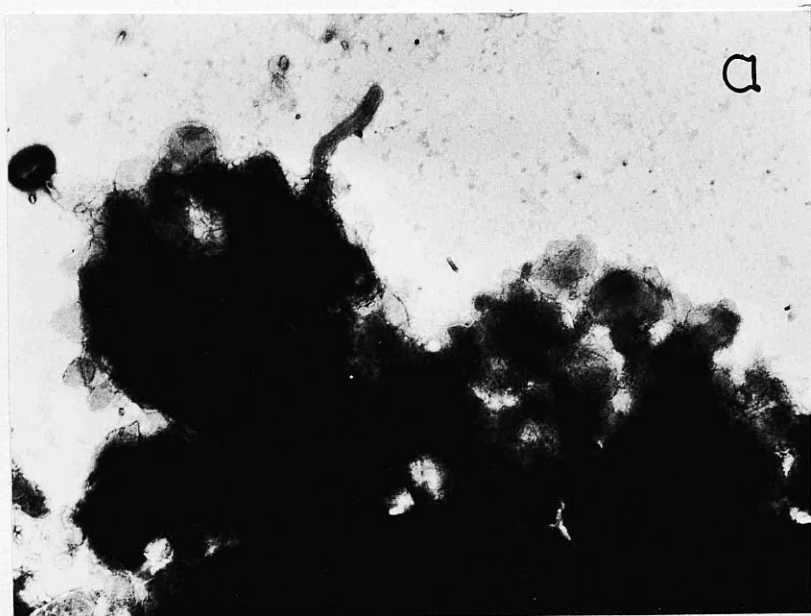


Figure 21

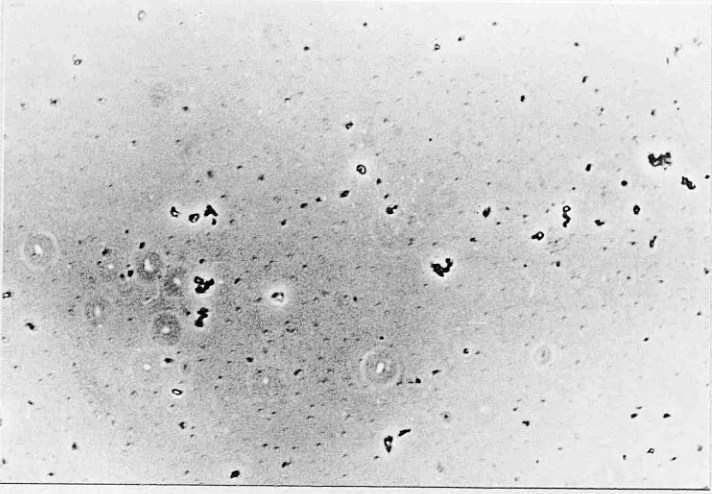
Titration of the Site Specific Antiserum by Agglutination of
Isolated Gap Junctions

Phase light micrographs of a mouse liver gap junction preparation incubated with (a) preimmune serum, (b) 1:8 dilution of site specific antiserum (SS), (c) 1:16 dilution of SS, (d) 1:32 dilution of SS

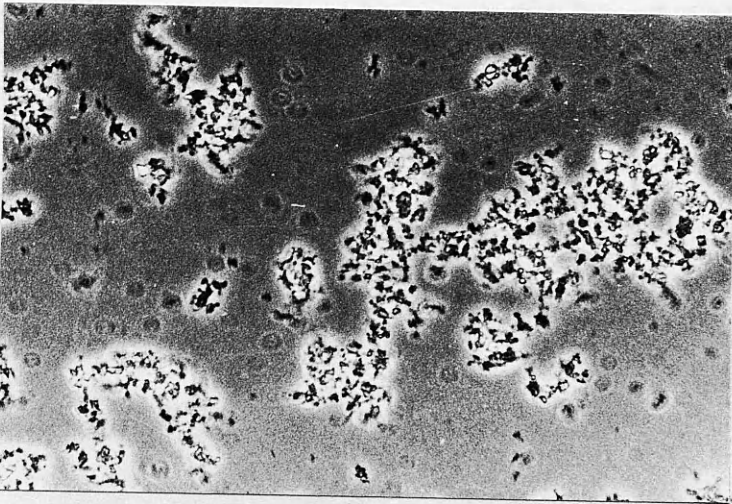
Magnification for all micrographs 900x.

The agglutination reaction was carried out as described in section 2.2.13.

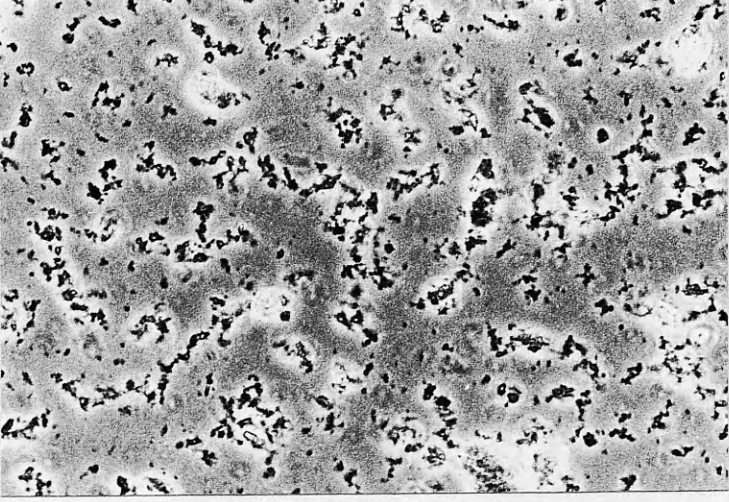
a



b



C



D

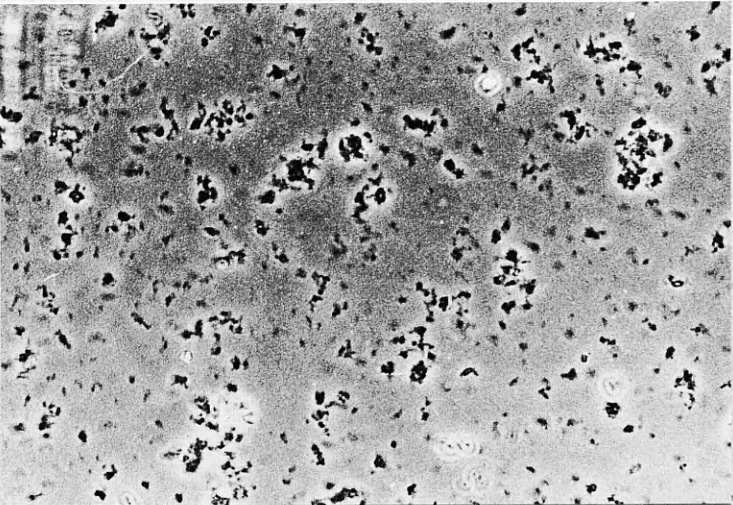


Figure 22

Peptide Inhibition of Agglutination

a) Phase light micrographs of examples of states of agglutination assigned arbitrary values for graphical representation of the peptide inhibition of agglutination (see b).

Agg = 1, agglutination.

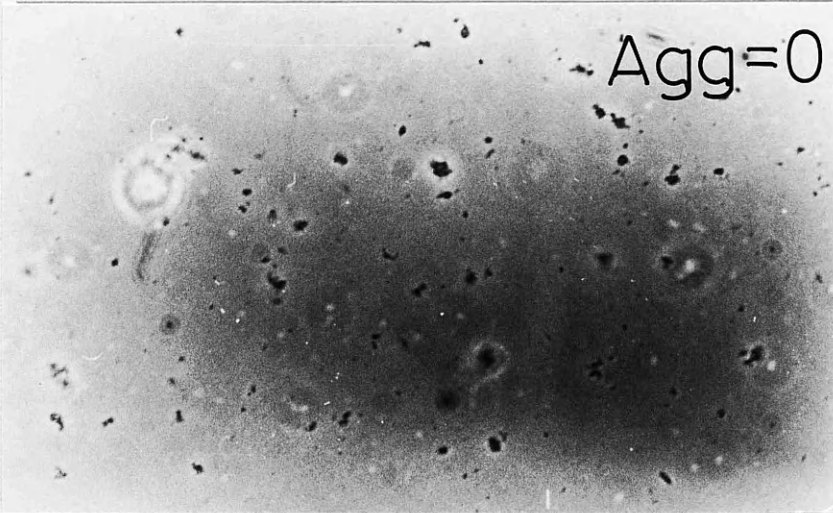
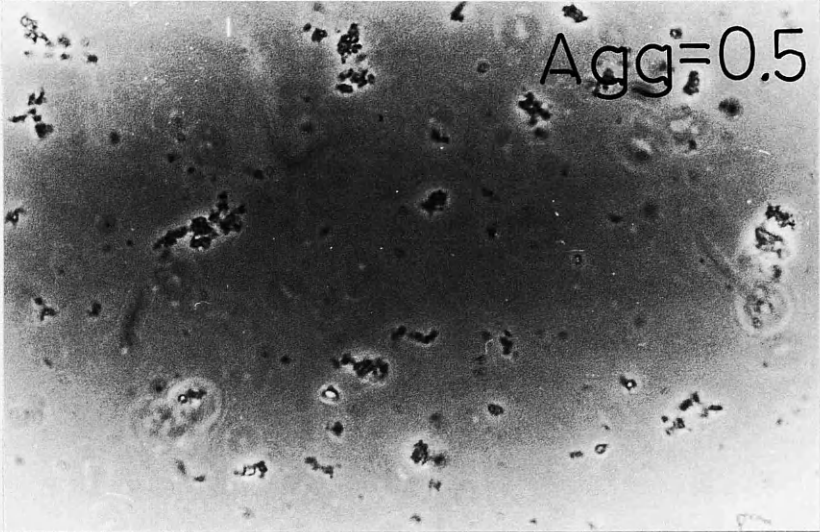
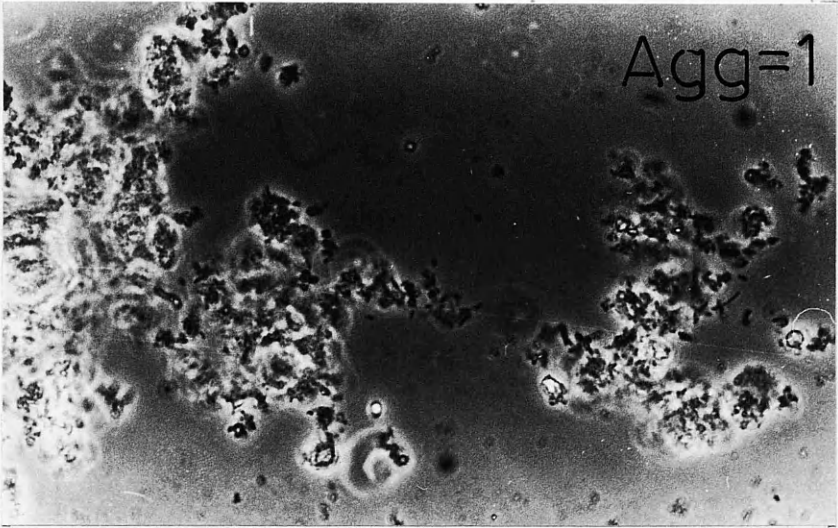
Agg = 0.5, partial agglutination.

Agg = 0, no agglutination.

Magnification 1400x

b) graphical presentation of peptide inhibition titration of agglutination complexes.

For experimental details see section 2.2.13.



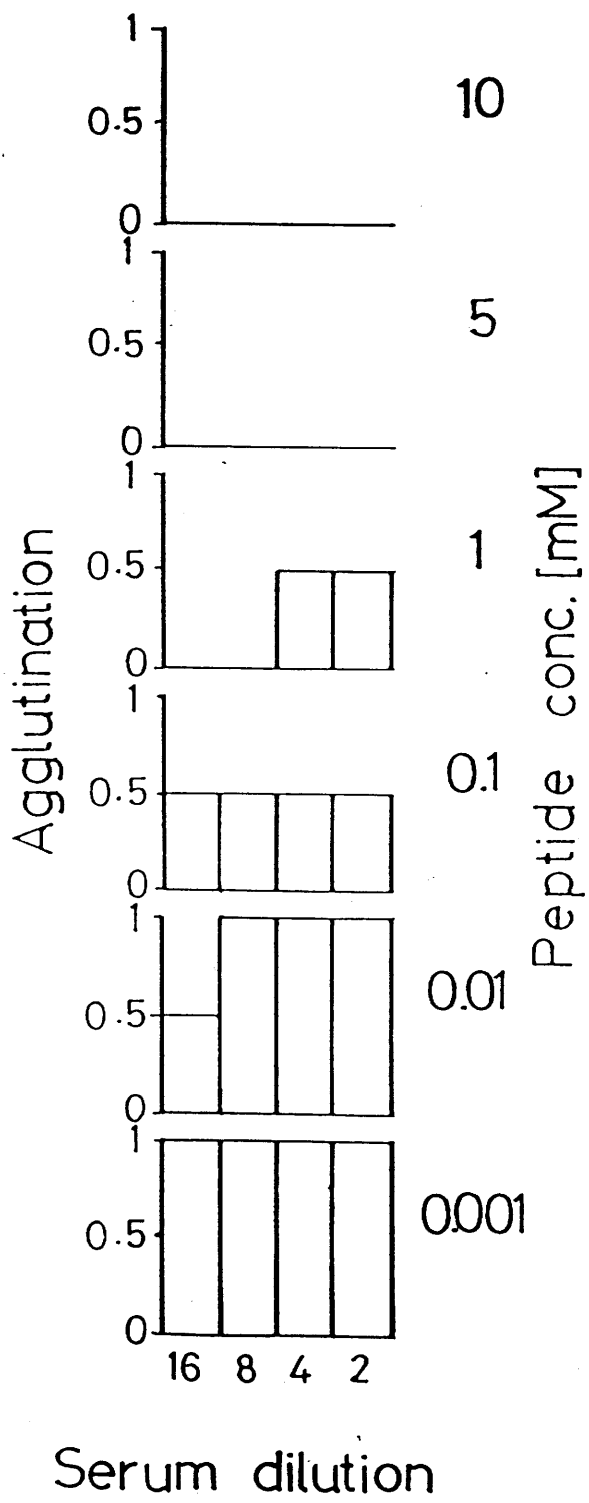


Figure 23

Fluorescent Labelling of Agglutinated Mouse Liver Gap Junction
Complexes

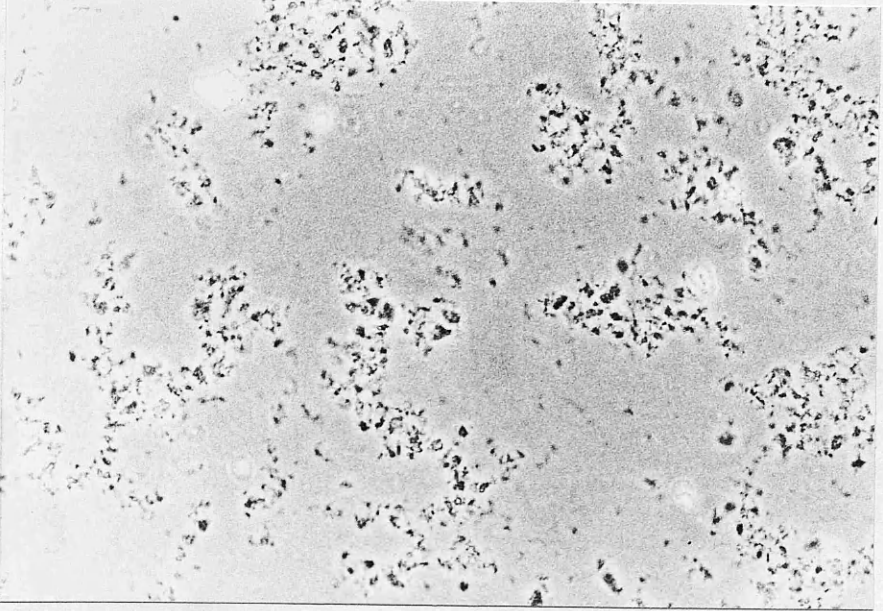
- a) Phase light microscope picture of agglutinated mouse liver gap junctions.
- b) Fluorescently labelled mouse liver gap junctional agglutination complexes. The field of view is the same as in (a).

Magnification 900x

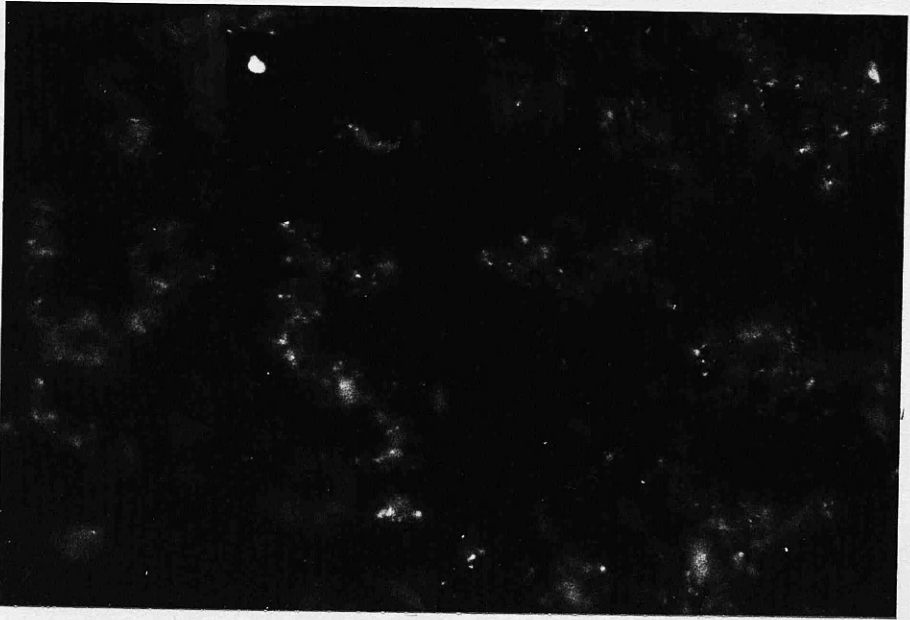
The agglutination reaction was carried out as described in section 2.2.13. The junction/antibody suspension was then incubated for 1 h with biotinylated donkey anti-rabbit antiserum followed by fluorescently labelled (FITC) biotin-streptavidin conjugate for 1 h. The aggregates were washed with PBS and examined by phase and fluorescent microscopy.

Punctate spots are observed after labelling agglutinated mouse liver junctions. The clumps move slightly due to Brownian motion but as they have settled onto the microscope slide the points of contact are held still and appear sharp. The phase picture freezes the movement of the clumps due to the fast shutter speed.

a



b



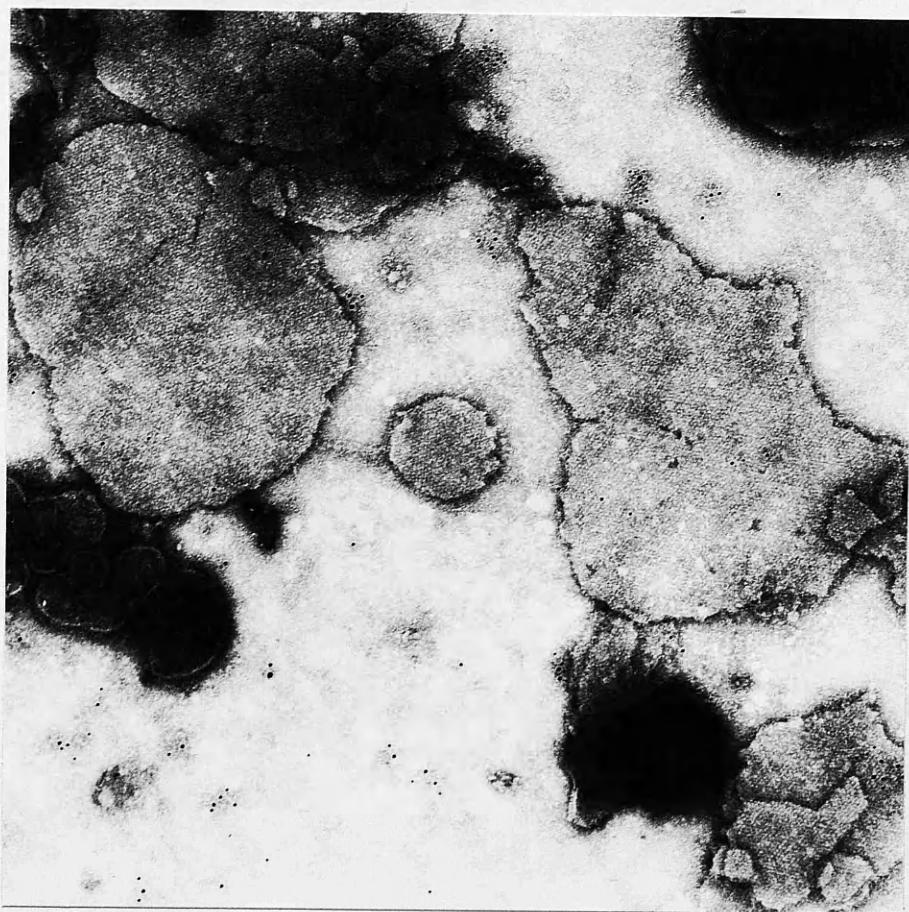
labelling of gap junctions suggested that gold immunolocalization of the antibody binding sites with Protein-A gold might be possible. Isolated mouse liver gap junctions were incubated with immune and preimmune serum. Conjugated Protein-A gold was then added to the junctions which after incubation and washing, were stained with PTA and applied to electron microscope grids. Results show (Fig. 24) that the clumps of gap junctions are decorated with gold and that the gold is spread over the free cytoplasmic faces.

These results can be summarized:

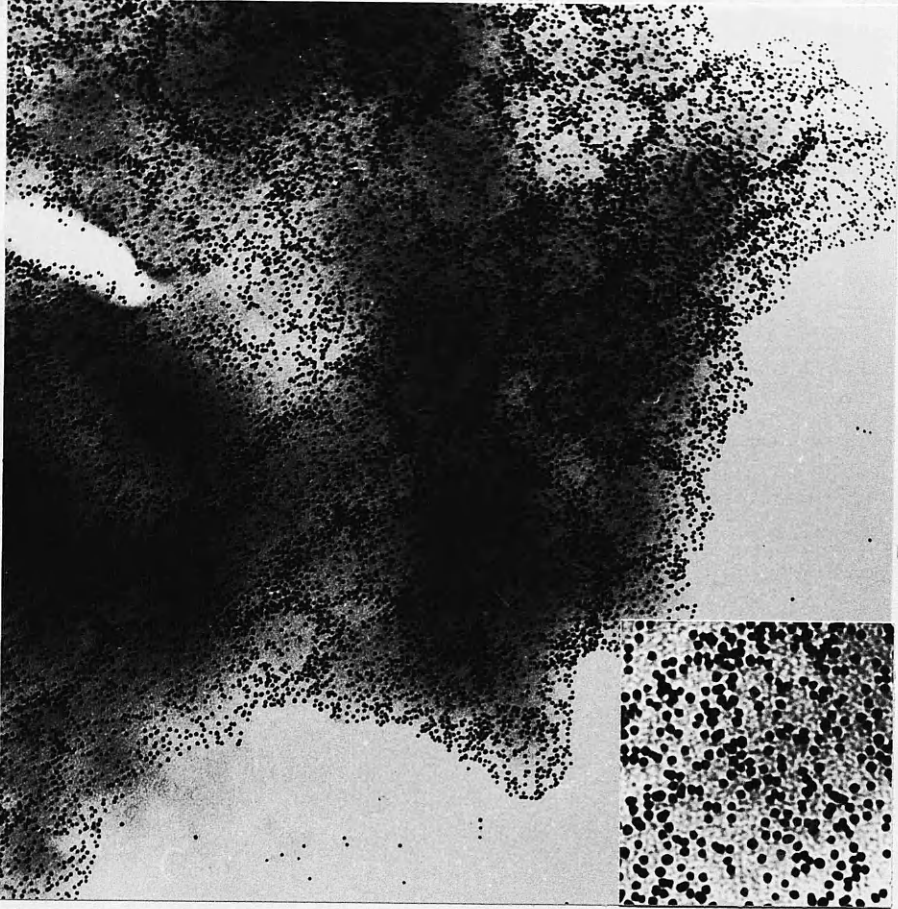
- i) the site specific antiserum recognize 16K protein from gap junctions before and after electroelution, and the 16K protein and its multimeric forms in plasma membrane preparations.
- ii) the site specific antiserum binds to the cytoplasmic faces of isolated gap junctions showing the localization of the N-terminus of the 16K protein.

This last result forms the basis for an investigation into the structural organization of the 16K protein within the gap junction, which is described in section 3.4. The site specific antiserum can also be used to analyse the tissue and species conservation of gap junctional proteins, which is described in the next section (3.3).

a



b



3.3 TISSUE AND SPECIES CONSERVATION OF GAP JUNCTION PROTEINS

3.3.1 Introduction

Gap junctions appear to be conserved at the structural level, as seen by electron microscopy (section 1.1), and at the functional level, as seen by coupling between cells from different tissues and between cells from different vertebrate species in tissue culture (section 1.4), which suggests that the structural protein is likely to be conserved. Immunoblotting analyses with RaC 16K antiserum has indeed shown that the 16K proteins from different murine tissues and different vertebrate species are immunologically related. This immunological relationship has been extended to the Nephrops norvegicus 18K protein by its cross reactivity with RaC 16K antiserum (Finbow et al., 1984; Buultjens et al., 1986).

An advantage of site specific polyclonal antisera over polyclonal antisera is that they can be used to pinpoint regions of homology. The site specific antisera raised against the N-terminal octapeptide of the mouse liver 16K protein were therefore used to examine the proteins isolated from gap junction preparations made from different murine tissues and tissues of different species.

3.3.2 Microimmunodiffusion Analysis

3.3.2a Analysis of Murine Tissues.

Using the isolation procedure of Finbow et al. (1983) gap junctions were prepared from mouse brain, heart, kidney and liver (see section 2.2.1).

The SDS PAGE profiles of these preparations (Fig. 25) shows that a single major protein, Mr 16K, is present in all four

Microimmunodiffusion Analysis of Various Mouse Tissue Gap
Junctional Preparations

a) Coomassie stained SDS polyacrylamide gel of the proteins isolated from the various mouse tissues: brain, B; heart, H; kidney, Ki; and liver, L; Bio-rad Mol. Wt. marker proteins ($M_r \times 10^{-3}$).

b) Coomassie stained microimmunodiffusion plate after reaction of the various mouse tissue gap junction antigens with the site specific antiserum. The code for the antigens is as in (a) with the additions: keyhole limpet haemocyanin (K) and keyhole limpet haemocyanin coupled to the peptide (K/P). The site specific antiserum (SS) and the preimmune serum (PreI) were placed in the central wells as indicated. (b,1 i) and (b,2 i) are duplicates except that the distance from the central to the outer wells is smaller in (b,2,i). (b,i,ii) has the antigens L, H, and K placed in alternate outer wells. (b,2,ii) has the antigens Ki, B, and K/P placed in alternate outer wells. (b,1,iii) and (b,2,iii) are the same as (b,1,i) and (b,2,i) respectively, except the central well contains preimmune serum (PreI)

SDS PAGE was carried out as described in section (2.2.2). The samples for microimmunodiffusion analysis were diluted with an equal volume of water (final [SDS] 0.5%) before application to the microimmunodiffusion plates. The plate was incubated overnight at 4°C, washed in several changes PBS over 2-3 h and stained with Coomassie blue.

Each of the mouse tissue antigens formed an immunoprecipitate with the site specific antiserum. In (b,2,i) it is possible to observe that the precipitin line is continuous for the kidney, heart, and brain gap junctional preparations. This suggests that the epitope recognized by the site specific antiserum is the same in each of these preparations. The major protein present in each of these preparations comigrate on SDS PAGE (Fig. 17a) so it is likely that these proteins isolated from the different mouse tissues are the same.

preparations confirming earlier observations. The yield of 16K protein from mouse liver and kidney was 2 µg/g wet weight. The yield from mouse heart and brain was less at 1 µg/g wet weight. These agree with the findings of Buultjens et al. (1986).

The microimmunodiffusion system was used to test the site specific antiserum against the proteins of the four different murine gap junction preparations. The results show that there is an immunoprecipitate formed with each of the junction preparations tested (Fig. 25). In the set of wells containing all four tissue samples, the precipitin lines are continuous indicating that the site specific antiserum is recognizing the same antigens. The preimmune serum does not form detectable precipitates.

These results suggest that the 16K gap junctional proteins derived from the three different germ layers of the mouse: endoderm, ectoderm and mesoderm all have the same or closely related N-terminal region. Furthermore these results show that the 16K protein can be isolated from excitable and non-excitable cell types.

3.3.2b Species Analysis

Finbow et al. (1984) have shown that the 16K proteins present in gap junction fractions isolated from chicken and mouse liver are immunologically related to each other and to the 18K protein present in junction fractions isolated from Nephrops norvegicus hepatopancreas. Therefore to investigate further the species conservation, with regard to the N-terminal region of the mouse liver 16K gap junctional protein, gap junctions were prepared from the livers of mouse, chicken and Xenopus laevis, and from the hepatopancreas of Nephrops norvegicus (see section 2.2.1).

The SDS PAGE profiles of these preparations (Fig. 26) again show a major 16K band for mouse, chicken and Xenopus liver. The Nephrops hepatopancreas SDS PAGE profile shows the 18K protein and its dimeric form, 28K (Finbow et al., 1984). (Other proteins are present due to the overloading of the gel.)

The proteins from these four different sources of gap junctions were analysed using the microimmunodiffusion system. Each

Figure 26

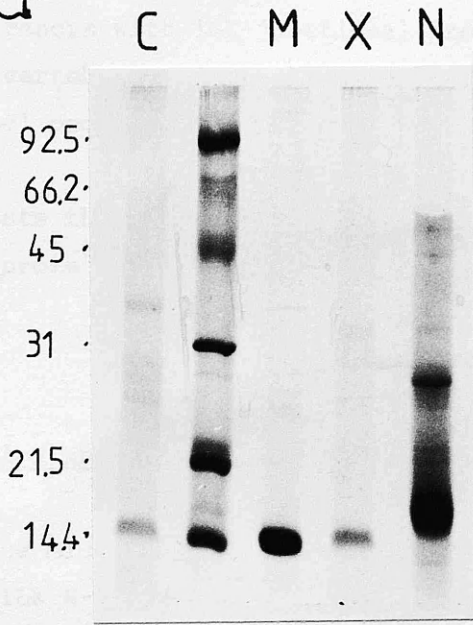
Microimmunodiffusion Analysis of Gap Junctions Preparations from
Different Species

a) Coomassie stained SDS polyacrylamide gel of gap junction preparations isolated from different species: chicken liver, C; mouse liver, M; Nephrops hepatopancreas, N; Xenopus liver, X. Lane 2 shows Bio-rad. Mol. Wt. marker proteins ($M_r \times 10^{-3}$).

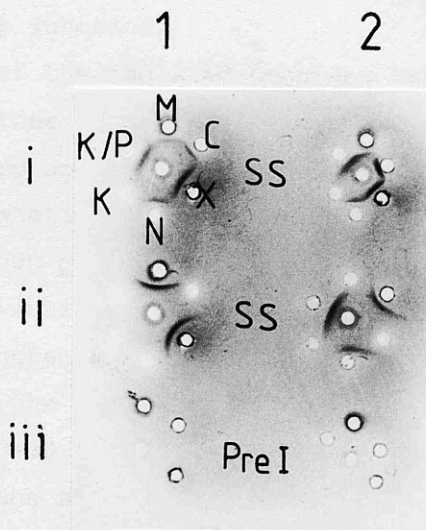
b) Coomassie stained microimmunodiffusion plate after reaction of the antigens from different species with the site specific antiserum. The labelling for the antigens is as in (a) with the addition of keyhole limpet haemocyanin (K) and keyhole limpet haemocyanin coupled to the peptide (K/P). The pattern of wells and reagents were as in the legend to figure 25.

The preparations from each of the different species formed an immunoprecipitate with the site specific antiserum. The precipitates between mouse liver and chicken liver and between Xenopus liver and Nephrops hepatopancreas appear to fuse. This suggests that there is species conservation of the N-terminal region of the various proteins.

a



b



of the junction preparations form an immunoprecipitate when tested against the site specific antiserum (Fig. 26). The precipitin lines appear continuous in the set of wells that contain the four different species. The preimmune serum did not form detectable precipitates.

The microimmunodiffusion results show that the site specific antiserum cross reacts with 16K junctional proteins isolated from three different vertebrate classes, Amphibia, Aves and Mammalia and the 18K junctional protein from the invertebrate Nephrops (phylum Arthropoda).

This suggests that the epitope(s) at the N-terminus of the mouse liver 16K protein has been highly conserved over long periods of evolution.

3.3.3 Agglutination Analysis

Although the microimmunodiffusion assays show conservation of the mouse liver 16K N-terminal epitope across species it does not give any indication of the location of the conserved epitopes in the gap junctional protein. The agglutination assay however can be used to identify the position of the epitope in the isolated Nephrops hepatopancreas gap junction.

Incubation of the isolated Nephrops hepatopancreas gap junctions with either the site specific antiserum or the affinity purified antibodies agglutinates isolated Nephrops hepatopancreas gap junction preparations (Fig. 27). A similar agglutination reaction occurs when Nephrops hepatopancreas gap junctions are incubated with an antiserum raised in rabbits against isolated Nephrops hepatopancreas gap junctions (RaN 18K) (Buultjens *et al.*, 1986) except that the reaction occurs faster, within 2-5 minutes, as compared to the 20-30 minutes using the site specific antiserum. Preimmune serum does not clump isolated Nephrops hepatopancreas gap junction preparations. The aggregates observed in the agglutination assay can be seen by electron microscopy of negatively stained samples to consist of gap junctions (Fig. 28).

Figure 27

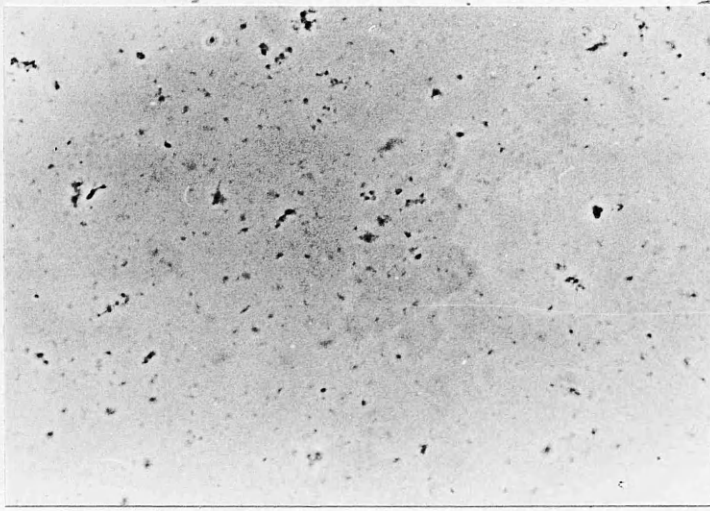
Agglutination of Nephrops Hepatopancreas Gap Junctional
Preparation

Phase light micrographs of Nephrops hepatopancreas gap junctional preparation incubated with preimmune serum (a), site specific antiserum (b), and affinity purified antibodies (c).

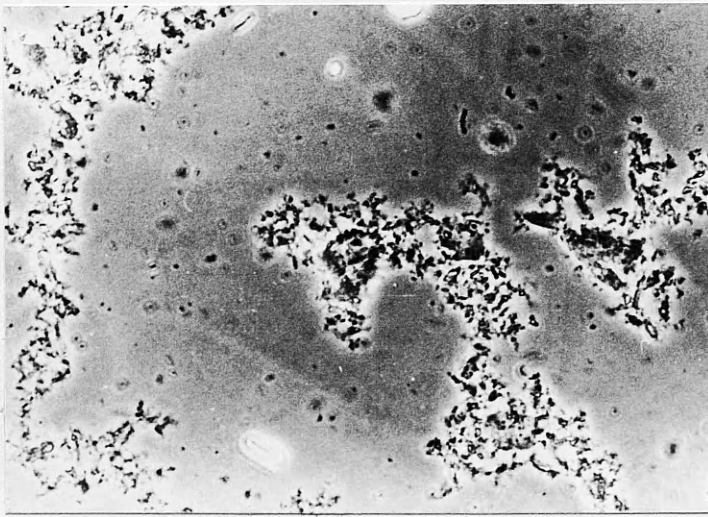
Magnification 900x

The agglutination reaction was carried out as described in section 2.2.13.

a



b



c

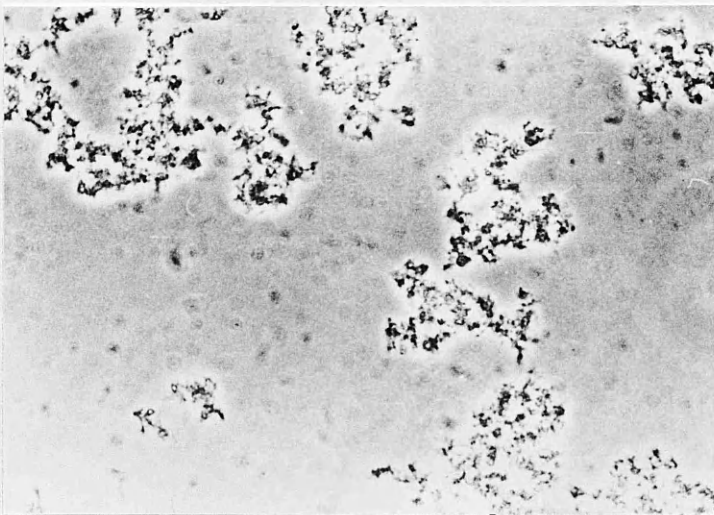


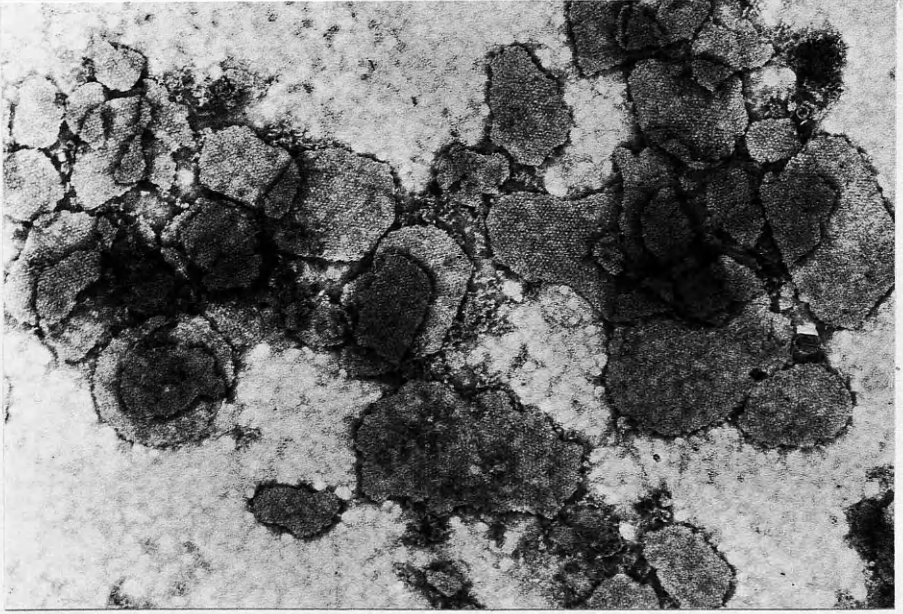
Figure 28

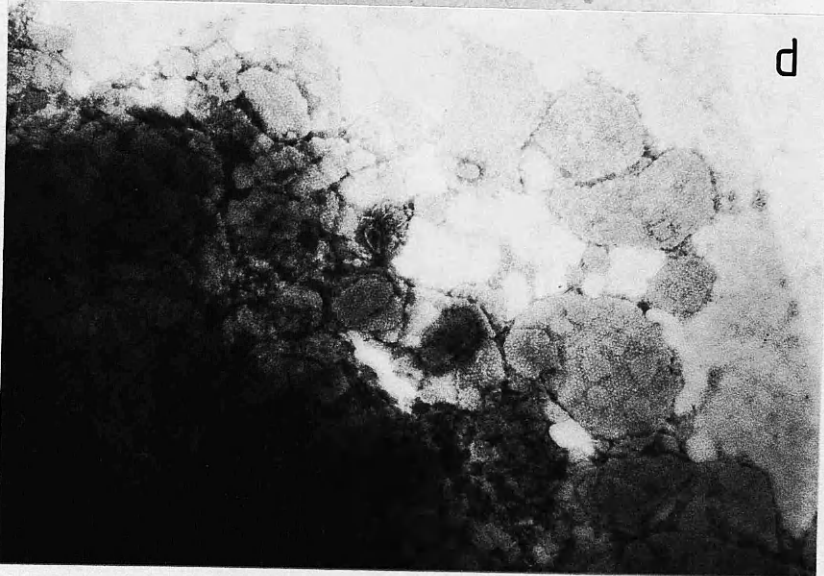
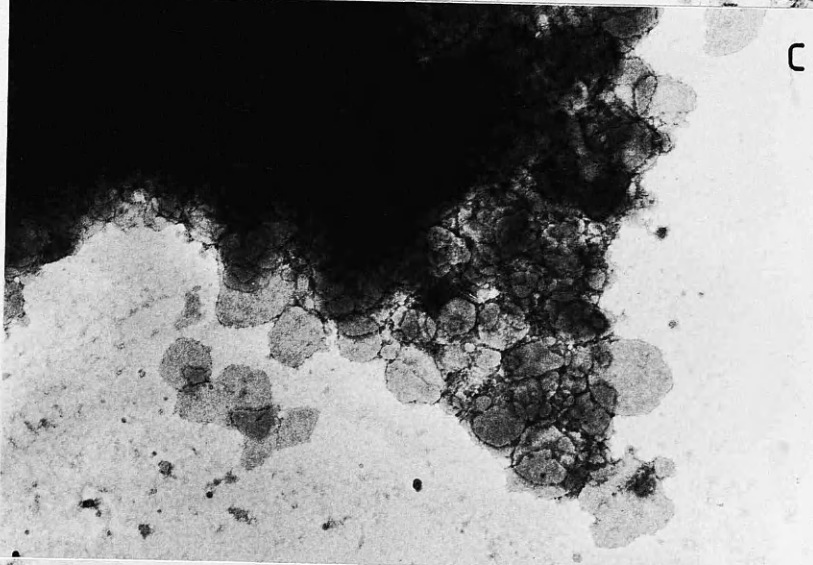
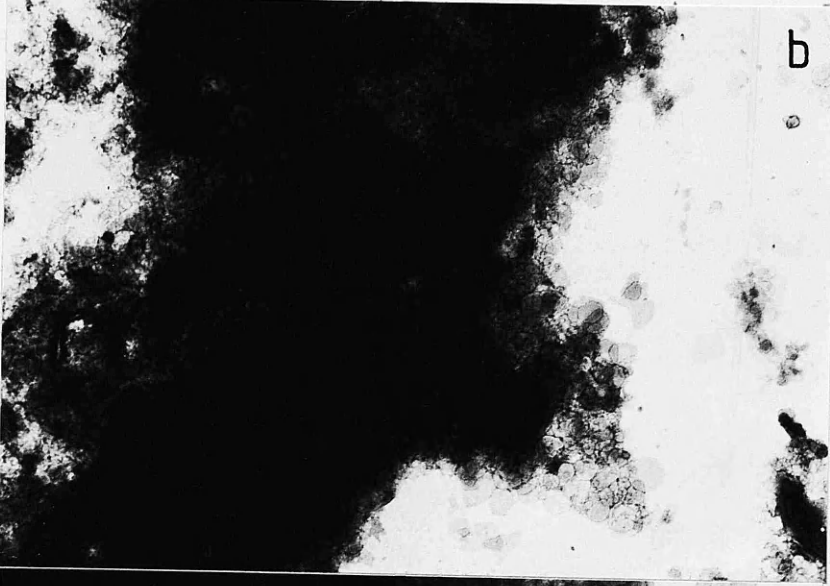
Electron Microscopy of Negative Stained Agglutinated Nephrops
Hepatopancreas Gap Junctional Preparation

Electron micrographs of negative stained agglutinated Nephrops hepatopancreas gap junctions with (a) preimmune serum (Mag. 84,000x), (b-d) site specific antiserum (b, Mag. 10,000x; c, Mag. 15,500x; d, Mag. 64,000x).

The agglutination reaction was carried out as described in section 2.2.13 and the preparations were stained with PTA as described in section 2.2.5.

a





These agglutination results provide further evidence that the N-terminal region of the mouse liver 16K protein is conserved and that in the mouse liver and Nephrops hepatopancreas gap junctions, the N-terminus is located on the cytoplasmic face of isolated gap junctions.

3.4 THE STRUCTURAL ORGANIZATION OF PROTEIN WITHIN THE GAP JUNCTION

3.4.1 Introduction

Gap junctional plaques are isolated with their extracellular faces apposing one another and their cytoplasmic faces exposed to the aqueous environment. Thus the structure of isolated gap junctions enables selective examination of their cytoplasmic domains. Reagents which are used to examine and probe the cytoplasmic domains should not enter the gap between the membranes or the channel (which may or may not be open in isolated gap junctions, but are likely to be closed, section (1.1.5)) and should not dissolve in the lipid. Antibodies and proteolytic enzymes are therefore ideal reagents with which to examine these domains.

3.4.2 N-terminal localization

The agglutination and gold immunolocalization experiments, reported in section 3.2 and 3.3, showed that the site specific antiserum binds to the cytoplasmic face of isolated mouse liver (section 3.2) and Nephrops hepatopancreas (section 3.3) gap junctions. To confirm this, isolated junctions were treated with pronase, a mixture of non specific endo- and exopeptidases obtained from Streptomyces griseus, which should cleave accessible regions on the cytoplasmic faces of isolated junctions and thereby prevent agglutination and immunoprecipitation.

Isolated whole mouse liver and Nephrops hepatopancreas gap junctions were incubated with various amounts (0.1 μ g to 30 μ g) of pronase for 30 min at 37°C to determine a dose response. The pronase treated junctions were then pelleted using an MSE bench top microfuge and washed (3x) with distilled water to remove

pronase. After solubilising the pellets, SDS PAGE analyses showed that increasing pronase concentrations results in an increasing degradation of both the mouse liver 16K protein and the Nephrops hepatopancreas 18K protein (Fig. 29) to lower molecular weight forms. The low molecular weight products formed by pronase digestion of intact gap junctions implies that the pronase is cutting the protein at at least one site on the cytoplasmic face of the gap junction. This site would have to be a loop or loops of the protein domain.

Quantitative analyses (Fig. 30) of the SDS PAGE profiles (Fig. 29) show that the amount of protein lost (not recovered in the lower Mr bands) due to the digestion of protein by pronase (30 μg) is $\sim 3\%$ in the case of the mouse liver protein and $\sim 5\%$ in the case of the Nephrops hepatopancreas gap junctions.

The effects on the density of Nephrops hepatopancreas gap junctions after pronase treatment was investigated by isopycnic buoyant density centrifugation in potassium iodide gradients. Measurements showed that there was less than 1% change in the buoyant density after pronase treatment (1.228 g/cm^3 to 1.225 g/cm^3) (Fig. 31). This result suggests that either there is little protein present on the cytoplasmic surface, which supports the structural studies of Unwin and Ennis (1983) and Hirokawa and Heuser (1982) (see section 1.1.4), or suggests that any protein which is present is inaccessible to pronase.

Preparations of both mouse and Nephrops gap junctions were treated with 30 μg of pronase at 37°C for 30 min and washed as described above, the pellets were analysed by electron microscopy after negative staining. When analysed the pellets show that they contain gap junctions and that with both mouse liver (Fig. 32) and Nephrops hepatopancreas (Fig. 33) pronase treatment does not produce a detectable change in their morphology as compared to those junctions left untreated.

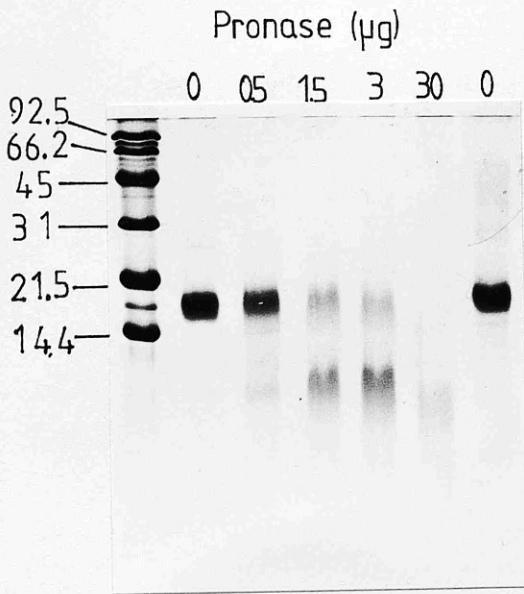
Gap junctions from mouse and Nephrops after being digested with pronase (30 μg , 37°C , 30 min) and washed were analysed by the agglutination assay. The pronase treatment removed or altered the N-terminal region of both mouse liver (Fig. 34) and Nephrops hepatopancreas (Fig. 35) junctional proteins such that the site

Figure 29

Treatment of Gap Junctions with Pronase

Coomassie stained SDS PAGE gels of (a) mouse liver gap junctions, (b) Nephrops hepatopancreas gap junctions. Gap junctions were treated with different amounts of pronase (0.5 - 30 μ g) for 30 min at 37°C. The junctions were then pelleted by centrifugation on an MSE bench top microfuge. The pellets were resuspended and washed (3x) with distilled water before solubilizing and analysing by SDS PAGE as described in section 2.2.2.

a



b

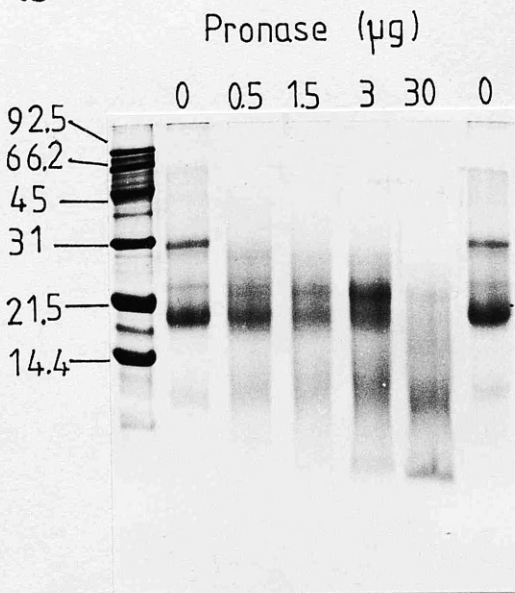


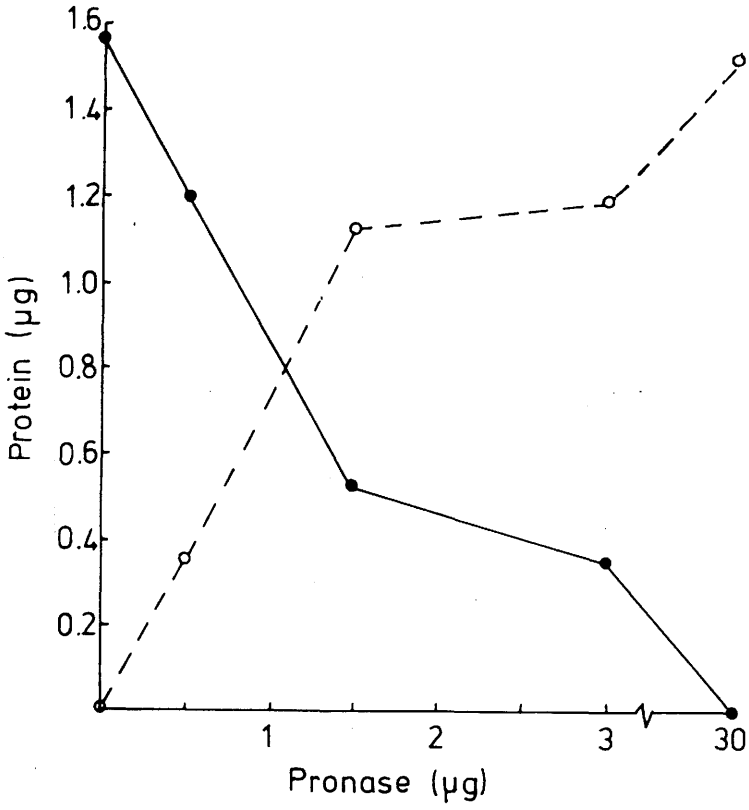
Figure 30

Quantitation of Pronase Treatment of Gap Junctions

Graphs showing the quantitation of the SDS PAGE analysis as shown in figure 29. (a) Mouse liver gap junctions (b) Nephrops hepatopancreas gap junctions.

The graphs show the loss of the 16K (a), and 18K (b) proteins(●—●) of the 28K dimer (○—○) and the formation of the the digestion products (△—△) after treatment with pronase for 30 min at 37°C. The points of the graph were obtained by scanning the SDS PAGE profile with a Helena Laboratories Gel Scanner as described in section 2.2.4.

a



b

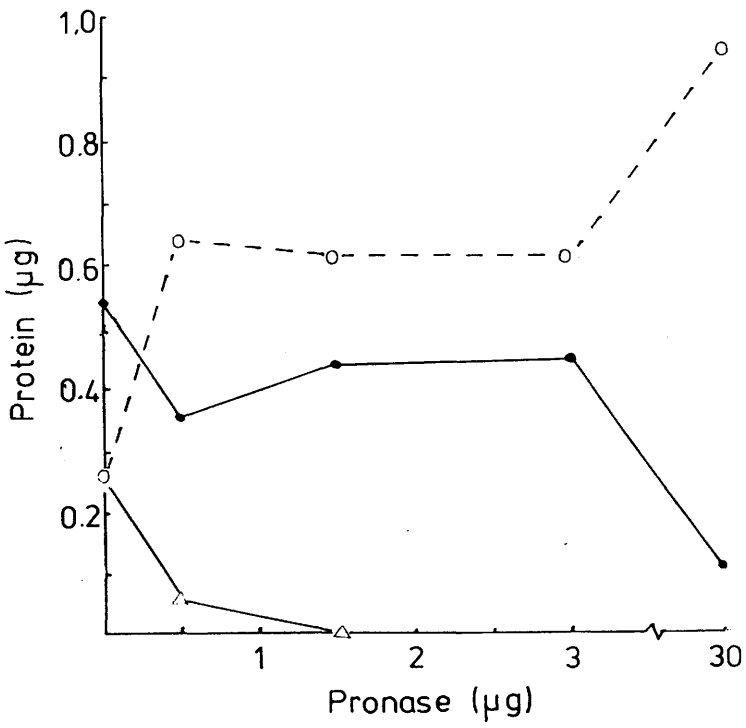


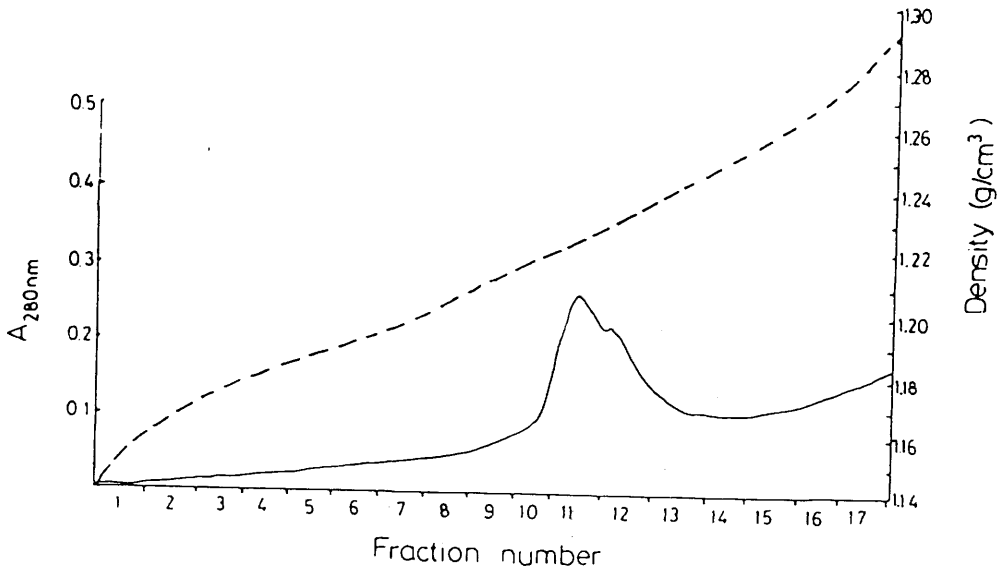
Figure 31

Isopycnic Centrifugation of Nephrops Hepatopancreas Gap Junctions
in Potassium Iodide Gradients

Buoyant density centrifugation of (a) Nephrops hepatopancreas gap junctions treated or (b) untreated with pronase.

Gap junctions were prepared as described in section 2.2.1. The junction pellets were suspended in PBS. One pellet was treated with pronase (30 μ g, 30 min, 37°C) as described in the legend to figure 29. The final pellets with and without pronase treatment were suspended in 0.5 ml 40% KI and layered underneath a 12 ml linear gradient (20-38.3% KI, w/vol). The gradient was centrifuged in a 6 x 14 rotor of an International B60 ultracentrifuge at 209,000g, 15°C for 20 h and harvested by upward displacement with fluorochemical oil. A_{280} nm (—) was monitored using an LKB "Uvicord" and 0.6 ml fractions were collected. The refractive index of each fraction was measured (---) with an Abbe refractometer (calibrated with KI solutions of measured density).

a



b

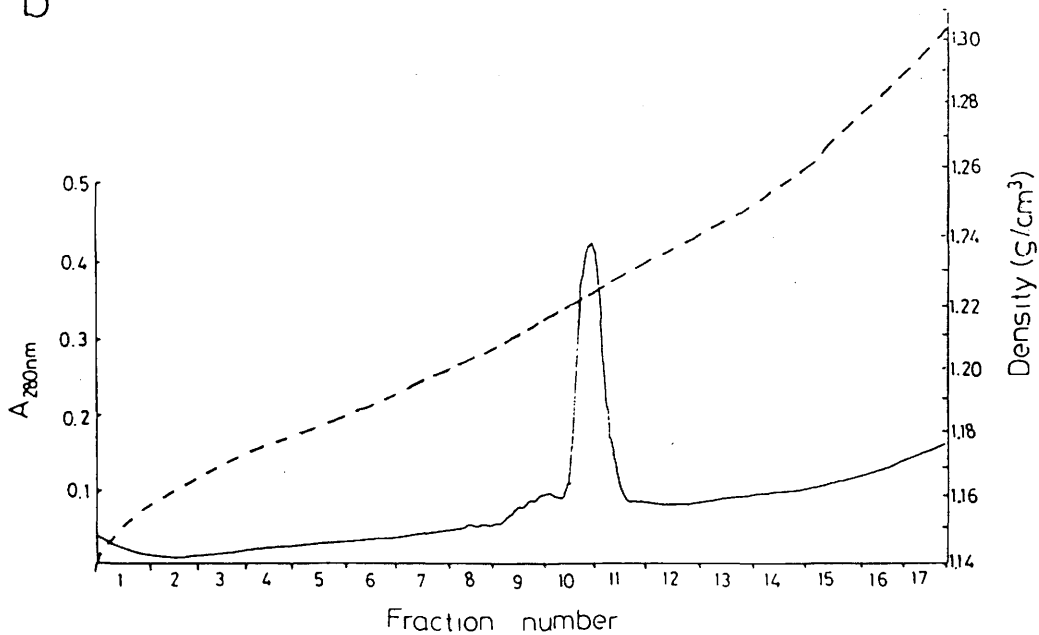


Figure 32

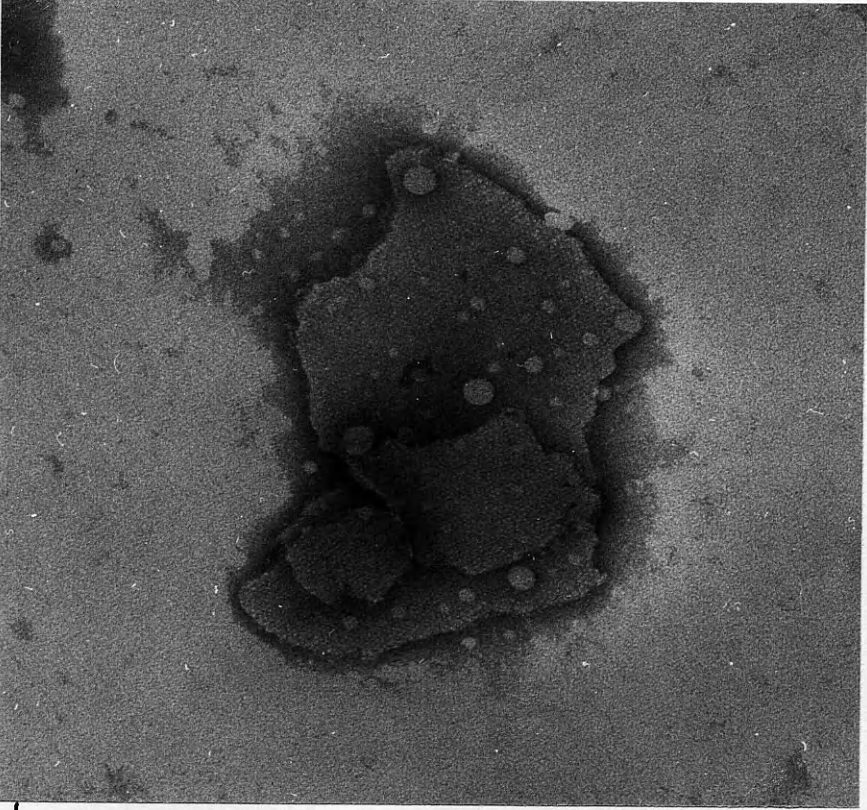
Electron Microscopy of Negative Stained Mouse Liver Gap Junctions
Treated with Pronase

Electron micrographs of (a) untreated mouse liver gap junctions and, (b) pronase treated (30 μg pronase per 1-2 μg 16K protein, 30 min, 37°C) mouse liver gap junctions.

Magnification (a) and (b) 110,000x.

Electron microscopy of negative stained gap junctions was carried out as described in section 2.2.5. The junctions were treated as described in the legend to figure 29.

a



b

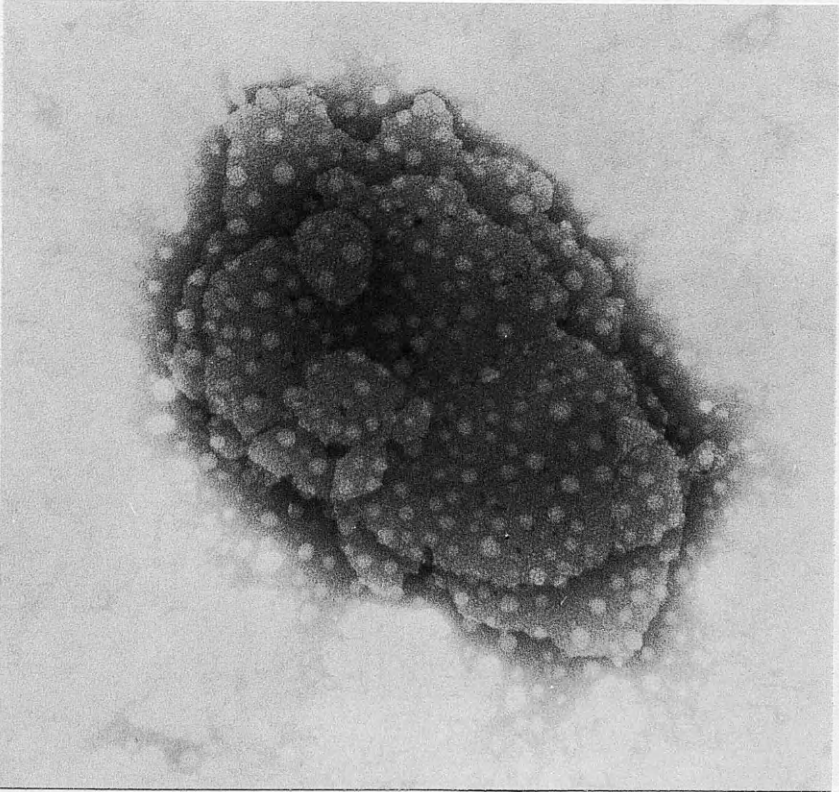


Figure 33

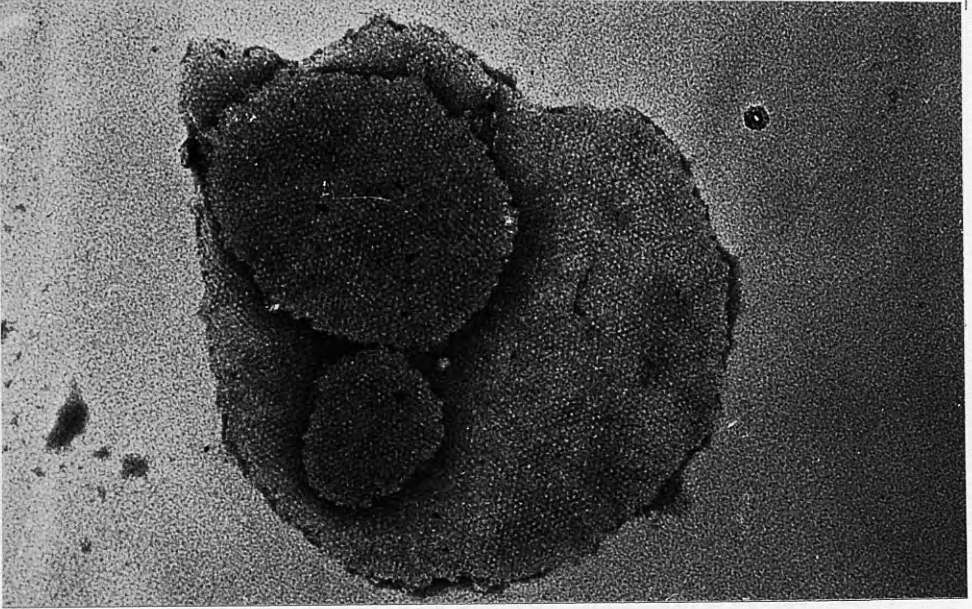
Electron Microscopy of Negative Stained Nephrops Hepatopancreas
Gap Junctions Treated with Pronase

Electron micrographs of (a) untreated and (b) pronase treated (30 μg pronase per 1-2 μg 18K protein, 30 min, 37°C) Nephrops hepatopancreas gap junctions.

Magnification (a) and (b) 110,000x.

Electron microscopy of negative stained gap junctions was carried out as described in section 2.2.5. The junctions were treated as described in the legend to figure 29.

a



b

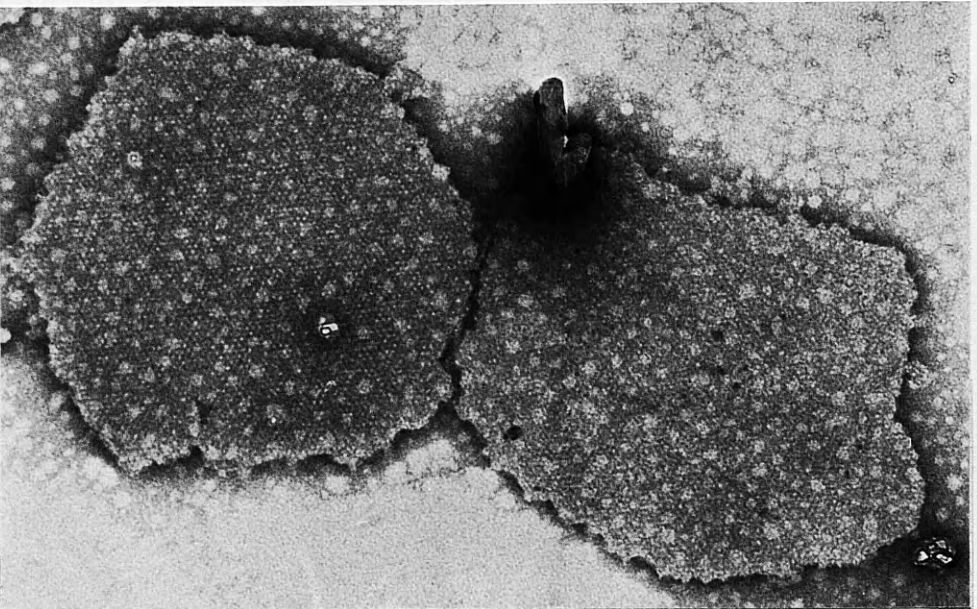


Figure 34

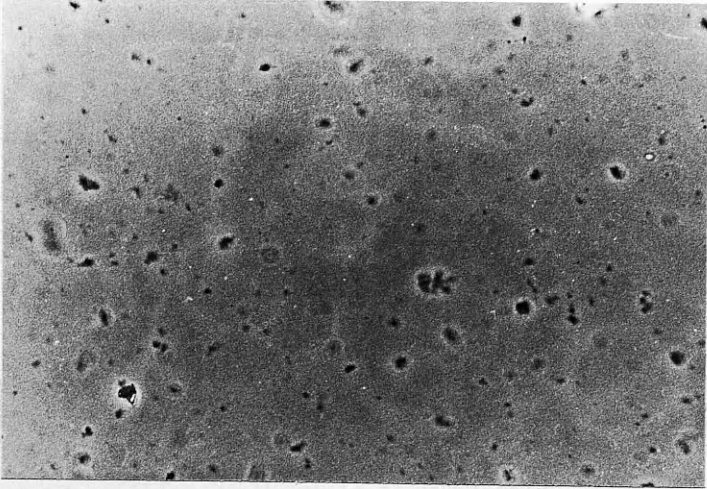
Agglutination of Pronase Treated Mouse Liver Gap Junctions

Phase light micrographs of a mouse liver gap junction preparation incubated with (a) preimmune serum, (b) site specific antiserum or, (c) affinity purified antibodies prepared from the site specific antiserum. The mouse liver gap junction preparation after pronase treatment and then incubated with (d) the site specific antiserum or, (e) the affinity purified antibodies.

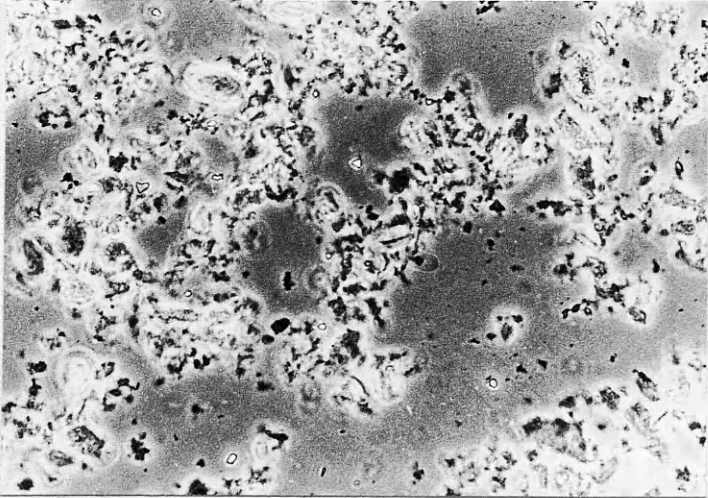
The agglutination was carried out as described in section 2.2.13. Junctions were treated with 30 μg pronase per 1-2 μg 16K protein for 30 min at 37°C. The junctions were then pelleted by centrifugation on an MSE bench top microfuge. The pellets were resuspended and washed (3x) with distilled water and then the agglutination assay was performed.

Magnification for all micrographs, 900x.

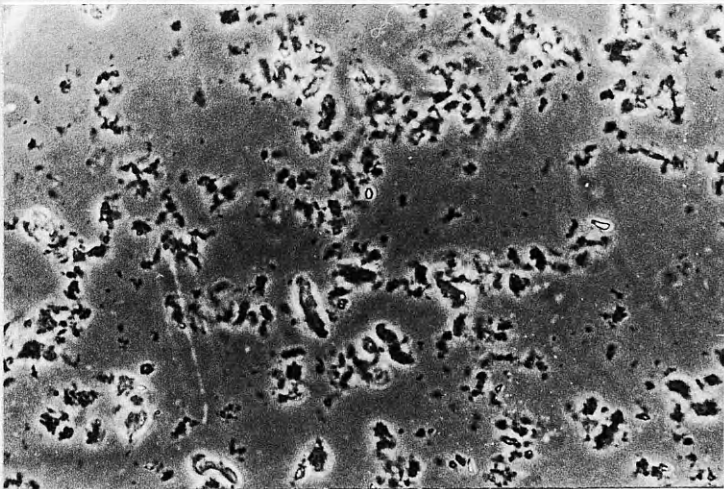
a



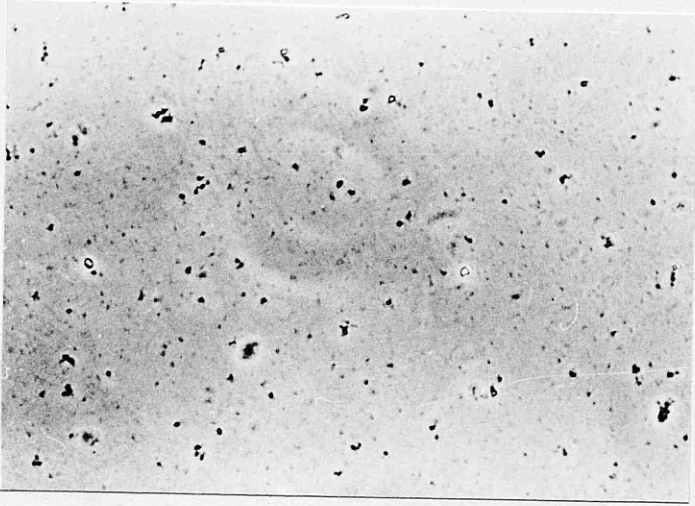
b



c



d



e

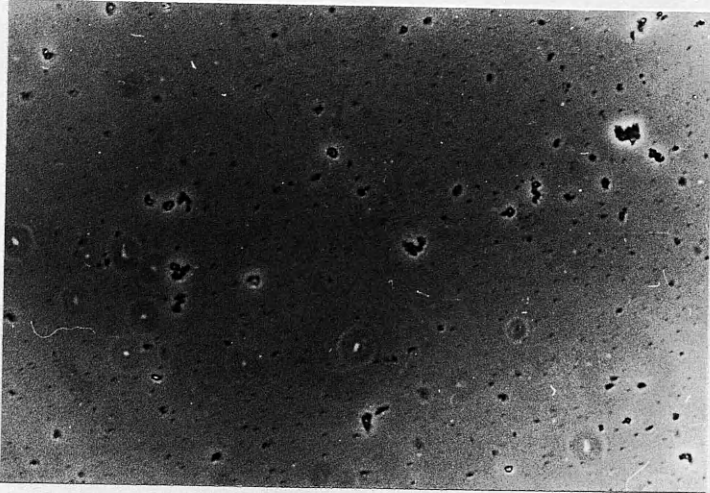


Figure 35

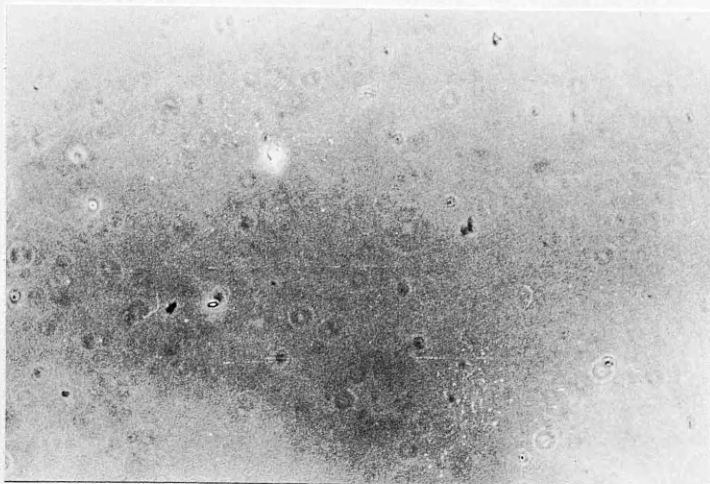
Agglutination of Pronase Treated Nephrops Hepatopancreas Gap Junctions

Phase light micrographs of a Nephrops hepatopancreas gap junction preparation incubated with (a) preimmune serum, (b) site specific antiserum or, (c) affinity purified antibodies prepared from the site specific antiserum. The Nephrops hepatopancreas gap junction preparation after pronase treatment and then incubated with (d) the site specific antiserum or, (e) the affinity purified antibodies.

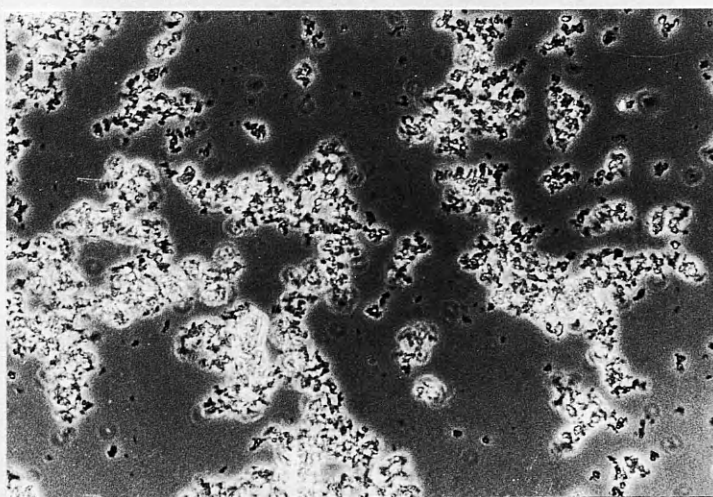
The agglutination was carried out as described in section 2.2.13. Conditions for pronase treatment were those described in the legend to figure 34.

Magnification for all micrographs, 900x.

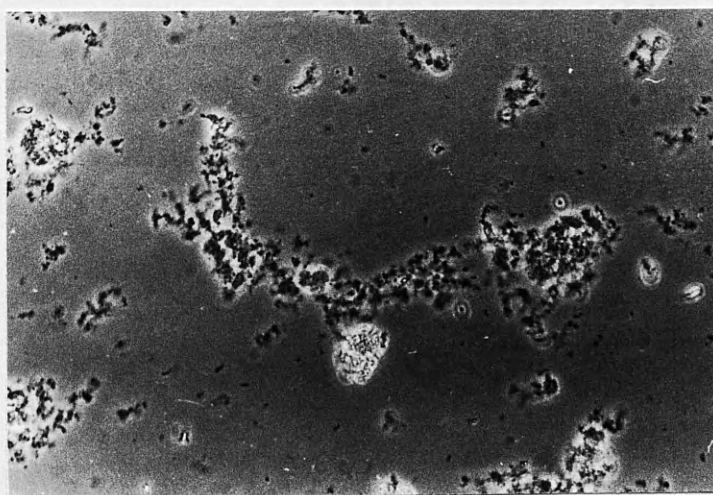
a



b



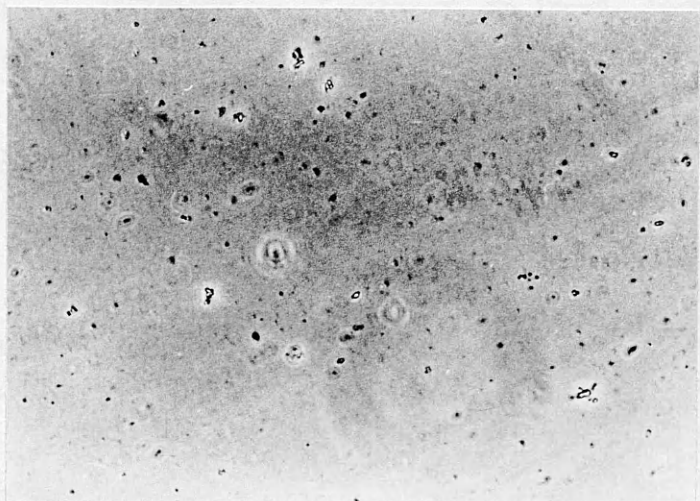
c



specific antibodies and the 1977 influenza A virus were on
founder able to form 2-3 µm diameter particles. These particles
agglutinate rapidly and are 100 nm in diameter.

Protein transfer and electron transfer were also analyzed
also analyzed using the silver-impregnation method. The results
(Fig. 36) show that the protein transfer particles, which

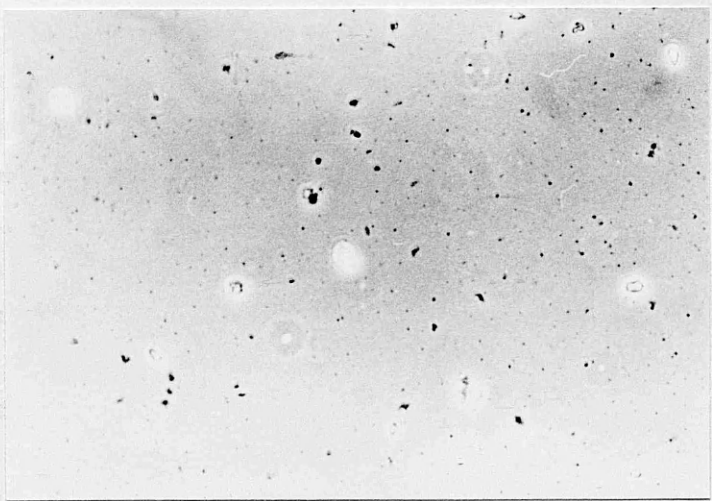
have been
immunoprecipitated
or had no
functions
antigenic
the
in
molecules
they are



immunoprecipitated
of hepatitis

e

The
of the
the ver
PAGE an
15K and
with ele
analysis
that pro
maintain
accessib
function



specific antiserum and the affinity purified antibodies were no longer able to form agglutination complexes. Pronase treated Nephrops hepatopancreas gap junctions also failed to form agglutination complexes with the RaN 18K antiserum.

Pronase treated gap junctions from mouse and Nephrops were also analysed using the microimmunodiffusion assay. The results (Fig. 36) show that the protein of mouse liver gap junctions, which have been treated with 30 µg of pronase, no longer form immunoprecipitates with the site specific antiserum, the RaC 16K or RaN 18K antisera. Similarly treated Nephrops hepatopancreas gap junctions no longer form immunoprecipitates with the site specific antiserum, the RaC 16K or the RaN 18K antisera (Fig. 37).

The agglutination and microimmunodiffusion results show that the N-terminal region of the 16K and 18K proteins are accessible, in their conformations in isolated junctions, to both antibody molecules and to the enzyme pronase. Pronase removes or alters those epitopes (N-terminal) responsible for the agglutination and immunoprecipitation by the site specific antiserum and in the case of Nephrops hepatopancreas gap junctions those responsible for the agglutination and immunoprecipitation by the RaN 18K antiserum.

The results add support for the suggestion that the N-termini of the 16K and 18K proteins are located on the cytoplasmic faces of the vertebrate and invertebrate gap junctions. Moreover the SDS PAGE analyses indicates that at least one other site (loop), of the 16K and 18K proteins, is accessible to pronase. In conjunction with electron microscopy of negatively stained junctions, SDS PAGE analyses show that the protein remaining in the gap junction (i.e. that present intramembranously or extracellularly) is sufficient to maintain the characteristic morphology and indicate that little accessible protein is present on the cytoplasmic faces of gap junctions.

Figure 36

Microimmunodiffusion Analysis of Mouse Liver Gap Junctions Treated
with Pronase

Coomassie stained microimmunodiffusion plate.

SS- site specific antiserum.

RaC- rabbit anti-chicken liver gap junction antiserum, (RaC/2, antiserum diluted twofold with PBS).

RaN- rabbit anti-Nephrops hepatopancreas gap junction antiserum, (RaN/2, antiserum diluted twofold with PBS).

M mouse liver gap junction preparation.

M:P mouse liver gap junction preparation treated with pronase as described in the legend to figure 29.

M:P/2 mouse liver gap junction preparation treated with pronase and diluted with an equal volume of PBS.

The antigens were placed in the central wells and the antisera placed in the outer wells (same for each set) of 1% agarose gels (buffer PBS). The microdiffusion plates were incubated overnight at 4°C. Washed over 3-4 h with several changes of PBS and stained with Coomassie blue.

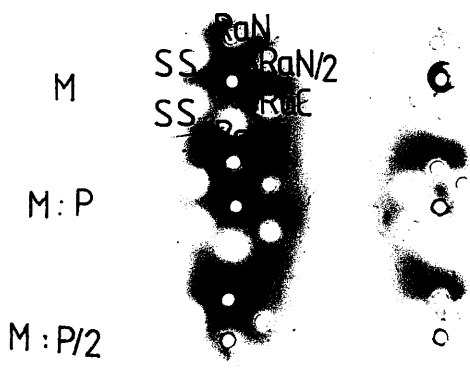


Figure 37

Microimmunodiffusion Analysis of Nephrops Hepatopancreas Gap
Junctions Treated with Pronase

Coomassie stained microimmunodiffusion plate

SS- site specific antiserum

RaC- rabbit anti-chicken liver gap junction antiserum (RaC/2,
antiserum diluted twofold with PBS)

RaN- rabbit anti-Nephrops hepatopancreas gap junction antiserum
(RaN/2, antiserum diluted twofold with PBS)

N- Nephrops hepatopancreas gap junction preparation

N:P- Nephrops hepatopancreas gap junction preparation treated with
pronase as described in the legend to figure 29.

Microimmunodiffusion was carried out as described in the legend to
figure 36.

3.3.3 The Effect of Nitrogen and Phosphorus

To establish the effect of substrate nitrogen and phosphorus on the growth of the yeast, a series of experiments were conducted. The yeast was grown on a medium containing 10% glucose and 1% yeast extract. The nitrogen and phosphorus concentrations were varied as follows: N: 0, 0.5, 1, 2, 4, 8, 16, 32, 64, 128, 256, 512, 1024, 2048, 4096, 8192, 16384, 32768, 65536, 131072, 262144, 524288, 1048576, 2097152, 4194304, 8388608, 16777216, 33554432, 67108864, 134217728, 268435456, 536870912, 1073741824, 2147483648, 4294967296, 8589934592, 17179869184, 34359738368, 68719476736, 137438953472, 274877906944, 549755813888, 1099511627776, 2199023255552, 4398046511104, 8796093022208, 17592186044416, 35184372088832, 70368744177664, 140737488355328, 281474976710656, 562949953421312, 1125899906842624, 2251799813685248, 4503599627370496, 9007199254740992, 18014398509481984, 36028797018963968, 72057594037927936, 144115188075855872, 288230376151711744, 576460752303423488, 1152921504606846976, 2305843009213693952, 4611686018427387904, 9223372036854775808, 18446744073709551616, 36893488147419103232, 73786976294838206464, 147573952589676412928, 295147905179352825856, 590295810358705651712, 1180591620717411303424, 2361183241434822606848, 4722366482869645213696, 9444732965739290427392, 18889465931478580854784, 37778931862957161709568, 75557863725914323419136, 151115727451828646838272, 302231454903657293676544, 604462909807314587353088, 1208925819614629174706176, 2417851639229258349412352, 4835703278458516698824704, 9671406556917033397649408, 19342813113834066795298816, 38685626227668133590597632, 77371252455336267181195264, 154742504910672534362390528, 309485009821345068724781056, 618970019642690137449562112, 1237940039285380274899124224, 2475880078570760549798248448, 4951760157141521099596496896, 9903520314283042199192993792, 19807040628566084398385987584, 39614081257132168796771975168, 79228162514264337593543950336, 158456325028528675187087900672, 316912650057057350374175801344, 633825300114114700748351602688, 1267650600228229401496703205376, 2535301200456458802993406410752, 5070602400912917605986812821504, 10141204801825835211973625643008, 20282409603651670423947251286016, 40564819207303340847894502572032, 81129638414606681695789005144064, 162259276829213363391578010288128, 324518553658426726783156020576256, 649037107316853453566312041152512, 1298074214633706907132624082305024, 2596148429267413814265248164610048, 5192296858534827628530496329220096, 10384593717069655257060992658440192, 20769187434139310514121985316880384, 41538374868278621028243970633760768, 83076749736557242056487941267521536, 166153499473114484112975882535043072, 332306998946228968225951765070086144, 664613997892457936451903530140172288, 1329227995784915872903807060280344576, 2658455991569831745807614120560689152, 5316911983139663491615228241121378304, 10633823966279326983230456482242756608, 21267647932558653966460912964485513216, 42535295865117307932921825928971026432, 85070591730234615865843651857942052864, 170141183460469231731687303715884105728, 340282366920938463463374607431768211456, 680564733841876926926749214863536422912, 1361129467683753853853498429727072845824, 2722258935367507707706996859454145691648, 5444517870735015415413993718908291383296, 10889035741470030830827987437816582766592, 21778071482940061661655974875633165533184, 43556142965880123323311949751266331066368, 87112285931760246646623899502532662132736, 174224571863520493293247799005065244265472, 348449143727040986586495598010130488530944, 696898287454081973172991196020260977061888, 1393796574908163946345982392040521954123776, 2787593149816327892691964784081043908247552, 5575186299632655785383929568162087816495104, 11150372599265311570767859136324173632990208, 22300745198530623141535718272648347265980416, 44601490397061246283071436545296694531960832, 89202980794122492566142873090593389063921664, 178405961588244985132285746181186778127843328, 356811923176489970264571492362373556255686656, 713623846352979940529142984724747112511373312, 142724769270595988105828596944949422502274664, 285449538541191976211657193889898845004549328, 570899077082383952423314387779797690009098656, 1141798154164767904846628775559595380018197312, 2283596308329535809693257551119190760036394624, 4567192616659071619386515102238381520072789248, 9134385233318143238773030204476763040145578496, 18268770466636286477546060408953526080291156992, 36537540933272572955092120817907052160582313984, 73075081866545145910184241635814104321164627968, 14615016373309029182036848327162820864232925536, 29230032746618058364073696654325641728465851072, 58460065493236116728147393308651283456931702144, 116920130986472233456294786617302566913863404288, 233840261972944466912589573234605133827726808576, 467680523945888933825179146469210267655453617152, 935361047891777867650358292938420535310907234304, 1870722095783555735300716585876841070621814468608, 3741444191567111470601433171753682141243628937216, 7482888383134222941202866343507364282487257874432, 14965776766268445882405732687014728564974515748864, 29931553532536891764811465374029457129949031497728, 59863107065073783529622930748058914259898062995456, 119726214130147567059245861496117828519796125990912, 239452428260295134118491722992235657039592251981824, 478904856520590268236983445984471314079184503963648, 957809713041180536473966891968942628158369007927296, 1915619426082361072947933783937885256316738015854592, 3831238852164722145895867567875770512633476031709184, 7662477704329444291791735135751541025266952063418368, 15324955408658888583583470271503082050533904126836736, 30649910817317777167166940543006164101067808253673472, 61299821634635554334333881086012328202136165067346944, 122599643269271108668667762172024656404272330134693888, 245199286538542217337335524344049312808544660269387776, 490398573077084434674671048688098625617089320538775552, 980797146154168869349342097376197251234178641077551104, 1961594292308337738698684194752394502468357282155102208, 3923188584616675477397368389504789004936714564310204416, 7846377169233350954794736779009578009873429128620408832, 15692754338466701909589473558019156019746858573240817664, 31385508676933403819178947116038312039493717146481635328, 62771017353866807638357894232076624078987434292963270656, 125542034707733615276715788464153248157974868585926541312, 251084069415467230553431576928306496315949737171873082624, 502168138830934461106863153856612992631899474343746165248, 1004336277661868922213726307713225973263798948687492330496, 2008672555323737844427452615426451946527597897374984660992, 4017345110647475688854905230852903893055195794749969321984, 8034690221294951377709810461705807786110391589499938643968, 16069380442589902755419620923411615572220783178999877287936, 32138760885179805510839241846823231144441566357999754575872, 64277521770359611021678483693646462288883132715999509151744, 128555043540719222043356967387292924577766265431999018283488, 257110087081438444086713934774585849155532530863998036567968, 514220174162876888173427869549171698311065061727996073135936, 1028440348325753776346855739098343396622130123455992146271872, 2056880696651507552693711478196686793244260246911984292543744, 4113761393303015105387422956393373586488520493823968585087488, 8227522786606030210774845912786747172977040987647937170174976, 1645504557321206042154969182557349434595408197529587434034992, 3291009114642412084309938365114698869190816395059174868069984, 6582018229284824168619876730229397738381632790118349736139968, 13164036458569648337239753460458795476763265800236699472279936, 26328072917139296674479506920917590953526531600473398944559872, 52656145834278593348959013841835181907053063200946797889119744, 105312291668557186697918027683670363814106126401893595778239488, 210624583337114373395836055367340727628212252803787191556478976, 421249166674228746791672110734681455256424505607574383112957952, 842498333348457493583344221469362910512849011215148766225915904, 1684996666696914987166688442938725821025698022430297532451831808, 3369993333393829974333376885877451642051396044860595064903663616, 6739986666787659948666753771754903284102792089721190129807327232, 13479973333575319897333507543509806568205584179442380259614654464, 26959946667150639794667015087019613136411168358884760519229308928, 53919893334301279589334030174039226272822336717769521038458617856, 10783978666860255917866806034807845254564467343553904207691723712, 21567957333720511835733612069615690509128934687107808415383447424, 43135914667441023671467224139231381018257869374215616830766894848, 86271829334882047342934448278462762036515738748431233661533789696, 172543658669764094685868896556925524073031477496862467323067579392, 345087317339528189371737793113851048146062954993724934646135158784, 690174634679056378743475586227702096292125909987449869292270317568, 1380349269358112757486951172455404192584251819974899738584540635136, 2760698538716225514973902344910808385168503639949799477169081270272, 5521397077432451029947804689821616770337007279899598954338162540544, 11042794154864902059895609379643233540674014559799197908676325081088, 22085588309729804119791218759286467081348029119598395817352650162176, 44171176619459608239582437518572934162696058239196791634705300324352, 88342353238919216479164875037145868325392116478393583269410600648704, 176684706477838432958329750074291736650784232956787166538821201297408, 353369412955676865916659500148583473301568465913574333077642402594816, 706738825911353731833319000297166946603136931827148666155284805189632, 1413477651822707463666638000594333893206273863654297332310569610379264, 2826955303645414927333276001188667786412547727308594664621139220758528, 5653910607290829854666552002377335572825095454617189329242278441517056, 11307821214581659709333104004754671145650190909234378658484556883034112, 22615642429163319418666208009509342291300381818468757316969113766068224, 45231284858326638837332416019018684582600763636937514633938227332136448, 90462569716653277674664832038037369165201527273875029267876454664272896, 180925139433306555349329664076074738330403054547750058535752909328545792, 361850278866613110698659328152149476660806109095500117111505818657091584, 723700557733226221397318656304298953321612218191000234223011637314183168, 1447401115466452442794637312608597906643224436382000468446022746228366336, 2894802230932904885589274625217195813286448872764000936892045492456732672, 5789604461865809771178549250434391626572897745528001873784090984913465344, 11579208923731619542357098500868783253145795491056003747568181969826930688, 23158417847463239084714197001737566506291590982112007495136363939653861376, 46316835694926478169428394003475133012583181964224014982720727879307722752, 92633671389852956338856788006950266025166363928448029965441455758615445504, 185267342779705912677713576013900532050332727856896059930882911517230891008, 370534685559411825355427152027801064100665455713792119861765823034461782016, 741069371118823650710854304055602128201330915427584239723531646068923564032, 1482138742237647301421708608111204256402661830855168479447063292137847128064, 2964277484475294602843417216222408512805323661710336958894126584275694256128, 5928554968950589205686834432444817025610647323420673917788253168551388512256, 11857109937901178411373668864889634051221294646841347835576506370102777024512, 23714219875802356822747337729779268102442589293682695671153012740205554049024, 47428439751604713645494675459558536204885178587365391342306025480411108098048, 94856879503209427290989350919117072409770357174730782684612050960822216196096, 189713759006418854581978701838234144819540714349461565369224101921644432392192, 379427518012837709163957403676468289639081426998923130738448203843288864784384, 758855036025675418327914807352936579278162853997846261476896407686577729568768, 1517710072051350836655829614705873158556325707995692522953792815373155459137536, 3035420144102701673311659229411746317112651415991385045907585630746310918275072, 6070840288205403346623318458823492634225302831982770091815171261492621836550144, 12141680576410806693246636917646985268450605663965540183630342522985243673100288, 24283361152821613386493273835293970536901211327931080367260685045970487346200576, 48566722305643226772986547670587941073802422655862160734521370091940974692401152, 97133444611286453545973095341175882147604845311724321469042740183881949384802304, 194266889222572907091946190682351764295209690623448642938085480367763898769604608, 388533778445145814183892381364703528590419381246897285876170960735527797

3.4.3 Two Dimensional Peptide Mapping

To examine the effects of proteolytic enzymes on the cytoplasmic faces of gap junctions in more detail a technique with higher resolving power than SDS PAGE is required. One such technique is two dimensional peptide mapping. Peptide mapping experiments in this laboratory have been used to examine the homology of proteins isolated from preparations containing gap junctions from different tissues and species (Buultjens et al., 1986). The peptide mapping technique has been extended to examine the effects of pronase on the mouse liver gap junctional protein and to try and identify which peptide, produced by tryptic digestion, is N-terminal.

Preparations of gap junctions from mouse liver and Nephrops hepatopancreas were radioiodinated by the chloramine T method (Hunter and Greenwood, 1962) which, under the conditions used, labels predominantly tyrosine residues (see section 2.2.14).

The preparations were divided in two. One half of each preparation was run on preparative SDS PAGE and the 16K and 18K proteins eluted in water overnight. The band purified iodinated mouse and Nephrops proteins showed more components than were in the initial preparations (16K, Fig. 38; 18K, Fig. 39), however the higher molecular weight bands represent aggregates of the 16K (Finbow et al., 1983) and 18K (Finbow et al., 1984) proteins.

The remaining half of each preparation and the band purified protein were both digested with trypsin (E.C. 3.4.21.4) using the procedure described by Finbow et al. (1984). Peptide mapping was carried out on cellulose TLC plates. Horizontal flat bed high voltage electrophoresis (22°C, pH 2.1) was followed by ascending chromatography (section 2.2.14). The peptide maps prepared from the total protein present in the mouse liver gap junction and those from band purified 16K protein are the same with respect to the number, the intensity and migration of labelled peptides (Fig. 38).

Likewise, peptide maps of the total protein present in Nephrops hepatopancreas gap junctions and 18K protein are the same with respect to the number, the intensity and migration of labelled

Figure 38

Two Dimensional Tryptic Peptide Maps of Eluted 16K Protein and
Total Protein from Mouse Liver Gap Junctions

a) Autoradiograph of SDS PAGE of (1) eluted ^{125}I labelled 16K protein and (2) ^{125}I labelled total protein from mouse liver gap junctions.

b) Autoradiographs of two dimensional tryptic peptide maps of (1) eluted ^{125}I labelled 16K protein and (2) total protein from ^{125}I labelled mouse liver gap junctions. Electrophoretic separation is from left to right and chromatographic separation is from bottom to top.

Gap junctions were labelled and digested with trypsin as described in section 2.2.14.

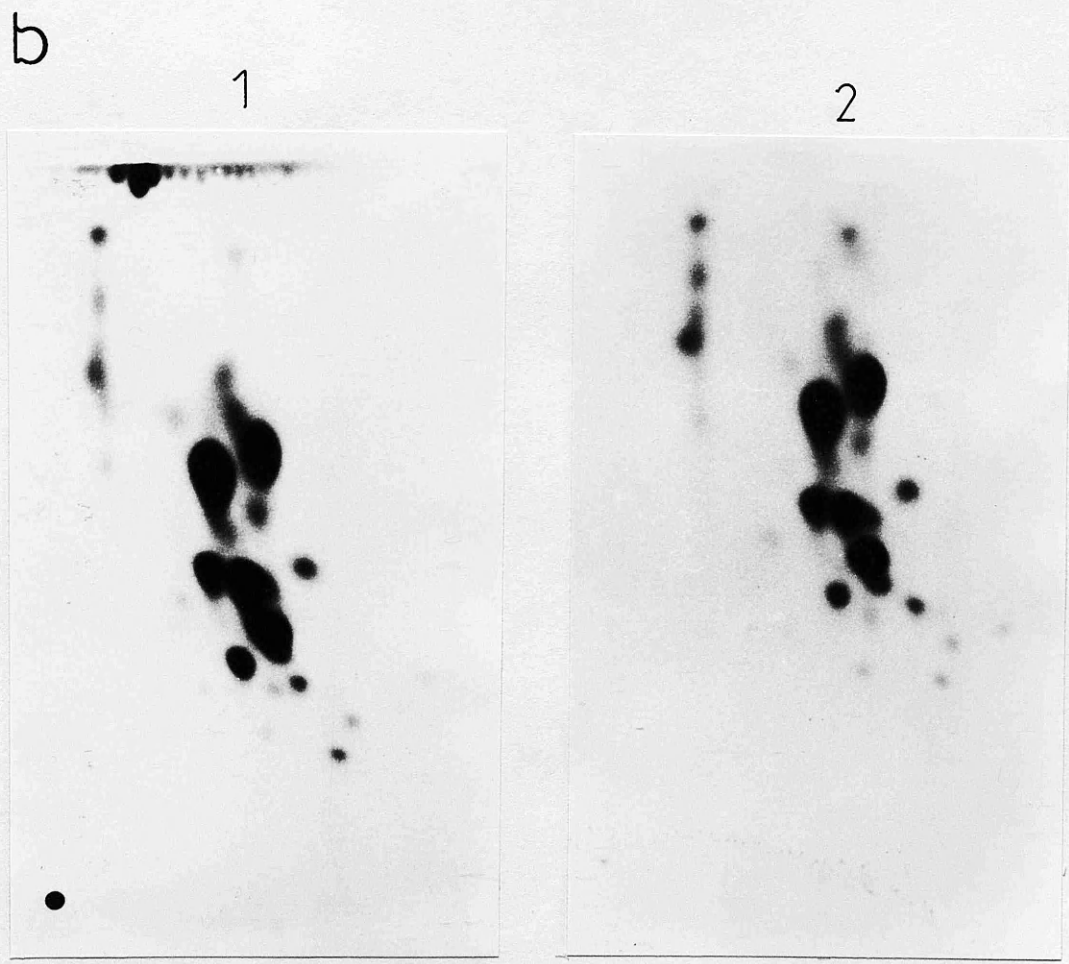
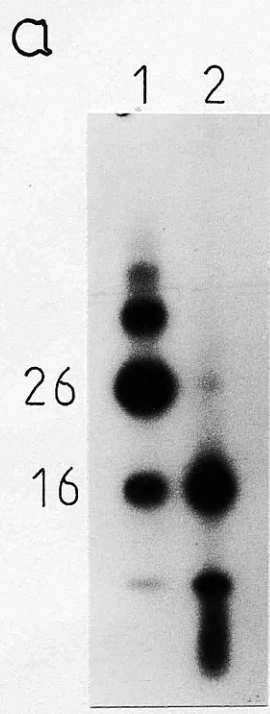


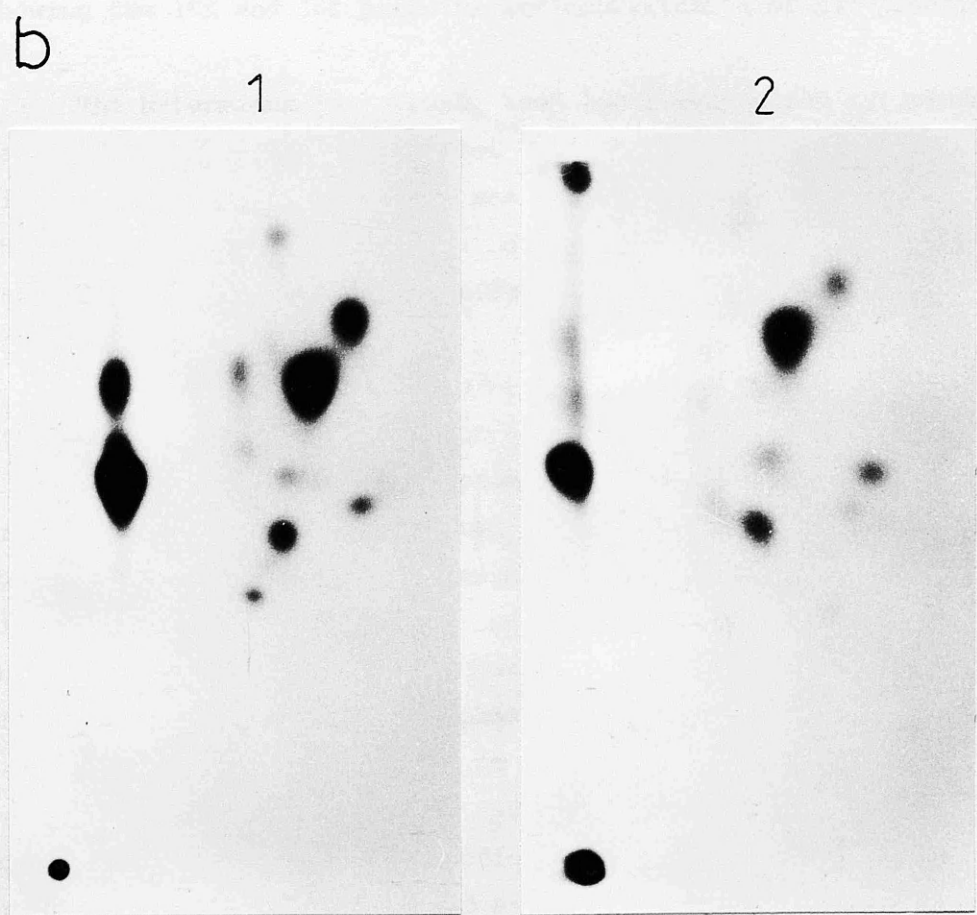
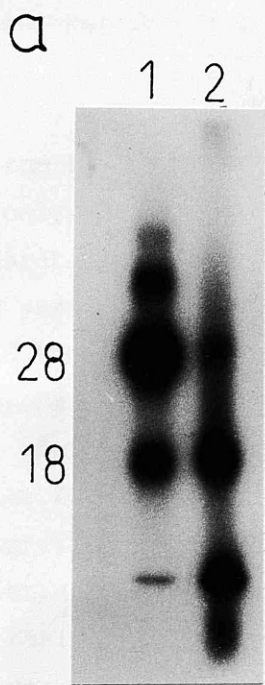
Figure 39

Two Dimensional Tryptic Peptide Maps of Eluted 18K Protein and
Total Protein from Nephrops Hepatopancreas Gap Junctions

a) Autoradiograph of SDS PAGE of eluted ^{125}I labelled 18K protein (1) and ^{125}I labelled total protein from Nephrops hepatopancreas gap junctions (2).

b) Autoradiographs of two dimensional tryptic peptide maps of (1) eluted ^{125}I labelled 18K protein and (2) total protein from ^{125}I labelled Nephrops hepatopancreas gap junctions. Electrophoretic separation is from left to right and chromatographic separation is from bottom to top.

Gap junctions were labelled and digested with trypsin as described in section 2.2.14



peptides (Fig. 39). (Although larger, as judged by SDS PAGE, than the mouse liver gap junctional protein, it has fewer labelled peptides.)

The conclusions from the peptide mapping experiments are that the 16K protein is the only detectable protein present in the mouse liver gap junction preparation. Similarly, the 18K protein is the only detectable protein present in Nephrops hepatopancreas gap junction preparation and therefore provides further evidence for the 16K, 18K proteins being the major components of the junction preparations. However, there must be the proviso that there could be proteins present with the following characteristics: insoluble in SDS (although the gap junctional structure is SDS soluble; Finbow et al., 1983), not digested by trypsin or not labelled with ^{125}I . These data support the earlier published evidence (Finbow et al., 1983; 1984) and the evidence reported in sections 3.2 and 3.3 showing the 16K and 18K proteins are constituents of gap junctions.

The N-terminus has already been localized to the cytoplasmic face of the gap junction (section 3.2.4 and 3.4.2). With two dimensional peptide mapping it should now be possible to determine which is the N-terminal peptide on the map. The sequence shows that it has a tyrosine in position 4 and it should therefore be labelled.

The identification of the N-terminal peptide was first attempted by immunoprecipitation using the site specific antiserum.

As stated earlier the peptide mapping experiments were initially carried out using a two dimensional system on cellulose TLC plates. Recovery of the separated peptides is inefficient in this system, so to isolate the individual peptides, trypsin digested iodinated 16K protein was fractionated by HPLC. Digests were applied to a C18 reverse phase column and eluted with a linear acetonitrile gradient (0-100%) in 0.1% TFA. Fractions (0.5 ml) were collected and counted for radioactivity. The resulting plot of counts recovered versus fraction number is shown in figure 40. Four major peaks were collected and samples were run, using the two dimensional electrophoretic and chromatographic system, on the TLC

Figure 40

HPLC Tryptic Peptide Map of 16K Protein

Tryptic peptides from ^{125}I labelled 16K protein resolved on a C18 reverse phase column.

Column: TSK C18 reverse phase.

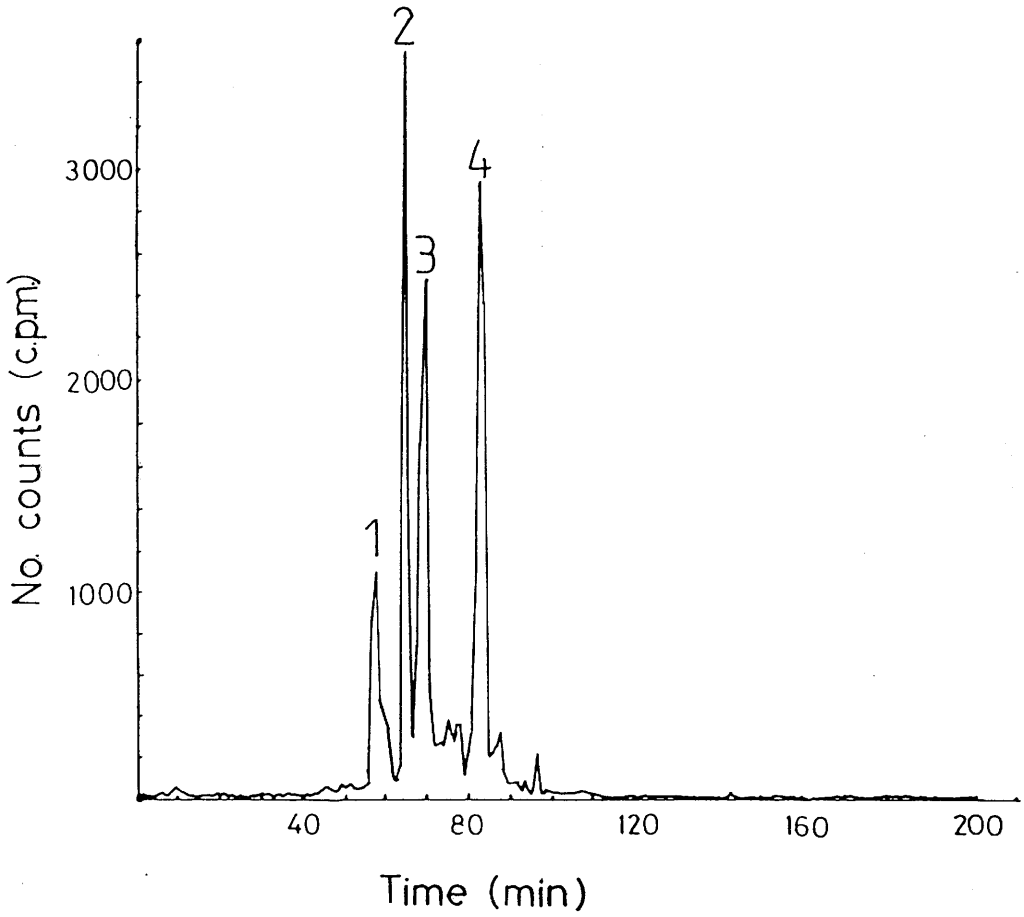
Temp: Ambient

Flow rate: 1 ml/min

Solvent A: 0.1% TFA in water (vol/vol)

Solvent B: 0.1% TFA in acetonitrile (vol/vol)

Labelled 16K protein was digested with trypsin as described in section 2.2.14. The digest was dissolved in 0.1% TFA in water and applied to the column. The peptides were eluted with a linear gradient of (0%) A to (100%) B over 100 min. 0.5 ml (0.5 min) fractions were collected and 50 μl of each counted by using an "LKB" liquid scintillation counter (10 ml of "Ecoscint" scintillation fluid, 1 min).



plates to check for purity. A mixture of the peaks was also applied to TLC plates to see if the peptide map of unfractionated trypsin digested iodinated protein could be regenerated.

The results show that the four major peaks regenerated much of the "original" peptide map (Fig. 41). One major labelled peptide is absent. For the "missing spot" it is summarized that it is either not soluble in the starting buffer of the HPLC gradient (0.1% TFA in water, pH 2) or that it remains attached to the C18 reverse phase column.

The individual peptides were then used in a solution immunoprecipitation assay, to try and detect the N-terminal peptide and other epitopes, either by the site specific or RaC 16K antisera. The immunoprecipitation experiments proved inconclusive as neither the the site specific antiserum nor the RaC 16K antiserum immunoprecipitated any peptides above the level of that produced by the preimmune serum. It is possible that the "missing spot" represented the N-terminal peptide so an alternative approach was devised. This approach was based on the agglutination and microimmunodiffusion assays.

It has been shown (section 3.4.2) that incubation of isolated junctions with pronase abolishes agglutination (e.g. Fig. 34) and precipitation of the residual protein in the microimmunodiffusion assay (e.g. Fig. 36). From these results it may be concluded that the N-terminus is removed or altered. Using the peptide maps of the protein from isolated gap junction preparations as controls, the protein of pronase treated mouse liver gap junctions was peptide mapped under the same conditions (Fig. 42). Under these conditions pronase should also affect other accessible cytoplasmic sites so the data produced may not lead directly to the identification of the N-terminal peptide.

After pronase treatment of iodinated, intact mouse liver gap junctions, SDS PAGE shows the 16K protein has been cleaved to what appears to be a mixture of peptides which form an unresolved broad band (Fig. 42). The peptide maps of these pronase treated mouse liver junctions show only two major labelled peptides so three major labelled peptides have been lost or modified by pronase treatment. The N-terminal peptide should be one of these three

Figure 41

Analysis of Peaks from HPLC Map by Two Dimensional TLC
Chromatography

- a) Autoradiograph of two dimensional tryptic peptide map of 16K protein.
- b) Autoradiograph of a mixture of peaks (1-4) obtained from HPLC peptide map as shown in figure 40.

Two dimensional peptide maps were prepared as described in section 2.2.14.

a



b

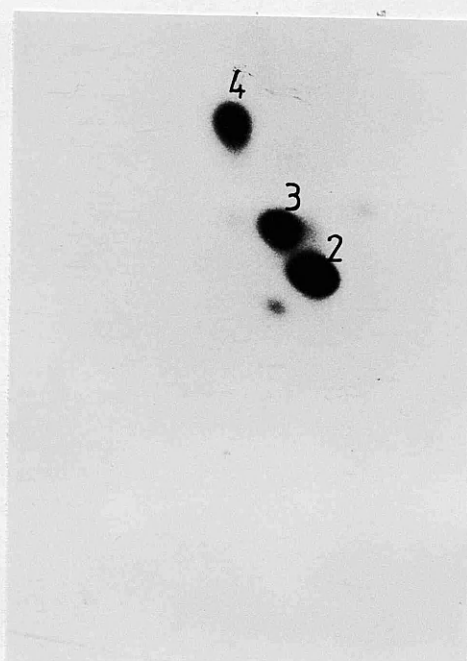


Figure 42

Two Dimensional Tryptic Peptide Map of Pronase Treated Mouse Liver
Gap Junctions

a) Autoradiograph of SDS PAGE (20% acrylamide) ^{125}I labelled mouse liver gap junctions (1), and pronase treated ^{125}I labelled mouse liver gap junctions (2).

b) Autoradiograph of two dimensional tryptic peptide map of untreated ^{125}I labelled mouse liver gap junctions.

c) Autoradiograph of two dimensional tryptic peptide map of pronase treated ^{125}I labelled mouse liver gap junctions.

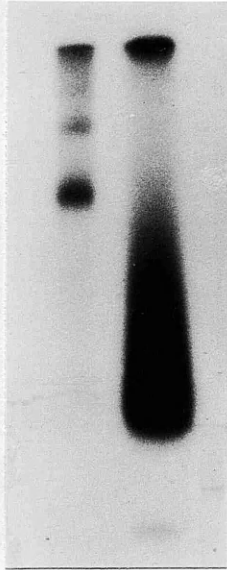
d) Autoradiograph of two dimensional tryptic peptide map of pronase treated ^{125}I labelled mouse liver gap junctions mixed with tryptic digest of untreated ^{125}I labelled mouse liver gap junctions (b).

^{125}I labelled mouse liver gap junctions were treated with pronase as described in the legend to figure 29 (30 μg pronase, 30 min, 37°C) and then digested with trypsin and peptide mapped as described in section 2.2.14.

a

1 2

16



spots. The peptide maps after pronase show that the "missing spot" (from the HPLC fractionation, Fig. 41) is also removed, so that the possibility still existed that it was the N-terminal peptide.

Identification of the N-terminal peptide was attempted using leucine aminopeptidase (E.C. 3.4.11.1) to specifically digest the N-terminal residues. Unfortunately the Asn-Pro peptide bond is only slowly digested by the peptidase. Initial experiments showed that incubation of the isolated mouse liver gap junction with aminopeptidase did not produce a change in the iodinated SDS PAGE profile nor the peptide map. Therefore the iodinated 16K protein was isolated and digested with leucine aminopeptidase. It did not produce a change in the SDS gel profile (Fig. 43) but it did alter the peptide map (Fig. 43). The map shows that the peptide x has been removed. The N-terminal peptide is then identified as x.

Figure 43

Two Dimensional Tryptic Peptide Map of Leucine Aminopeptidase
Treated Eluted 16K Protein

a) Autoradiograph of SDS PAGE gel of ^{125}I labelled mouse liver 16K protein (1), and leucine aminopeptidase treated ^{125}I labelled mouse liver 16K protein (2).

b) Autoradiograph of two dimensional tryptic peptide map of untreated ^{125}I labelled 16K protein.

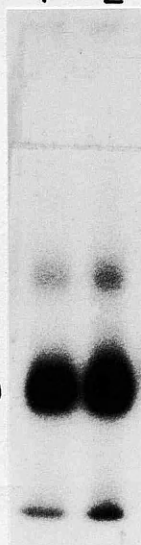
c) Autoradiograph of two dimensional tryptic peptide map of leucine aminopeptidase treated ^{125}I labelled 16K protein.

d) Autoradiograph of two dimensional peptide map of mixture of leucine aminopeptidase treated ^{125}I labelled 16K protein digested with trypsin and ^{125}I labelled 16K protein digested with trypsin. The peptide which is lost due to leucine aminopeptidase digestion is marked x.

^{125}I labelled mouse liver 16K protein was digested for 1 h with 10 μg of leucine aminopeptidase and then supplemented with 10 μg of leucine aminopeptidase and left 16-18 h at 37°C in 0.5 M tris, 0.025 M MnCl_2 , 0.0625 M MgCl_2 , pH 8.5. Total protein was precipitated and peptide mapped as described in section 2.2.14.

a

1 2



16

b



c



d



3.5 FUNCTIONAL STUDIES

The localization of the N-terminal region of the peptide to the cytoplasmic domain of the gap junction raised the question as to whether the site specific antiserum could be used for functional studies.

If the antigenic site was available in isolated whole gap junctions would it be available in vivo and if so would the antiserum block junctional communication when injected into cells?

In collaborative studies with Dr. Ephraim Kam (Beatson Institute, Glasgow) the site specific antiserum was used to test these questions. Buffalo rat liver (BRL) cells were grown as monolayers. When they reached confluence, cells were iontophoretically injected with the site specific antiserum or the preimmune serum. The serum was driven into three neighbouring cells by pulses of current (20 nA, 500 msec at 1 Hz for 20 s). After the cells had been injected with the serum the same cells were iontophoretically injected with Lucifer Yellow. Again pulses of current were used to drive the Lucifer Yellow into the cells (10 nA, 500 msec at 1 Hz for 15 s). Lucifer Yellow was injected alone into one cell at a distant site to act as negative control.

The site specific antiserum prevented the transfer of Lucifer Yellow to neighbouring cells (Fig. 44) in 73% of injections (16/22). No transfer was defined as no detectable fluorescence beyond the three injected cells. Partial blockage i.e. the detection of fluorescence beyond the three cells or no blockage accounted for the remaining (6/22) injections. The preimmune serum prevented the transfer of Lucifer Yellow to neighbouring cells (Fig. 44) in 12% of injections (2/17). The remaining injections (15/17) showed no blockage of the transfer of the dye to neighbouring cells.

Figure 44

Phase and Fluorescence Micrographs of Buffalo Rat Liver Cells
Injected with the Site Specific Antiserum or the Preimmune serum,
and Lucifer Yellow

a) Phase light micrograph of BRL cells growing as monolayers injected with either preimmune serum and Lucifer Yellow (top right 3 cells injected with both) or with Lucifer Yellow alone (bottom left, 1 cell injected).

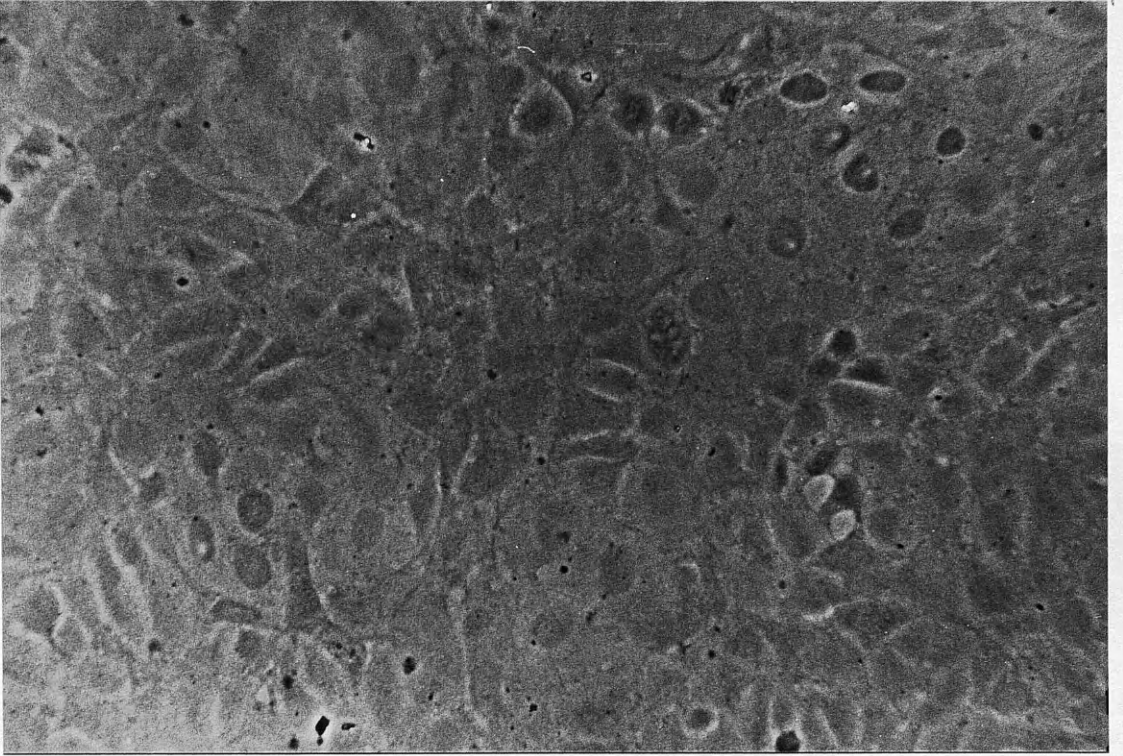
b) Fluorescent light micrograph of the field shown in (a).

c) Phase light micrograph of BRL monolayers injected with the site specific antiserum and Lucifer Yellow (top right, 3 cells injected with both, marked, x) or with Lucifer Yellow alone (bottom left, 1 cell injected, marked, o).

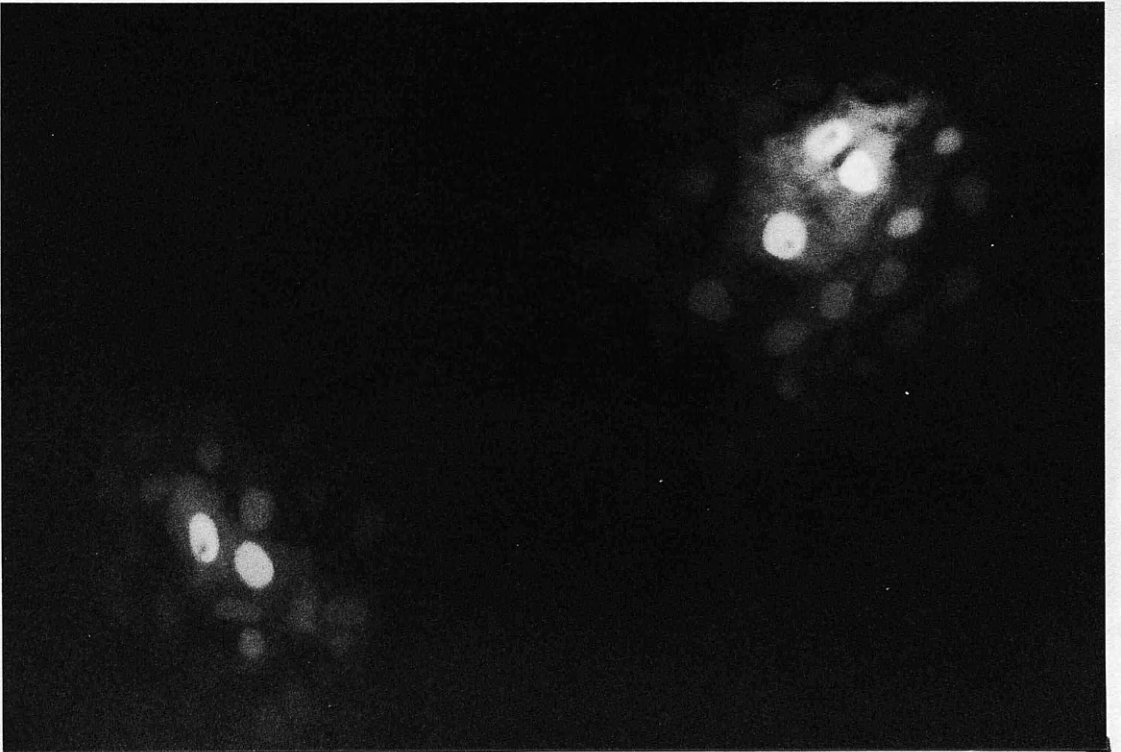
d) Fluorescent light micrograph of the field shown in (c).

Magnification (a) and (b) 900x. (c) and (d) 1100x

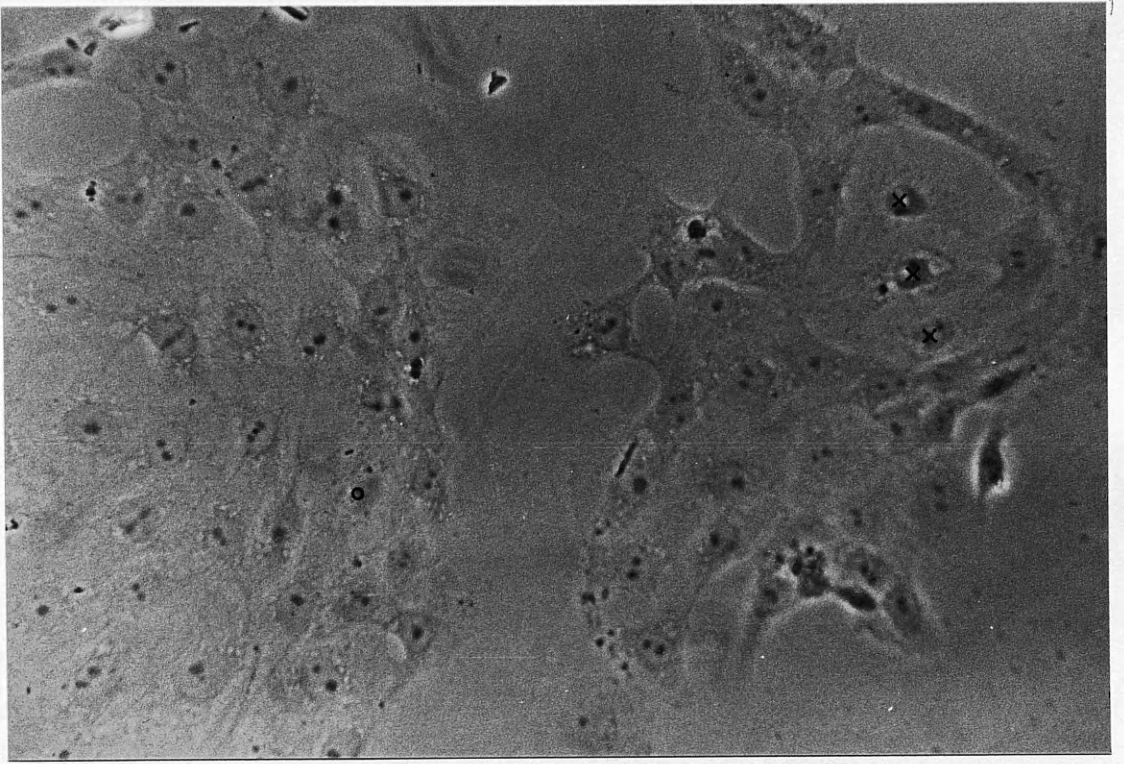
a



b



C



d



These results suggest that the N-terminus of the 16K protein is available for antibody binding in the intact cell which is consistent with the cytoplasmic location of the N-terminal octapeptide used to raise antisera. The result also suggests that the structure of the N-terminal site is the same in the isolated protein, isolated junctions and in situ.

The implication for this result will be discussed in section 4.6.

CHAPTER IV

DISCUSSION

4.1 Introduction

A site specific antiserum has been raised against the N-terminal octapeptide of the 16K mouse liver protein. The antiserum has been used to show that the 16K protein is a structural component of mouse liver gap junctions. This result confirms and extends the earlier results of Finbow et al. (1983). In addition, evidence has been shown for the presence of immunologically related proteins in gap junctions isolated from different murine tissues and from the livers of other species.

Finbow et al. (1984) and more recently Bultjens et al. (1986) have used conventional polyclonal antisera raised in rabbits against mouse liver and Nephrops hepatopancreas gap junctional preparations to show tissue and species conservation of the 16K protein. However, the specificity of conventional polyclonal antisera depends on the purity of the antigen used to produce the immune response and the success of any affinity purification. This point is illustrated by reference to other work on gap junctions.

A protein with an SDS PAGE estimated molecular weight of 27,000 (27K protein) has been reported by others (see section 1.5) to be the major structural protein of rodent liver gap junctions. A polyclonal antiserum produced in sheep against rat liver gap junctional preparations by Hertzberg (1984) recognizes the 27K and 16K proteins, which have subsequently been shown (Hertzberg, 1985; Finbow et al., 1986) to be unrelated. This raises important questions as to which antibodies, those directed against the 27K protein or those directed against the 16K protein, are responsible

for functional activities of the antiserum such as the blocking of dye and electrical coupling (see section 4.6).

Traub et al. (1982) have also produced an antiserum against gap junctions, although they used junctions isolated from mouse liver and raised the serum in rabbit. This antiserum is likely to have reactivity against both the 27K and 16K proteins because both proteins (50% 27K protein, 30% 16K protein, Finbow, personal communication) are present in the preparation of the gap junctions.

Similarly, the affinity purified rabbit antiserum raised against SDS PAGE band purified 27K protein by Warner et al. (1984) also recognizes a 54K protein, which was initially said by these authors to be a biochemical precursor form of the 27K protein, but is now known not to be (Paul, 1986; Kamur and Gilula, 1986). Hence one rationale for synthesizing a peptide, corresponding to a part of the 16K protein and using this as the immunogen, was the hope of raising a more specific reagent which would in principle avoid some of the pitfalls of conventional polyclonal antisera and which might be used to provide evidence for the gap junctional origin of the 16K protein.

An alternative strategy would have been to raise monoclonal antibodies. They too have the advantage of specificity, but have the disadvantage that without further characterization they are against unknown sites and are not so helpful for studies on structure and structure-function relationships.

Site specific antibodies have several advantages over conventional polyclonal antisera:

- 1) The antibodies should specifically react with a predetermined region of the protein
- 2) The antibodies can be used to examine homology between specific known regions of possibly related proteins
- 3) The antibodies can be used to examine aspects of the structural organization of the protein, by identifying antigenic sites accessible on a protein
- 4) The antibodies are directed against the synthetic peptide where the potential contaminants (related peptides, the carrier protein and its possible contaminants) are less likely to interfere with the useful specificity of the antiserum (i.e. they are not

contaminants of the natural immunogen)

5) The antibodies can be affinity purified against the peptide

6) It is easier to obtain a similar immune response in different animals, as the scope for variability is much reduced.

In this thesis I describe the first polyclonal site specific antiserum which recognizes a putative gap junctional protein, the 16K protein, in the intact gap junction structure. This site specific antiserum, apart from providing evidence for the 16K protein being a structural component of mouse liver gap junctions, has shown that the N-terminus of the 16K protein is on the cytoplasmic face of these junctions. Other studies, reported below, have used polyclonal site specific antisera directed against parts of the 27K putative gap junctional protein, but these antisera have not been shown to bind to the gap junctional structure.

4.2 Characterization of Site Specific Antiserum

4.2.1 Microimmunodiffusion Analysis

The major principle of the microimmunodiffusion (Ouchterlony) technique is that a single antigen gives rise to a single precipitin line. The precipitates are formed by non-covalent cross-linking interactions between the bivalent antibodies and the usually multivalent antigens (with respect to different antibodies). However, as mentioned in the Results (see section 3.2.3), it is unexpected, on theoretical grounds, that antibodies raised against such a small antigenic site, in this case an octapeptide, can form such immunoprecipitates because each protein molecule is in effect monovalent.

Using monoclonal antibodies it has been shown that an epitope (a single antigenic site) can be as small as three amino acids. Thus the eight amino acids of the immunogen used in this study may represent several sequentially overlapping epitopes, with possibly each epitope recognized by several antibodies with differing

affinities. Steric hinderance is likely though, to prevent more than one antibody molecule binding to the 16K protein and hence no precipitate should form. However precipitates are formed with the site specific antibodies and the 16K protein (Fig.16, section 3.2). The precipitation observed in the microimmunodiffusion assays appears to be specific (in no case did precipitation occur with the preimmune serum) and the position of the precipitin line varies with the concentration of antigen and antibody in the normal way.

One possible explanation for the precipitation reaction is based on the 16K protein's propensity to aggregate. The protein when solubilized in 1% SDS from gap junctional preparations (see Fig. 16) runs at 16K on SDS PAGE but when the protein is heated, concentrated or purified away from SDS, it aggregates to stable dimeric and higher multimeric forms. Examples of this aggregation are shown in other parts of this work e.g. after heating gap junctional preparations in the presence of 1% SDS (Fig. 18) and after electroelution in 0.1% SDS (Fig. 5). Aggregates might therefore be expected to form as the SDS diffuses away through the agarose gel faster than the protein.

When solubilized mouse liver gap junctions are heated in SDS, the SDS PAGE gel profile (Fig. 18) shows that the 16K monomer dimerizes and aggregates to higher molecular weight forms. The higher molecular weight forms can be of such high molecular weight that are unresolved in the running gel (13.7% acrylamide), but they do enter the stacking gel (6% acrylamide), so all aggregate forms should therefore be able to diffuse in the 1% agarose gel used in the immunodiffusion assay.

The immunoprecipitates seen in the immunodiffusion assay are single lines which have uniform intensity and form at the same distance from the antigen well for each of the samples examined (under the same conditions of antigen and antibody concentration), whether it be solubilized junctions, electroeluted monomer or electroeluted dimer. This suggests only one of the multimeric forms predominates in the precipitates, which, on the basis of the SDS PAGE analysis is more likely to be the dimer (Fig. 18, section 3.2). In a somewhat analogous situation Cazenave (1973) has reported that antibodies which did not form a precipitate with a

protein could be made to do so by treating the protein with glutaraldehyde (forming soluble multimers) which then formed immunoprecipitates with the antibody.

It is also possible because the N-terminus is a hydrophilic region that the binding of an antibody molecule to the 16K protein induces the dimerization or multimerization process.

The ease of dimerization and the stability of this form may have implications for the arrangement of the protein within the junction. As mentioned previously (section 1.1 and 1.5) the analysis of isolated gap junctions has suggested that the connexon is made up from six subunits each occupying a space equivalent to 20-30K of protein. This together with the stability of the dimer could mean that two 16K proteins make up the subunit structure of the connexon (twelve 16K proteins to each connexon). Furthermore the stability of the dimer may play a role in the formation of connexons. The insertion of 16K protein into the plasma membrane may result in spontaneous dimer formation and the dimers may then self assemble to form the connexon.

At present insufficient sequence data for the 16K protein is available to produce a model of the polypeptide path within the membrane and therefore the use of the various algorithms used to predict protein secondary structure are not yet applicable. However amino acid analysis by Dr. Findlay (Leeds) has shown a high proportion (~ 46%) of hydrophobic residues. If α -helices or β -strands are incorporated into the membrane, they must be sufficiently hydrophobic. For an aqueous channel, such as the gap junction, the pore must have a hydrophilic lining. This implies that at least some membrane spanning domains, be they α -helices or β -strands, should be amphipathic i.e. only the side facing the aqueous environment (the channel) need be hydrophilic.

4.3 Other Site Specific Antisera

Two different antisera have been raised in rabbits by Evans and his colleagues against peptides (amino acid residues 1-7, Hope et al., 1984; and 7-21, Zervos et al. 1985) of the 27K protein

sequence (as determined by Nicholson et al. 1983).

4.3.1 Immunoblotting Analysis

Immunoblotting analysis of a rat liver gap junctional preparation has shown that the rabbit 1-7 antiserum (Ra 1-7), recognizes bands running at 28K, 26K, 24K, 18K, and 10K. Hope et al. 1984 and Zervos et al. 1985 call the protein 28K based on its migration in SDS PAGE but they believe it to be the same as the 27K observed by other workers in the field. These bands are presumed to be N-terminally derived degradation products, produced by endogenous proteolysis of the 28K protein. Such immunoblot analyses suggests that the N-terminal region of the protein is inaccessible to the endogenous proteases i.e. the N-terminus is intramembranous or located extracellularly.

Interestingly the rabbit 7-21 antiserum (Ra 7-21) when used for immunoblotting analysis fails to bind to any bands other than the 28K in rat liver gap junctional preparations (Zervos et al., 1985). This could be due to better preparation of the gap junctions with reduced endogenous proteolysis, although the methods described were the same. Alternatively the fragments produced (a 10K fragment is visible on the Coomassie stained SDS PAGE profile of the preparation) have adopted a different conformation which prevent this particular antiserum from binding to the partially degraded proteins.

Immunoblotting studies using the site specific antibodies reported in this thesis (Fig. 15, section 3.2), have shown binding to a 16K band in gap junctional preparations and higher molecular weight bands (aggregation products suggested by comigration studies) in profiles of the total protein from mouse liver plasma membranes and electroeluted proteins. At present the site specific antiserum has not detected any proteins with molecular weights lower than 16K. Such a finding is not unexpected as 16K protein is present when gap junctions are isolated in the presence or absence of trypsin (Finbow et al., 1983) i.e. the 16K protein is trypsin resistant when present in the intact gap junction structure.

4.3.2 Immunoprecipitation Analysis

Hope et al. (1984) have investigated the binding of the Ra 1-7 antiserum to iodinated 28K protein in solution radioimmunoassay. Unfortunately the details of the methods they used for this procedure were not given and a direct comparison with the results reported in this thesis is not possible. However, Hope et al. (1984) established that under their conditions the Ra 1-7 antiserum did not bind to the iodinated 28K protein. They suggested that this was due to the conformation adopted by the protein in solution as binding was observed to several tryptic fragments after isolation by reverse phase HPLC.

Conversely, the results in this thesis show that the site specific antiserum to the 16K protein failed to immunoprecipitate from solution radioiodinated 16K protein (section 3.2.2) or its fragments produced by tryptic digestion and isolation by reverse phase HPLC (section 3.4.2). Failure to precipitate the protein may be due to the iodine altering the antigen recognized by the antibody (there is a tyrosine residue in position 4 of the octapeptide).

The site specific antisera produced and characterized by Hope et al. (1984) and Zervos et al. (1985), recognize by immunoblot analyses proteins derived from rat liver gap junctional preparations but such analyses in themselves, cannot distinguish between proteins which are merely associated with gap junctions or those which are structural components.

One way to identify the structural protein of gap junctions is to immunolocalize the antigen to the isolated gap junction structure. Neither Hope et al. (1984) nor Zervos et al. (1985) have been successful in using their antisera to localize the protein to the gap junction structure. This may mean that the N-terminus is located intramembranously or extracellularly (in the gap).

In this thesis site specific antibodies have been produced which fortuitously bind on the cytoplasmic face of gap junctions and therefore can be used to bind to and agglutinate isolated mouse

liver junctions (Fig. 19). Agglutination reactions which can be inhibited by incubation of the antiserum with free peptide (complete inhibition of agglutination reaction at ~ 5 mM; see Fig. 22), or by removal/modification of the antigenic site by pronase treatment of the isolated junctions (section 3.4.2). This confirms the cytoplasmic or edge location as pronase is too large to enter the gap between the membranes or to penetrate into the channels. Further support for the suggestion that the antibody binds to isolated mouse liver junctions is provided by immunofluorescence (Fig. 23) and gold immunolocalization studies (Fig. 24).

4.4 Tissue and Species Conservation

4.4.1 Tissue Conservation

The evidence from the microimmunodiffusion studies (section 3.3.2) showing that the 16K proteins from gap junctions derived from different tissues cross react is consistent with experiments which show functional coupling between cells from different tissues. For example rat ovarian granulosa cells and mouse myocardial cells can couple in tissue culture (Lawrence et al., 1978).

The tissues chosen for this work are derived from the three germ layers of the mouse, the ectoderm (brain), the endoderm (liver) and the mesoderm (heart and kidney). Other work (Buultjens et al., 1986) has also shown that proteins isolated from these tissues are immunologically related by using a polyclonal antiserum raised in rabbits against isolated chicken liver gap junctions and by peptide map analyses of the iodinated 16K proteins derived from these tissues. However there is as yet no sequence data to provide unequivocal evidence that these proteins are identical. It seems reasonable to conclude from the above discussion, and the results presented (section 3.3.2) that the gap junctional protein from different tissues are similar, if not identical.

N-terminal sequence data available for the other putative gap junctional protein, 27K indicates that the rat liver 27K protein

has a 43% homology with a 29K protein isolated from rat heart (Nicholson et al., 1985, see section 1.5). This implies that the "27K" proteins, which are unrelated to 16K, form a set of tissue specific proteins. However, Zervos et al. (1985) have shown by immunoblotting that the Ra 7-21 antiserum binds to 28K proteins in gap junctional preparations from heart, uterus and brain.

4.4.2 Species Conservation

The site specific antisera described by Hope et al. (1984) and Zervos et al. (1985) have not been used to examine gap junction preparations from other species. Finbow et al. (1984) report that a polyclonal antiserum raised in rabbits against isolated gap junctions from chicken and a second polyclonal antibody raised in rabbits against isolated Nephrops hepatopancreas gap junctions (Buultjens et al., 1986) both show reactivity against mouse liver 16K protein, chicken liver 16K protein and Nephrops hepatopancreas 18K protein (Buultjens et al., 1986). Antibodies affinity purified, from the RaC 16K antiserum, against either mouse liver 16K protein or Nephrops hepatopancreas 18K protein bind to, as shown by immunoblot analysis, 16K proteins in chicken and mouse and an 18K protein of Nephrops hepatopancreas. These results show that there is considerable evolutionary conservation. Consistent with these data, experiments in tissue culture show that mammalian cells form junctions with cells from vertebrates in different classes (avian, amphibian, and pisces, Epstein and Gilula, 1977; Pitts, 1977).

Results reported in this thesis (section 3.3.2) have extended these findings by showing that liver gap junction preparations derived from mouse, chicken, Xenopus and Nephrops all form immunoprecipitates with the site specific antiserum in the microimmunodiffusion assay. The SDS PAGE profile (Fig. 26) indicates that there is a major Coomassie staining band, from preparations from each of the species in the molecular weight range at 16-18000 daltons. Moreover the site specific antibodies agglutinates junctions from mouse liver and Nephrops hepatopancreas

(Fig 27). The conclusion drawn from these results is that the protein of the gap junctions from each of these species has a conserved N-terminal region, which is located on the cytoplasmic surface of the junctions. Such a conclusion is consistent with the uniform morphology of gap junctions from different sources and their similar physiological properties. Sequence analysis will be required to obtain more definitive information about the species conservation of the gap junctional proteins.

The conclusion suggesting that a ubiquitous, or highly conserved protein (16K), is the gap junctional structural protein, contrasts with that most recently propounded by Revel et al. (1986). They propose that the proteins which constitute gap junctions belong to several protein families. In support of their argument they note that a protein Mr 21,000 (judged by SDS PAGE), is present on heavily loaded gels of mouse and rat liver gap junctional preparations. Sequencing studies show that the 21K and 28K proteins are related (Revel et al., 1986). However the amount of 21K protein which can be isolated after partial hepatectomy remains constant with time in contrast to the fall and rise in amount of the 28K (Finbow et al., 1980; Traub et al., 1982) and 16K (Finbow et al., 1983) proteins. There is also a fall and rise in gap junctional area measured by morphometry of freeze fractured tissue which follows the same time course (Yee and Revel, 1978; Meyer et al., 1981).

The support for the junctional origin of the 21K protein therefore, relies merely upon its partial sequence homology with the 28K protein, and the fact that it represents 10% of the protein in the final junctional fractions from rat liver and as much as 30-40% in that from mouse liver preparations. Revel et al. (1986) further argue that this "multiplicity" of junctional proteins is confirmed as the protein isolated from arthropods (18K) is distinct from the 28K protein. The results presented in this thesis however, support those of Finbow et al. (1984) which show that the arthropod 18K protein is related to the vertebrate 16K protein, providing a much simpler picture of a conserved structure, conserved function and a conserved protein.

An explanation for these contrasting views may hinge on the nature of the association of the protein with the gap junction i.e. whether it is a structural or associated protein. At present insufficient evidence is available to distinguish between these possibilities. However, no matter which isolation procedure is followed (see section 1.5) the 16K protein has always been detected. In contrast the 27K protein (26K, 28K) has not been detected using the isolation procedures developed by Goodenough (1974) or Finbow et al. (1983). These procedures use conditions under which the 27K protein becomes disassociated from the gap junction or is degraded by proteolysis.

4.4 Monoclonal Antibodies.

At present there are two reports in the literature describing monoclonal antibodies directed against liver gap junctions. One has been produced by immunizing Balb/c mice with whole rat liver gap junctions (Paul, 1985). The other has been produced in BDIX rats by immunizing alternately with whole mouse liver gap junctions followed by mouse liver gap junctions treated with 0.2% SDS (Janseen-Timmen et al., 1986).

The anti-rat junctional monoclonal antibodies bind to the cytoplasmic face of gap junctions isolated from mouse, rat, and human liver as shown by immunofluorescent labelling on frozen unfixed sections. However the monoclonal antibody does not appear to react with sections from brain, kidney, pancreas, heart, or stomach. Results which suggest that the epitope is unique to the liver type protein. However the identification of the protein to which the monoclonal antibodies bind was not possible as no reaction was detectable using immunoblot analyses (providing an example of an immunogenic response which has limited practical application).

Further evidence for the nature of the antigen recognized by the monoclonal reported by Paul (1985) will be required before it can be used to help resolve the present uncertainty about the nature of the gap junction protein.

The anti-mouse liver junction monoclonal antibodies recognize 26K proteins from mouse and rat liver as well as mouse pancreas, as shown by immunoblotting (Janseen-Timmen et al., 1986). In addition the monoclonal antibody reacts in situ, as shown by indirect immunofluorescence, with cryosections from the livers of mouse and rat and mouse exocrine pancreas and seminiferous epithelium (Willecke et al., 1985). However the monoclonal does not react with cryosections or immunoblots of brain, kidney or heart, tissues known to have gap junctions.

The gold immunolocalization studies using the monoclonal antibody are on thin sectioned liver plasma membranes. The junctions have the gold particles lying directly on the cytoplasmic faces (rather than being separated by ~ 7 nm as is expected from binding via antibodies and gold conjugated anti-rat IgG), as though the gold particles are non-specifically adsorbed. Unfortunately Janseen-Timmen et al. (1986) do not show control micrographs.

4.6 Functional studies

As outlined in section 1.4 the suggestions for the functional roles of gap junctions have mainly been based on their known permeability properties. To further define the functions of gap junctions a means of specifically interrupting or controlling gap junctional communication is required. Two possible ways to do this with specific antibodies are readily apparent: one is to block gap junction formation by the topical application of antibodies, through interactions with extracellular sites on the precursors to the gap junction; the other is to block or interrupt gap junctional communication by injection of antibodies into cells, which would act on the cytoplasmic faces of established junctions or could possibly interact with cytoplasmic sites on precursors to prevent gap junction formation. This latter procedure has the disadvantage that the number of cells that can be injected is limited. Conversely the extracellular application of antibodies would mean that whole populations of cells could be examined for any perturbations in gap junctional formation.

To date there are only three published reports on attempts to directly modulate gap junctional permeability with antibodies. Two of these reports have described unsuccessful experiments based on the topical application of antibodies to cells grown in tissue culture.

Traub et al. (1982) used the antibodies raised in rabbits against mouse liver gap junctions and found they had no effect, as judged by the transfer of radiolabelled metabolites, on junctional communication in cultures of mouse 3T6 fibroblasts. Similar results were reported by Hertzberg et al. (1985). They showed that in this case the topical application of antibodies, raised in sheep against purified rat liver gap junctions and affinity purified against the 27K protein, had no effect on electrical coupling between primary cultures of hepatocytes isolated from rat liver, neurons isolated from neonatal rat superior cervical ganglion cells and myocardial cells isolated from adult rat ventricles.

These results of Traub et al. (1982) and Hertzberg et al. (1985) are perhaps not surprising as the antigens used in both cases were isolated gap junctions, which may therefore have only produced antibodies to determinants on the cytoplasmic surfaces. Moreover if the protein is highly conserved then tolerance may be shown to extracellular epitopes.

In contrast, when these antibodies are injected into cells, junctional communication is disturbed. Hertzberg et al. (1985) pressure injected antibodies into one of a pair of coupled cells to examine the effects of antibody on dye transfer and electrical coupling. They used the same three cell types, hepatocytes, myocardiocytes, and cervical ganglion neurons. They looked at the passage of the dye Lucifer Yellow. By co-injecting Lucifer Yellow and the affinity purified antibodies they showed that the antibodies blocked dye transfer in all three cell types. All three cell types when injected with antibodies showed decreased, but not completely inhibited electrical coupling. The cervical ganglion neurons showed that coupling was reduced to ~20% of control values in 50 s. In the hepatocytes and myocardiocytes the electrical coupling was reduced to < 10% of control values in ~150 s.

The antibody may be acting either by sterically hindering the

passage of molecules through the channel, or by binding to the protein and to altering its conformation to reduce the diameter of the channel. Alternatively, it is conceivable that, in some way, antibody binding triggers the normal gating mechanism and fully closes the channels.

Hertzberg et al. (1985) use the physiological data (sic), outlined above to conclude that similar or identical 27K proteins constitute gap junctions in brain, heart and liver and extend this conclusion to include most vertebrate tissues. They further argue that the failure of the other antibodies, specifically those raised against the 26K protein, monoclonal and polyclonal, to react with heart tissue may be due to tissue preparation. This is a valid point but only applicable to the failure of the antibody to detect 26K protein on immunoblots. Such an argument is less likely to apply to failure to detect antigen when using cryosections of unfractionated tissue. However Hertzberg et al. (1985) do concede that they might be identifying homologous but tissue specific proteins. This would seem the more likely explanation as Paul (1986) has shown by northern blot analyses, mRNAs in brain, liver and kidney of the same size, implying homologous proteins of similar size. However these analyses also showed, at lower stringency, smaller mRNA in heart, a finding which is at odds with the claim of Hertzberg et al. (1985) that the 27K protein is found in heart.

The preliminary study reported in this thesis used the transfer of the fluorescent dye, Lucifer Yellow, to monitor the effects of antiserum injection in Buffalo rat liver (BRL) cells grown as monolayers. In distinction to Hertzberg et al. (1985) the antiserum was not co-injected with the dye, but the antiserum was first iontophoresed into the cell followed by the iontophoretic injection of dye (Fig. 44). 73% of the cells injected with antiserum failed to transfer the dye. Until electrical coupling is measured it is difficult to obtain quantitative results and thereby to make direct comparisons with the data of Hertzberg et al. (1985).

The blocking of the cell to cell transfer by the site specific antiserum provides further evidence that the 16K protein

is a structural or closely associated gap junctional protein and also confirms that the octapeptide recognized by the antiserum is located on the cytoplasmic face of gap junctions in vivo.

More ambitious functional studies have been carried out by Warner et al. (1984). They have attempted to delineate the role of gap junctional communication in embryonic development by injecting antibodies into a cell located in the region of the grey crescent in 8 cell stage Xenopus embryos.

The antibodies used were raised in rabbits against SDS PAGE band purified 27K protein derived from rat liver and affinity purified on an affinity column containing the 27K protein. By immunoblot analyses the antibodies recognize a 27K protein and its dimer, 47K, and an uncharacterized 54K protein in rat liver homogenates. In the protein homogenate from unfertilized Xenopus eggs the antibodies recognized the 27K protein and a 54K protein with the 54K protein being the most abundant antigenic species present. In the protein homogenate of Xenopus 8 cell stage embryos the antibodies only detected the 54K protein.

In common with the preliminary data reported here and those of Hertzberg et al. (1985), Warner et al. (1984) used in part of their study the transfer of the dye Lucifer Yellow to monitor the effects of antibody injection. The antibody was injected at the 8 cell stage and dye transfer assayed at the 32 cell stage. This they argue provides sufficient time for the antibody to diffuse throughout the four daughter cells. Between 70 and 80% of those embryos injected with Lucifer Yellow failed to transfer dye. As they assayed for dye transfer at the 32 cell stage they conclude that the antibodies can block the permeability both of the junctions already formed at the 8 cell stage and of new junctions established during the 16 and 32 cell stages.

Warner et al. (1984) confirmed the blockage of dye transfer, by examining the effect of antibody injections on electrical coupling. In contrast to Hertzberg et al. (1985) Warner et al. (1984) found that the injection of antibody caused complete inhibition of electrical coupling.

Warner et al. (1984) monitored embryos injected with antibody until the tadpole stage. They found that those cells injected with

antibody maintained normal resting potentials and continued to divide at the same rate as the "non-injected" cells although until what stage is not specified. Warner et al. (1984) showed that the injected embryos developed a characteristic set of abnormalities. The most common defect was varying degrees of right/left asymmetry and some embryos failed to form brains and eyes on the right side.

This study is the first attempt at producing evidence for a "pivotal role" of gap junctions in embryonic development. However with the publication of the full cDNA sequence (Paul, 1986), the question as to the identity of the 54K protein arises. It does not appear to be a precursor of the 27K protein as Warner et al. (1984) suggest. As the identity of the 54K protein is unknown, the presence of reactivity to it in the affinity purified antibody preparation casts doubt on Warner et al.'s (1984) claim that it is the activity directed against the 27K protein which is causing blockage of cell to cell communication and the right/left asymmetry. Furthermore it is not readily apparent why the antibody detects 27K protein in the unfertilized eggs of Xenopus but not at the 8 cell stage. Xenopus eggs do not have gap junctions (although some form of precursor could be present) and junctions only begin to develop at the 8 cell stage, the converse of what might be predicted.

It seems premature to conclude from these experiments that the junctional pathway is used for developmental signalling. Blockage of cell to cell communication by such invasive techniques as antibody injection, could be due to secondary factors e.g. cell damage causing an influx of calcium ions. Moreover even if such secondary effects could be ruled out, the blocking of cell to cell communication could merely be interfering with cellular homeostasis. This could be sufficient to prevent normal clonal expansion, and thus resulting developmental abnormalities do not necessarily mean the junctional pathway is used for developmental signalling.

However such a potential or putative role for junctional communication remains a powerful enticement for the further study of gap junctions and their functions.

CHAPTER V

REFERENCES

- Anderson, E. and Albertini, D.F. (1976) *J. Cell Biol.*, 71, 680-686.
- Asada, Y. and Bennett, M.V.L. (1971) *J. Cell Biol.*, 49: 159-172.
- Atherton, E., Fox, H., Harkiss, D., Logan, C.J., Sheppard, R.C. and Williams, B.J. (1978) *J. Chem. Soc. Chem. Commun.*, 13: 537-539.
- Atkinson, M.M., Anderson, S.K. and Sheridan, J.D. (1986) *J. Membr. Biol.*, 91: 53-64.
- Atkinson, M.M., Menko, A.S., Johnson, R.G., Sheppard, J.R. and Sheridan, J.D. (1981) *J. Cell Biol.*, 91: 573-578.
- Azarnia, R. and Loewenstein, W.R. (1984) *J. Membr. Biol.*, 82: 191-205.
- Baker, T.S., Casper, D.L.D., Hollingshead, C.J. and Goodenough, D.A. (1983) *J. Cell Biol.*, 96: 204-216.
- Baker, T.S., Sosinsky, G.S., Caspar, D.L.D., Gall, C. and Goodenough, D.A., (1985) *J. Mol. Biol.*, 184: 81-98.
- Baldwin, K. (1979) *J. Cell Biol.*, 82: 66-79.
- Benedetti, E.L., Dunia, I., Bentzel, J., Vermoken, A.J.M., Kibbelaar, D. and Bloemendal, H. (1976) *Biochim. Biophys. Acta.*, 457: 353-384.
- Benedetti, E.L. and Emmelot, P. (1967) *J. Cell Biol.*, 38: 15-24.
- Bennett, M.V.L. (1973) In: "Intracellular Staining Techniques in Neurobiology" (Kater, S.D. and Nicholson, J. eds.) pp115-133, Elsevier, New York.
- Bennett, M.V.L., Brown, J.E., Harris, A.L. and Spray, D.C. (1978) *Biol. Bull.*, 155: 442.

- Bennett, M.V.L., Spray, D.C., Harris, A.L. (1981) *Amer. Zool.*, 21: 413-427.
- Berdan, R.C. and Caveney, S. (1985) *Cell Tissue Res.*, 239: 111-122.
- Bernardini, G., Peracchia, C. and Peracchia, L.L. (1984) *Eur. J. Cell Biol.*, 34: 207-312.
- Blumberg, P.M. (1980) *CRC Crit. Rev. Toxicology.*, 8: 153-169.
- Bok, D., Dockstader, J. and Horwitz, F. (1983) *J. Cell Biol.*, 92: 213-220.
- Brink, P.R. and Dewey, M.M. (1978) *J. Gen. Physiol.*, 72: 67-86.
- Buultjens, T.E.J., Finbow, M.E., Lane, N.J. and Pitts, J.D. (1986) (submitted)
- Canipari, R., Palombi, F., Riminucci, M. and Mangia, F. (1984) *Dev. Biol.*, 102: 519-524.
- Caspar, D.L.D., Goodenough, D.A., Makowski, L. and Phillips, W.C., (1977) *J. Cell Biol.*, 74: 605-628.
- Caveney, S., Berdan, R.C. and Mclean, S. (1980) *J. Insect. Physiol.*, 26: 557-567.
- Cazenave, P.-A. (1973) *FEBS Lett.*, 31: 348-357.
- Chang, J.Y., Brauer, D. and Wittmann-Liebold, B. (1978) *FEBS Lett.*, 93: 205-214.
- Charest, R., Blackmore, P.F., Berthon, B. and Exton, J.H. (1983) *J. Biol. Chem.*, 258 : 8769-8773.
- Cooper, M.S. (1984) *J. Theor. Biol.*, 111: 123-130.
- Culvenor, J.G. and Evans, W.H. (1977) *Biochem. J.*, 168: 475-481.
- Dahl, G. and Isenberg, G. (1980) *J. Membr. Biol.*, 53: 63-75.
- Davidson, J.S., Baumgarten, I.M. and Harley, E.H., (1985) *Carcinogenesis.*, 6: 1353-1358.
- Dekel, N. and Beers, W.H. (1980) *Dev. Biol.*, 75: 247-254.
- Dekel, N. and Beers, W.H. (1981) *Dev. Biol.*, 80: 356-362.
- Dekel, N., Lawrence, T.S., Gilula, N.B. and Beers, W.H. (1981) *Dev. Biol.*, 86: 356-362.
- Dermietzel, R., Leibstein, A., Frixen, U., Janseen-Timmen, V., Traub, O. and Willecke, K. (1984a) *EMBO J.*, 3: 2261-2270.
- Dermietzel, R., Janseen-Timmen, V., Willecke, K. and Traub, O., (1984b) *Eur. J. Cell Biol.*, 33: 84-89.

- Dorman,B.H. and Boreiko,C.J. (1983) Carcinogenesis., 4: 873-877.
- Enomoto,T., Sasaki,Y., Shiba,Y., Kanno,Y. and Yamasaki,H. (1981)
Proc. Natl. Acad. Sci. U.S.A., 78: 5628-5632.
- Eppig,J.J (1982) Dev.Biol., 89: 268-272.
- Epstein,M.L. and Gilula,N.B. (1977) J. Cell Biol., 75: 769-787.
- Fentiman,I., Taylor-Papadimitriou,J. and Stoker,M. (1979) Nature.,
264: 760-762.
- Finbow,M.E. (1981) In:" The Functional Integration of Cells In
Animal Tissues. " (eds Pitts,J.D. and Finbow,M.E.) pp 1-37.
Cambridge University Press.
- Finbow,M.E. and Pitts,J.D., (1981) Exp. Cell Res., 104: 1-13.
- Finbow,M.E., Buultjens,T.E.J., John,S., Kam,E., Meagher,L. and
Pitts,J.D. (1986) In: " Molecular Structure of the Gap
Junctional Channel. " CIBA Symp., no 125 (in press)
- Finbow.M.E., Buultjens,T.E.J., Lane,N.J., Shuttleworth,J. and
Pitts,J.D., (1984) EMBO J., 3: 2271-2278.
- Finbow,M.E., Shuttleworth,J., Hamilton,A.E., and Pitts,J.D., (1983)
EMBO J., 2: 1479-1486.
- Finbow,M.E., Yancey,S.B., Johnson,R. and Revel,J.-P. (1980) Proc.
Natl. Acad. Sci.USA., 77: 970-974.
- Fitzgerald,P.G., Bok,D. and Horwitz,J. (1983) J. Cell Biol., 97:
1491-1499.
- Flagg-Newton,J.L., Simpson,I. and Loewenstein,W.R., (1979) Science
205: 404-407.
- Flower,N.E., (1972) J.Cell Sci., 10:683-691.
- Furshpan,E.J. and Potter,D.D. (1959) J. Physiol., 145: 289-325.
- Furshpan,E.J. and Potter,D.D. (1968) Current Topics in
Developmental Biology, 3: 95-127.
- Gainer,H. and Murray,A.W. (1985) Biochem. Biophys.Res. Commun.,126
1109-1113.
- Garfield,R.E. and Hayashi,R.H. (1982) Am.J.Obstet.Gynecol., 140:
254-260.
- Garfield,R.E., Sims,S. and Daniel,E.E. (1977) Science., 198:
958-960.

- Garfield,R.E., Sims,S. Kannan,M.S. and Daniel,E.E. (1978) Am. J. Physiol., 253: C168-C179.
- Gilula, N.B. (1972) J.Ultrastruct.Res., 38: 215-216 abstr.
- Gilula,N.B., Epstein,M.L. and Beers,W.H. (1978) J. Cell Biol., 78: 58-75.
- Gilula,N.B., Reeves,D.R. and Steinbach,A. (1972) Nature, 235: 262-265.
- Goodenough,D.A. (1974) J. Cell Biol., 61: 557-563.
- Goodenough,D.A. (1979) Invest. Ophthalmol. Visual. Sci., 18: 1104-1122.
- Goodenough,D.A. and Gilula,N.B. (1974) J. Cell Biol., 61: 575-590.
- Goodenough,D.A. and Revel, J.-P. (1970) J.Cell Biol., 45: 272-290.
- Goodenough,D.A. and Stoeckenius,W. (1972) J. Cell Biol., 54: 646-656.
- Gray,W.R. and Hartley,B.S. (1969) Biochem. J., 89: 59-68.
- Green,C.R. and Severs, N.J. (1984) J. Cell Biol., 99: 453-463.
- Gullick,W.J., Downward,J. and Waterfield,M.D. (1985) EMBO J., 4: 2869-2877.
- Gunning,B.E.S. and Robards,A.W. (eds) (1976) in Intercellular Communication in Plants: Studies on Plasmodesmata. Springer-Verlag, Berlin.
- Hagiwara,S. and Morita,H. (1962) J. Neurophysiol., 25: 721-731.
- Hand,A.R. and Gobel,S. (1972) J. Cell Biol., 52: 397-408.
- Hanna,R.B., Ornberg,R.L. and Reese,T.L. (1985) In "Gap Junctions" (Bennett.M.V.L. and Spray,D.C.)pp23-32. Cold Spring Harbour. New York.
- Hanna,R.B., Pappas,T.S. and Bennett,M.V.L. (1984) Cell Tissue Res. 235: 243-249.
- Hartman,T.G. and Rosen,J.D., (1985) Carcinogenesis 6: 1315-1319.
- Haydon,D.A., Elliot,J.R. and Hendry,B.M. (1984) Curr. Top. Membr. Transp., 22: 445-482.
- Henderson,D., Eibl,H. and Weber,K., (1979) J. Mol. Biol., 132: 193-218.
- Hertzberg,E.L. (1985) Ann. Rev. Physiol.,47: 305-308.
- Hertzberg,E.L. (1984) J. Biol. Chem., 259: 9936-9943.

- Hertzberg,E.L. and Gilula,N.B. (1979) J. Biol. Chem., 254:
2138-2147.
- Hertzberg,E.L. and Skibbens,R.V. (1984) Cell, 39: 61-69.
- Hertzberg,E.L. and Spray,D.C.(1985) In : " Gap
Junctions"(Bennett,M.V.L.and Spray,D.C. eds) pp49-65. Cold
Spring Harbour. New York.
- Hertzberg,E.L. Spray,D.C. and Bennett,M.V.L. (1985) Proc. Natl.
Acad. Sci. USA., 82: 2412-2416.
- Hille,B. (1984) In " Ionic Channels of Excitable Membranes"
pp 329-353. Sinauar, Massachusetts.
- Hirowaka,H., and Heuser,J., (1982) Cell, 30: 395-406.
- Hope,J., Zervos,A. and Evans,W.H. (1984) In:" Matrices and Cell
Differentiation" (Hinchcliffe,J.R.and Kemp,R.B. eds) pp261-274
Alan R. Liss, New York.
- Hopp,T.P and Woods.K.R. (1981) Proc. Natl. Acad. Sci. USA 78:
3824-3828.
- Hunter,W.M. and Greenwood,F.C. (1962) Nature, 194:495-496.
- Hunter,G.K. and Pitts,J.D. (1981) J. Cell Sci., 49: 163-175.
- Iwatsuki.N and Peterson,D.H. (1979) Nature, 286:148-149.
- Janssen-Timmen,U., Dermietzel,R., Frixen,U., Leibstein,A., Traub,O.
and Willecke,K. (1983) EMBO J., 2: 295-302.
- Janseen-Timmen,U., Traub,O., Dermietzel,R., Rabes,H.M. and
Willecke,K. (1986) Carcinogenesis, 7: 1475-1482.
- Johnston,M., Simon,S. and Ramon,F. (1980) Nature, 286: 498-500.
- Kamur,N.M. and Gilula,N.B. (1986) J. Cell Biol., 103: 767-776.
- Kistler,J. and Bullivant,S. (1980) J. Ultrastruct. Res., 72: 27-38.
- Laemmli,U.K. (1970) Nature, 277: 680-685.
- Laseter,E.M. and Dowling,J.E. (1985) Proc. Natl. Acad. Sci. USA,
82: 3025-3029
- Lawrence,T.S., Beers,W.H. and Gilula,N.B. (1978) Nature, 272:
501-506.
- Leslie,T. (1955) In " The Nucleic Acids" (eds Chargaff,E. and
Davidson,J.N.)p 1-50 vol II Academic Press, New York.

- Loewenstein, W.R. (1966) *Ann. N. Y. Acad. Sci.*, 137: 441.
- Loewenstein, W.R. (1968) *Dev. Biol. Suppl.*, 2: 151-183.
- Loewenstein, W.R. (1979) *Biochim. et Biophys. Acta.* 560: 1-65.
- Loewenstein, W.R. and Kanno, Y. (1964) *J. Cell Biol.* 22: 565-586.
- McNutt, N.S. and Weinstein, R.S. (1973) *Prog. Biophys. Mol. Biol.*, 26: 45-101.
- Makowski, L. (1985) In: "Gap Junctions" (Bennett, M.V.L. and Spray, D.C. eds) pp1-7 Cold Spring Harbour. New York.
- Makowski, L., Caspar, D.L.D., Phillips, W.C. and Goodenough, D.L.D. (1977) *J. Cell Biol.*, 74: 629-645.
- Makowski, L., Caspar, D.L.D., Phillips, W.C. and Goodenough, D.L.D. (1984) *J. Mol. Biol.*, 174: 449-481.
- Manjunath, C.K., Goings, G.E. and Page, E. (1984) *Am. J. Physiol.*, 246: H865-H875
- Meyer, D.J., Yancey, S.B. and Revel, J.-P. (1981) *J. Cell Biol.*, 91: 505-523.
- Miller, T.M. and Goodenough, D.A. (1986) *J. Cell Biol.*, 102: 194-199.
- Moor, R.M., Smith, M.W. and Dawson, R.M.C. (1980) *Exp. Cell Res.*, 126: 15-29.
- Murray, A.W. and Fitzgerald, D.J. (1979). *Biochem. Biophys. Res. Commun.*, 91: 395-401.
- Neville, D.M. (1960) *J. Biochem. Biophys. Cytol.*, 8: 413-421.
- Newbold, R.G. (1981) In "The Functional Intergration of cells in animal tissue." (eds Pitts, J.D. and Finbow, M.E.) p 301-318. Cambridge University Press.
- Neyton, J. and Trautmann, A. (1985) *Nature*, 317: 331-335.
- Neyton, J., Piccolino, M. and Gerschenfeld, H.M. (1985) In: "Gap Junctions" (Bennett, M.V.L. and Spray, D.C. eds) pp381-391 Cold Spring Harbour. New York.
- Nicholson, B.J., Gros, D.B., Kent, S.B.H., Hood, L.E. and Revel, J.-P. (1985) *J. Bio. Chem.*, 260: 6514-6517.
- Nicholson, B.L., Hunkapiller, M., Grim, L.B., Hood, L. and Revel, J.-P. (1981) *Proc. Natl. Acad. Sci. USA*, 78: 7594-7598.
- Nicholson, B.J., Takemoto, L.J., Hunkapillar, M., Hood, L. and Revel, J.-P. (1983) *Cell*, 32: 967-978.

- Nishizuka, Y. (1986) *J.N.C.I.*, 76: 363-370.
- Obaid,A.L., Socolar,S.J. and Rose,B. (1983) *J.Membr. Biol.*, 73: 69-89.
- Paul,D.L. (1985) In "Gap Junctions" (Bennett,M.V.L. and Spray,D.C. eds) pp 107-122. Cold Spring Harbour. New York.
- Paul,D.L. (1986) *J. Cell Biol.*, 103: 123-134.
- Paul,D.L. and Goodenough,D.A. (1983) *J. Cell Biol.*, 96: 625-632.
- Peracchia,C. (1977) *J. Cell Biol.*, 72: 628-641.
- Peracchia,C. (1978) *Nature*, 271: 669-671.
- Peracchia,C. and Dalhanty,A.F. (1976) *J. Cell Biol.*, 70:419-439.
- Pincus,G. and Enzmann,E.V. (1935) *J.Exp. Med.*62:665-675.
- Pitts,J.D. (1971) In : " Growth Control in Cell Culyures"
(Wolstenholme,G.E.W. and Knight,J. eds.) p 89
Churchill-Livingstone, London.
- Pitts,J.D. (1976) In:" Developmental Biology of Plants and Animals"(Graham,C.F. and Wareing,P.F. eds) pp 96-110
Blackwell. Oxford.
- Pitts,J.D. and Burk,R.R. (1976) *Nature, Lond.*, 264: 762-764.
- Pitts,J.D. and Burk,R.R. (1986) (in press)
- Pitts,J.D. and Finbow,M.E. (1986) *J.Cell Sci. Suppl.*, 4: 239-266.
- Pitts,J.D. and Kam, E. (1985) *Exp. Cell Res.*, 156: 439-449.
- Pitts,J.D. and Simms,J.W. (1977) *Exp. Cell Res.*, 104:153-163.
- Pitts,J.D., Finbow,M.E., Bultjens,T.E.J., Kam,E. and Shuttleworth,J. (1985) In "Cellular and Molecular Control of Direct Cell Interactions in Developing Systems " (ed Marthy, H.J.) NATO/ASI Series Plenum. New York.
- Raviola,E., Goodenough,D.A. and Raviola,G. (1980) *J. Cell Biol.* 87: 719-723.
- Reber,W.R. and Weingart,R. (1982) *J. Phsiol.* 328: 87-104.
- Revel,J.-P. and Karnovsky, M.J. (1967) *J. Cell Biol.*, 33: 87-102.
- Revel,J.-P., Yancey,B.J. and Nicholson,B.J. (1986) *TIBS* 11:375-377.
- Revel,J.-P., Yancey,S.B., Meyer,D.J. and Nicholson,B.J. (1980) In *Vitro* 16: 1010-1017.

- Revel, J.P., Yee, A.G. and Hudspeth, A.J. (1971) Proc. Natl. Acad. Sci., 68: 2924-2929.
- Rose, B. and Loewenstein, W.R. (1975) Nature, Lond., 254: 250-252.
- Rose, B. and Rick, R. (1978) J. Membr. Biol. 44: 377-415.
- Rose, B., Simpson, I. and Loewenstein, W. (1977) Nature, 267: 625-627.
- Safranyos, R.G.A. and Caveney, S. (1985) J. Cell Biol., 100: 736-747.
- Sas, D.F., Sas, M.J., Johnson, K.R., Menko, A.S. and Johnson, R.G. (1985) J. Cell Biol., 100: 216-225.
- Seeman, P. (1972) Pharmacol. Rev. 24: 583-655.
- Sheridan, J.D. (1976) In "The Cell Surface in Animal Embryogenesis" (eds Poske, G. and Nicholson, G.L.) New York: Elsevier.
- Sheridan, J.D., Finbow, M.E. and Pitts, J.D. (1979) Exp. Cell Res. 123: 111-117.
- Sheridan, J.D., Hammer-Wilson, Preus, M. and Johnson, R.G. (1978) J. Cell Biol., 76: 532-544.
- Shibata, Y., Manjunath, C.K. and Page, E. (1985) Am. J. Physiol., 249: H690-H693.
- Simpson, I., Rose, B., and Loewenstein, W.R. (1977) Science 195: 294-296.
- Sims, S.M., Daniel, E.E., and Garfield, R.E. (1982) J. Gen. Physiol., 80: 353-375.
- Spira, M.E. and Bennett, M.V.L. (1972) Brain Res., 37: 294-300.
- Spray, D.C. and Hertzberg, E.L. (1985) Biophys. J., 47: 505a.
- Spray, D.C., Campos de Carvalho, A.C. and Bennett, M.V.L. (1986) Proc. Natl. Acad. Sci. USA., 83: 3533-3536.
- Spray, D.C., Stern, J., Harris, A.L. and Bennett, M.V.L. (1982) Proc. Natl. Acad. Sci. USA., 79: 441-445.
- Spray, D.C., White, R.L., Campos de Carvalho, A.C., Harris, A.L. and Bennett, M.V.L. (1984) Biophys. J., 45: 219-230.
- Spray, D.C., White, R.L., Versilis, V. and Bennett, M.V.L. (1985) In "Gap Junctions" (Bennett, M.V.L. and Spray, D.C. eds) pp 355-366 Cold Spring Harbour. New York.
- Subak-Sharpe, J.M., Burk, R.R. and Pitts, J.D. (1966) Hereditary 21: 342-343. Abstr.
- Subak-Sharpe, J.M., Burk, R.R. and Pitts, J.D. (1969) J. Cell Sci., 4: 353-367.

- Traub,O., Druge,P.M. and Willecke,K. (1983) Proc. Natl. Acad. Sci., 80: 255-259.
- Traub,O., Janseen-Timmen,V., Druge,P.M., Dermietzel,R. and Willecke,K. (1982) J. Cell Biochim., 18: 27-44.
- Towbin,H., Staehlin,T. and Gordon,J. (1979) Proc. Natl. Acad. Sci. USA, 76: 4350-4354.
- Trosko,J.E. and Chang, C-c.(1984) In:" Mechanisms of Tumour Promotion" (Sлага,T.J. ed) pp119-145 Vol IV CRC Press. Boca Raton. Florida.
- Turin,L. (1985) In "Cellular and Molecular Control of Direct Cell Interactions" (ed Marthy,H.-J.) pp 285-296. NATO ASI Series vol 99: Plenum. New York.
- Turin,L. and Warner,A.E. (1977) Nature, 270: 56-57.
- Turin,L. and Warner,A.E. (1980) J. Physiol.300: 489-504.
- Unwin,P.N.T. and Ennis,P.D. (1983) J. Cell Biol.97: 1459-1466.
- Unwin,P.N.T. and Ennis,P.D. (1984) Nature, 307: 606-613.
- Unwin,P.N.T. and Henderson,R. (1984) Scient. Am., 250: 56-66.
- Unwin,P.N.T. and Zampighi,G.S. (1980) Nature, 283: 545-549.
- Van Eldik,L.J., Hertzberg,E.L., Berdan,R.C. and Gilula,N.B. (1985) Biochim. Biophys. Res. Commun., 126: 825-832.
- Warner,A.E., Gutherie,S.C. and Gilula, N.B. (1984) Nature 311: 127-131.
- Watanabe,A. and Grundfest.H. (1961) J. Gen. Physiol., 45: 267-308.
- Weinstein,I.B., Lee,L.S., Fisher,P.B., Mufson,R.A. and Yamasaki.H. (1979) J.Supramol.Struct., 12: 195-201.
- Willecke,K. Traub,O., Jansseen-Timmen,U., Frixen,U., Dermietzel,R., Leibstein,A., Paul,D. and Rabes,H. (1985) In:" Gap Junctions" (Bennett,M.V.L. and Spray,D.C. eds) Cold Spring Harbour. New York.
- Wojtczak,J.A. (1985) In "Gap Junctions" (Bennett,M.V.L. and Spray, D.C. eds) pp 167-175 Cold Spring Harbour. New York.
- Wrigley,N.G. Brown,E. and Chillingworth,R.F. (1984) Biophys. J., 45: 201-207.
- Yamasaki,H. and Enomoto,T. (1985) Carcinogenesis 9: 179-194.

- Yancey, S.B., Easter, D., and Revel J.-P. (1979) J. Ultrastruct. Res., 67: 229-242.
- Yancey, S.B., Edens, J.E., Trosko, J.E., Chang, C.C. and Revel, J.-P. (1982) Exp. Cell Res., 139: 329-340.
- Yee, A.G. and Revel, J.-P. (1978) J. Cell Biol., 78: 554-564.
- Yotti, L.P., Chang, C.C. and Trosko, J.E. (1979) Science 206: 1089-91.
- Zampighi, G., Corless, J.M. and Robertson, J.D. (1980) J. Cell Biol., 86: 190-199.
- Zampighi, G., Simon, S., Robertson, J.D., McIntosh, T., and Costello (1982) J. Cell Biol., 93: 175-189.
- Zelcer, E. and Daniel, E.E. (1979) Can. J. Physiol. Pharmacol., 57: 590-595.
- Zervos, A.S., Hope, J. and Evans, W.H. (1985) J. Cell Biol., 101: 1363-1370.
- Zimmerman, A.L. and Rose, B. (1985) J. Membrane Biol., 84: 269-283.